KINETIC, THERMODYNAMIC AND MECHANISTIC FEATURES OF *ESCHERICHIA COLI* BCP, AN UNUSUALLY VERSATILE PEROXIREDOXIN

By

STACY REEVES

A Dissertation Submitted to the Graduate Faculty of

WAKE FOREST UNIVERSITY GRADUATE SCHOOL OF ARTS AND SCIENCES

In Partial Fulfillment of the Requirements

for the Degree of

DOCTOR OF PHILOSOPHY

In Molecular Genetics and Genomics

August 2011

Winston-Salem, North Carolina

Approved By:

Leslie Poole, Ph.D., Advisor

Examining Committee:

Rajendar Deora, Ph.D., Chair

Mark Lively, Ph.D.

W. Todd Lowther, Ph.D.

Doug Lyles, Ph.D.

ACKNOWLEDGEMENTS

I would to thank my advisor Leslie Poole for all her help and guidance during my studies as a graduate student and for fostering an environment of scientific growth and critical thinking. I am grateful to Derek Parsonage for imparting his expertise on a wide array of methods from protein purifications to stopped flow spectroscopy. I am especially grateful to my former and current labmates Chananat Beveridge, Laura Soito, Thomas Jonsson, Verena Wenzl, Erika Bechtold, and Amanda Day for the advice and counsel on various issues and topics. Special thanks goes to Kim Nelson for serving as a “second” mentor to me and for the many hours spent reviewing and editing this thesis.

TABLE OF CONTENTS

LIST OF ABBREVIATIONS

AhpC	alkyl hydroperoxide reductase C component
AhpF	alkyl hydroperoxide reductase F component, the specialized flavoprotein disulfide reductase for AhpC
AU	analytic ultracentrifugation
BCP	bacterioferritin comigratory protein
CHP	cumene hydroperoxide
C_p	peroxidatic cysteine (C45 of *E. coli* BCP)
C_r	resolving cysteine (C50 of *E. coli* BCP)
Cys(O)	2-electron oxidized form of cysteine, with a sulfenic acid (SOH) in place of a sulfhydryl group (SH)
DNA	deoxyribonucleic acid
DTNB	5,5'-dithiobis(2-nitrobenzoic acid)
DTPA	diethylenetriamine pentaacetic acid
DTT	1,4-dithiothreitol
EcBCP	*Escherichia coli* bacterioferritin comigratory protein
EDTA	ethylenediamine tetraacetic acid
Gpx	glutathione peroxidase
GR	glutathione reductase
Grx	glutaredoxin
$Grx1_{F6W}$	F6W mutant of Grx1
GSH	reduced glutathione
GSSG	oxidized glutathione,

GST	glutathione-S-transferase
GuHCl	guanidine hydrochloride
FAD	flavin adenine dinucleotide
FOX	peroxide detection assay that involves oxidation of Fe(II) and complex formation with xylenol orange
H_2O_2	hydrogen peroxide
HED	hydroxyethyldisulfide
HRP	horseradish peroxidase
IPTG	isopropyl-1-thio-β-D-galactopyranoside
MS	mass spectrometry
NEM	N-ethylmaleimide
NTD	N-terminal domain of *S. typhimurium* AhpF
PAGE	Polyacrylamide gel electrophoresis
PDI	protein disulfide isomerase
Prx	peroxiredoxin
ROS	reactive oxygen species
R-SOH	sulfenic acid
R-SO_2H	sulfinic acid
SOD	superoxide dismutase
SDS	sodium dodecyl sulfate
tBHP	*t*-butyl hydroperoxide
Tpx	thiol peroxidase
Trx	thioredoxin
TrxR	thioredoxin reductase

LIST OF ILLUSTRATIONS

ABSTRACT

In *Escherichia coli*, bacterioferritin-comigratory protein (*Ec*BCP) by definition is a peroxiredoxin (Prx) which catalyzes the reduction of hydrogen peroxide and organic hydroperoxides. EcBCP is a member of the most poorly characterized and least studied Prx subfamily. The experiments and data presented in this thesis were undertaken to elucidate the biochemical features of this poorly characterized Prx found in *E. coli*. EcBCP is one of 3 Prxs utilized by E. coli as defenders against oxidative stress. Contradicting studies claim that EcBCP is capable of efficiently scavenging peroxides by two different peroxiredoxin mechanisms, 1-Cys and atypical 2-Cys. However, EcBCP may be capable of utilizing either mechanism when needed. Our investigations using analytical ultracentrifugation approaches demonstrated that both oxidized and reduced BCP behaved as monomers in solution at concentrations as high as 200 μM, thus eliminating the possibility of intermolecular disulfide bond formation and typical 2-Cys mechanisms. In fact, mutational studies of the resolving cysteine revealed a 1-Cys peroxidase mechanism was possible. During thioredoxin-dependent peroxidase activity studies conducted by stopped flow spectroscopy, an increase in $V_{max,app}$ was observed with increasing reducing substrate concentrations, indicating a nonsaturable interaction with the reductant. At physiologically reasonable thioredoxin 1 (Trx1) concentration of 10 μM, the $K_{m,app}$ value for H_2O_2 is ~80 μM, and overall V_{max}/K_m for H_2O_2, which remains constant over the various Trx1 concentrations, is about 1.3×10^4 M^{-1} s^{-1}. Our kinetic analyses demonstrated the ability of BCP to utilize different reducing substrates,

including Trx1, thioredoxin 2 (Trx2), glutaredoxin 1 (Grx1) and glutaredoxin 3 (Grx3). EcBCP exhibited an unexpectedly high redox potential of – 145.9 ± 3.2 mV, the highest recorded value for a Prx. The unusually high redox potential increases the versatility of EcBCP by broadening its pool of reductants. Moreover, this protein exhibited a broad specificity for peroxides, with comparable rates for H_2O_2 and cumene hydroperoxide. We have now shown that BCP is a stable enzyme exhibiting broad specificity for reductants and peroxide substrates, potentially allowing BCP to remain fully active and functional under varying cellular conditions. Additionally, spectroscopic and activity titration studies showed that the pK_a of peroxidatic cysteine (Cys46) was ~5.8, which is common among Prxs. The combination of these biochemical features and its ability to remain active highlights its cellular importance and suggests that *Ec*BCP functions as a Prx stop-gap protein during times of increased oxidative stress.

Chapter 1: Introduction

The first prokaryotes lived in an environment devoid of oxygen (Berkner & Marshall, 1965). Approximately 3.5 billions years ago marked the appearance of photosynthetic oxygen-producing cyanobacteria. The introduction of oxygen into the atmosphere served as a catalyst for the generation of reactive oxygen species (ROS) for many bacteria inhabiting the earth during the proterozoic time period (Cloud, 1972, Holland, 1972, Garrels, 1978, Holland, 2002). In order to counter the deleterious effects of ROS, bacteria developed and expressed a wide variety of antioxidants. This thesis investigates the biochemical features of an antioxidant found in *Escherichia coli*, a poorly characterized, widely expressed member of the peroxiredoxin (Prx) family known as Bacterioferritin comigratory protein (*Ec*BCP). For the purpose of this thesis future references to *E. coli* BCP will be presented as "*Ec*BCP".

ROS Species. The generation of oxygen-derived toxins occurs during cellular respiration, a process in which oxygen normally accepts 4 electrons and is directly converted to water. Oxygen contains two unpaired electrons in its outer shell; as a result, reactive byproducts are occasionally formed during respiration. These reactive byproducts, formed from the incomplete reduction of oxygen during metabolism, are called reactive oxygen species (ROS). Reactions between ROS and macromolecules are unavoidable due the oxygen rich environment in which many bacteria exist (Fridovich, 1978, McCord & Fridovich, 1978, Halliwell & Gutteridge, 1984, Bannister *et al.*, 1987, Farr & Kogoma, 1991). Internal sources of ROS include autoxidation of NADH dehydrogenase, succinate dehydrogenase, and D-lactate dehydrogenase, and glutathione reductase

interaction with NADH (Massey *et al.*, 1969, Imlay *et al.*, 1988, Powell & Jackson, 2003). External ROS stem from ultraviolet light, radiolysis of water, and immune host response (Eisenstark, 1989, Segal, 2005, Segal, 2006). Despite their deleterious effects, ROS can function in a variety of ways that are beneficial to bacteria and mammals; such as cell signaling, apoptosis, gene expression, phagocytosis, and redox cycling of xenobiotics (Cha *et al.*, 1995, Hancock *et al.*, 2001). The types of ROS responsible for oxidative stress include but are not limited to superoxide, hydrogen peroxide, and hydroxyl radicals (Table I).

The superoxide radical ($O_2^{-\cdot}$) is formed from the addition of an electron to O_2 (Haber & Weiss, 1934). The intracellular concentration of $O_2^{-\cdot}$ in wild type *E. coli* under aerobic growing conditions is approximately 10^{-9} to 10^{-10} M ,(Imlay & Fridovich, 1991a & b). Superoxide is moderately reactive and capable of diffusing before reacting with its cellular targets and extracellularly generated $O_2^{-\cdot}$ can utilize cellular anion channels to traverse membranes and react with cellular targets (Ross *et al.*, 1984). Bacterial enzymes are among the targets of $O_2^{-\cdot}$, especially enzymes involved in the biosynthesis of branched amino acids (Kuo & Fridovich, 1988, Haas & Goebel, 1992). $O_2^{-\cdot}$ can cause inactivation of various *E. coli* dehydratases containing [4Fe-4S] clusters, including aconitase, α,β-dihydroxyacid dehydratase, 6-phosphogluconate dehydratase, and fumarases A and B (Gardner & Fridovich, 1991, Gardner & Fridovich, 1991, Flint *et al.*, 1993, Liochev & Fridovich, 1993). Superoxide can become protonated to form $HO_2^{\cdot}$, under low pH conditions, e.g. at inflammation sites. $HO_2^{\cdot}$ possesses a higher permeability due to its neutral charge and often reacts spontaneously with itself

Table 1-I: Various Reactions with Reactive Oxygen Species (Miller & Britigan 1997)

Reaction	Formula
Haber-Weiss reaction (Fenton chemistry)	$O_2^- + Fe^{3+} \rightarrow O_2 + Fe^{2+}$
	$H_2O_2 + Fe^{2+} \rightarrow {}^{\bullet}OH + OH^- + Fe^{3+}$
	$O_2^- + H_2O_2 \rightarrow {}^{\bullet}OH + OH^- + O_2$
Nitric oxide synthase	L-Arginine $\rightarrow$ L-citrulline + $NO^{\bullet}$
Peroxynitrite formation/ decomposition	$NO^{\bullet} + O_2^- \rightarrow ONOO^-$
	$ONOO^- + H^+ \rightarrow ONOOH$
	$ONOOH \rightarrow {}^{\bullet}OH + NO^{\bullet}$
Catalase	$2H_2O_2 \rightarrow 2H_2O + O_2$
SOD	$2O_2^- + 2H^+ \rightarrow H_2O_2 + O_2$
GSH	$2GSH + H_2O_2 \rightarrow G\text{-}S\text{-}S\text{-}G + 2H_2O$
GSH Reductase	$G\text{-}S\text{-}S\text{-}G + 2NADPH \rightarrow 2GSH + 2NADP$

to form hydrogen peroxide and oxygen. In the presence of the proper iron catalysts, $O_2^{-\cdot}$ is capable of producing additional toxic ROS via the Haber-Weiss reaction pathway; e.g., hydrogen peroxide and hydroxyl radical (Table I) (Haber & Weiss, 1934).

Hydrogen peroxide (H_2O_2) can be formed from the divalent reduction of $O_2^{-\cdot}$ during Haber-Weiss reactions (Haber *et al* 1934). Hydrogen peroxide is

highly cell permeable and is responsible for oxidation of enzymes and cellular membranes, inhibition of the membrane transport processes, and DNA damage and mutagenesis (Weiss, 1986). Additionally, it is capable of killing *E. coli* as a result of DNA damage in two different ways involving low (1 to 3 mM) and high (>20 mM) concentrations of H_2O_2. In fact, these levels are more lethal than intermediate concentrations (Imlay & Linn, 1988). These low levels of H_2O_2 cause DNA damage by reacting with Fe^{2+}, the second step in the Haber-Weiss reaction, to form intermediate ferryl radicals (Imlay *et al.*, 1988). In response, *E. coli* attempts to combat this exposure by boosting/bolstering recombinational DNA repair mechanisms thus increasing resistance to future H_2O_2 exposure (Imlay & Linn, 1987). The acute H_2O_2 response pathway inhibits other cellular targets in lieu of DNA and does not require an iron electron donor (Hassett, 1989).

The hydroxyl radical ($OH^{\cdot}$) is a more potent oxidizer than the previous two species and is sometimes the unassuming/undetected culprit in $O_2^{-\cdot}$ mediated cellular damage. Hydroxyl radicals are generated in the metal catalyzed interaction of $O_2^{-\cdot}$ and H_2O_2, known as the Haber Weiss reaction (Haber & Weiss, 1934). Superoxide induced oxidation is further exacerbated by hydroxyl radicals, which are capable of oxidizing many biomolecules including, DNA, proteins, and lipids. The diffusion and permeability of $OH^{\cdot}$ is limited due to its high reactivity. In fact, its high reactivity is what allows it to be a potent oxidizer despite its limited diffusion capabilities. Therefore, in order to be effective, $OH^{\cdot}$ must be generated near its cellular targets (Czapski, 1984).

Nitric oxide ($NO^{\cdot}$) is a water soluble free radical gas formed during the conversion of L-Arginine to L-Citrulline by nitric oxide synthase. It is both cytotoxic and cytostatic for prokaryotic (and eukaryotic) cells (Moncada & Higgs, 1993, Moncada & Martin, 1993, Freeman, 1994). Nitric oxide is not a ROS, it is classified as a reactive nitrogen species (RNS); nevertheless, it is capable of potentiating ROS oxidative effects in the cell. By itself, nitric oxide causes damage by interacting with iron-containing moieties in respiratory cycle enzymes and by interfering with DNA synthesis resulting in mutagenesis. Nitric oxide forms nitrosothiol groups on proteins causing inactivation and changes in protein function (Rockett *et al.*, 1991, Moncada & Higgs, 1993). Nitric oxide is capable of reacting with secondary amines to form alkylating agents. For example, peroxynitrite ($ONOO^{-}$) is generated by the interaction of $O_2^{-\cdot}$ with $NO^{\cdot}$ (Table I) and it is responsible for oxidizing DNA bases and sulfhydryl groups, reacting with metals or metalloproteins, and catalyzing iron-dependent membrane lipid peroxidation (Beckman *et al.*, 1990, Stark & Jackson, 1990, Radi *et al.*, 1991, Radi *et al.*, 1991, Hogg *et al.*, 1992, Imlay & Fridovich, 1992). During nitrosative stress investigations by microarray analysis, researchers exposed *E. coli* to $NO^{\cdot}$ under varying growth conditions and observed a universal increase in expression in 3 separate *E. coli* genes (Mukhopadhyay *et al.*, 2004, Flatley *et al.*, 2005, Justino *et al.*, 2005). Increases in gene expression are in part responsible for minimizing toxic effects of $NO^{\cdot}$ exposure in *E. coli* cells. However, the combination of $NO^{\cdot}$ and H_2O_2 increased (up to 1000-fold) the H_2O_2-mediated killing of cells/cytotoxicity. Nitric oxide was also shown to reduce the cellular

concentration of the antioxidant glutathione by 80-85% in *E. coli* (Pacelli *et al.*, 1995).

Antioxidants. In spite of the deleterious effects caused by ROS, organisms have proven themselves to be resilient and resourceful in dealing with the byproducts of oxygen metabolism. One of the ways in which bacteria defend themselves is through the expression of antioxidants enzymes, such as superoxide dismutase (SOD), catalase, glutathione (GSH), glutathione peroxidase (Gpx), and peroxiredoxins (Prx) (Table II).

Superoxide dismutase (SOD) was discovered in 1969, opening the door to investigations in free radical biology and oxidative stress defense (McCord & Fridovich, 1969, McCord & Fridovich, 1969). *E. coli* possesses 3 types of SODs: CuZnSOD, FeSOD, and MnSOD (Keele *et al.*, 1970, Yost & Fridovich, 1973). SODs are responsible for the dismutation of superoxide into oxygen and hydrogen peroxide (McCord & Fridovich, 1969). SOD is capable of reducing the concentration of $O_2^{-\cdot}$ by as much as 3 orders of magnitude (Imlay and Fridovich 1991). FeSOD is encoded by *sodB* and is mainly found in prokaryotes, while MnSOD is encoded by *sodA* and exists in both prokaryotes and eukaryotes (Greenberg *et al.*, 1990, Niederhoffer *et al.*, 1990). In *E. coli*, the combined concentration of SOD is approximately 10^{-5} M (Fridovich, 1983, Fridovich, 1983). As previously stated, H_2O_2 is produced as a result of the dismutation of $O_2^{-\cdot}$, which begs the question whether $O_2^{-\cdot}$ is more toxic than H_2O_2. Moreover, *E. coli* compensates for this by expressing other antioxidants capable of H_2O_2 removal, e.g. catalase.

Table 1-II: Antioxidant Proteins in the *Escherichia coli* Genone

Protein family	**Function**	**Present in *E.coli***
Peroxiredoxin	Reduces hydroperoxides (broad specificity)	1 AhpC group 1 Tpx group 1 BCP group
AhpF	Disulfide reductase (AhpC-specific)	1
Thioredoxin	Disulfide reductase (general)	2
TrxR	Thioredoxin reductase	1
Catalase	Peroxide scavenger (H_2O_2 specific)	2
Glutathione peroxidase	Reduces hydroperoxides (broad specificity)	No
BtuE	Bacterial Gpx homologue	1
Superoxide dismutase	Converts superoxide to H_2O_2 and O_2	3
Glutaredoxin	Removes glutathione from proteins	4
Glutathione reductase	Recycles oxidized glutathione	1
γ-Glutamatecysteine ligase	Biosynthesis protein for glutathione	1

The catalases in *E. coli*, HPI catalase (encoded by *katG*) and HPII catalase (encoded by *katE* and regulated by *katF*), remove H_2O_2 by converting it into H_2O and O_2 (Loewen, 1984, Loewen & Triggs, 1984, Loewen *et al.*, 1985, Triggs-Raine & Loewen, 1987, Storz *et al.*, 1990). HPI and HPII are differentially localized to the periplasm and cytoplasm, respectively (Heimberger & Eisenstark, 1988). The reaction is exothermic, requiring only the presence of H_2O_2 for activation. Therefore, the lack of requirement for a reducing source or ATP for energy activation makes catalase a powerful defender against H_2O_2. Studies by Hillar *et al* revealed a k_{cat}/K_m of 9×10^5 M^{-1} s^{-1} for catalase, but suggest that it is most protective against H_2O_2 concentrations equal to or greater than 5 μM where

it demonstrated the ability to degrade high concentrations of H_2O_2 at a rate of 10^7 M^{-1} s^{-1} (Hillar *et al.*, 2000, Seaver & Imlay, 2001).

On the opposite end of the discovery spectrum is glutathione. The tripeptide glutathione is synthesized by glutathione synthetase and capable of performing several cellular tasks in addition to functioning as a peroxidase (Hopkins, 1921, Kosower & Kosower, 1969, Holmgren, 1976, Meister, 1982, Meister, 1983, Meister, 1991). *E. coli* maintains high basal levels of GSH and concentrations can exceed 10 mM, thus ensuring a reducing environment in the cell (Fahey *et al.*, 1978, Loewen, 1979, Ferguson *et al.*, 1995). In its role as a peroxidase, GSH dimerizes upon reacting with H_2O_2, $O_2^{-\cdot}$, and hydroperoxides (ROOH) forming oxidized glutathione (GSSG) which then requires glutathione reductase to shuttle electrons from NADPH in order to return to its active form, i.e. GSH (Meister & Anderson, 1983, Cotgreave & Gerdes, 1998, Halliwell, 2007). Additionally, a synergistic role of GSH is its ability to reduce the disulfide bonds of peroxidase reducing factors, like glutaredoxin (Grx), caused by oxidative stress; in limited cases it can reduce peroxiredoxins as well (Holmgren, 1979, Russel *et al.*, 1990, Clarke *et al.*, 2010).

Peroxidases. Peroxidases, unlike catalase, require NADPH or NADH as an electron source for reduction (Hofmann *et al.*, 2002, Imai & Nakagawa, 2003, Wood *et al.*, 2003, Poole *et al.*, 2004, Arenas *et al.*, 2010). Unfortunately, the requirement for reducing factors serves as limiters for the potential effectiveness of peroxidases. Research has also shown that peroxidases often exhibit versatility through their broad specificity, reacting with a variety of ROS

(Ferguson & Booth, 1998, Wood *et al.*, 2003). *E. coli* utilizes peroxidases against oxidative stress, including the small molecule glutathione (GSH), as well as enzymes like peroxiredoxins (Prx) and a glutathione peroxidase (Gpx) homolog, BtuE. For years, scientist believed *E. coli* didn't possess Gpx family members due to the lack of GSH-dependent peroxidase activity; this changed when a recent study revealed the presence of BtuE, a Gpx homologue that is capable of decomposing H_2O_2, alkyl and lipid hydroperoxides (Arenas *et al.*, 2010, Arenas *et al.*, 2011). Research surrounding the newly discovered BtuE is in the early stages; therefore, its role and impact as a defender against peroxides require further investigation.

Peroxiredoxins. Peroxiredoxins (Prx) are almost ubiquitous in bacteria and mammals and are responsible for a wide range of cellular functions: proliferation, differentiation, immune response, and detoxification of peroxides (Kang *et al.*, 2005, Veal *et al.*, 2007, Poole & Nelson, 2008, Winterbourn & Hampton, 2008). These thiol-specific peroxidases and peroxynitrite reductases have an activated cysteine rather than a selenocysteine, as in the case of many glutathione peroxidases, and possess broad specificity for peroxides, such as H_2O_2, alkyl and organic hydroperoxides, and peroxynitrite (Lee *et al.*, 1999, Park *et al.*, 2000, Seaver & Imlay, 2001, Hofmann *et al.*, 2002, Comtois, 2003, Wood *et al.*, 2003, Cha, 2004, Poole *et al.*, 2004). Peroxiredoxins are among the most abundant classes of proteins in *E. coli* and typically comprise ~0.1 to 1% of the total cellular proteins in mammalian cells (Chae *et al.*, 1994, Link *et al.*, 1997, Hofmann *et al.*, 2002). Prxs range in size from 17 to 29 kDa and can exist as

homodimers or higher multimers of monomers (Chae *et al.*, 1999, Wood *et al.*, 2002, Choi *et al.*, 2005, Sarma *et al.*, 2005). In eukaryotes, the importance of Prxs in oxidative stress defense by H_2O_2 is underscored by their ability to reduce ~90% of mitochondrial H_2O_2 and practically 100% of cytoplasmic H_2O_2 (Winterbourn & Hampton, 2008, Cox *et al.*, 2010).

Peroxiredoxin Mechanisms. Peroxiredoxins possess a thioredoxin fold and PxxxTxxC active site motif centered around a cysteine that reacts with peroxide (called the "peroxidatic" cysteine) to form a cysteine sulfenic acid (Cys-SOH) and may subsequently form a disulfide bonds with the "resolving cysteine", either inter or intramolecular. Mutations of the peroxidatic cysteine (C_P) of peroxiredoxins result in a complete loss of activity. However, mutating the resolving cysteine (C_R) of various Prxs often still allows for the reduction of sulfenic acid; albeit, the reduction reaction experiences decreased activity (Ellis & Poole, 1997, Jeong *et al.*, 2000, Rouhier, 2002, Baker, 2003, Rouhier, 2004, Trujillo, 2006).

Three peroxidase mechanisms can be used to describe catalysis by Prxs; 1-Cys, typical 2-Cys, and atypical 2-Cys mechanisms (Figure 1-1). This mechanistic classification was introduced by Wood *et al* (2003), where 1-Cys enzymes generate cysteine sulfenic acid, Cys-SOH, in the oxidized form, typical 2-Cys Prxs generate an intersubunit disulfide, and atypical 2-Cys Prxs form an intrasubunit disulfide. Typical 2-Cys Prxs make up the largest class, containing bacterial AhpC, mammalian proteins PrxI-IV, and tryparedoxin peroxidase of trypanasomatids. Atypical 2-Cys Prxs are expressed in archae, bacteria,

mammals (PrxV), lower fungi and higher plants (PrxQ) (Hofmann *et al.*, 2002). Similarities exist across the classes in the form of a universal active site structure and a hydroperoxide-reducing mechanism based on the formation of sulfenic acid at the active site cysteine. However, the classes differ in the intermediates involved in recycling of the sulfenic acid to regenerate the active dithiol form of the Prx (Wood *et al.*, 2003, Poole, 2007).

The first universal phase of Prx-mediated catalysis is the production of sulfenic acid at the C_P. The C_P is located in the first turn of the α2 helix (Hall *et al.*, 2010) and is positioned at the base of the active pocket making it inaccessible to the resolving cysteine in the fully-folded form (Figure 1-2). It requires several residues working in conjunction in order to become active. These residues help lower the pK_a, promoting nucleophilic attack on the hydroperoxide substrate by the stabilized thiolate. Four absolutely conserved residues appear in the active site complex of Prxs: proline, threonine, arginine, and the catalytic cysteine. Mutational studies of some of these residues were conducted to determine their function and kinetic contributions, if any. During studies of Prxs in *Leishmania donovani*, *Crithidia fasciculata*, and barley; resolving cysteine mutants showed a 50% decrease in enzyme activity using a thioredoxin (Trx)-dependent assay, although an increase in activity was noted when dithiothreitol (DTT) was used as the reductant (Montemartini *et al.*, 1999, Flohe, 2002, Konig *et al.*, 2003). Of the four residues; Cys, Thr, and Pro are located within a PxxxTxxC active site motif, with the Thr and the distant (in sequence) Arg facilitating activation of the C_P (Figure 1-2).

A. 1-Cys Prxs

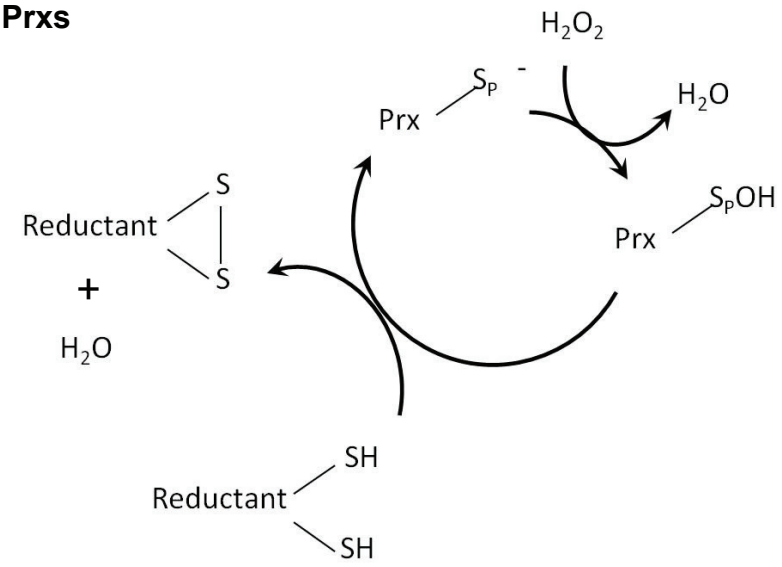

B. Typical 2-Cys Prxs

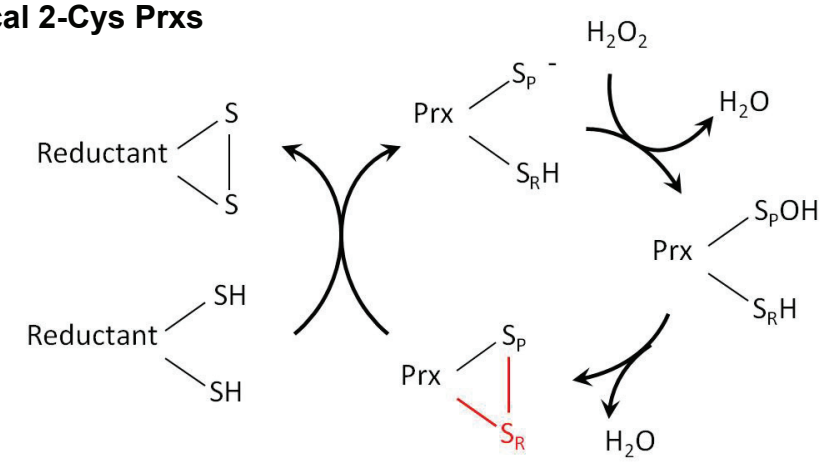

C. Atypical 2-Cys Prxs

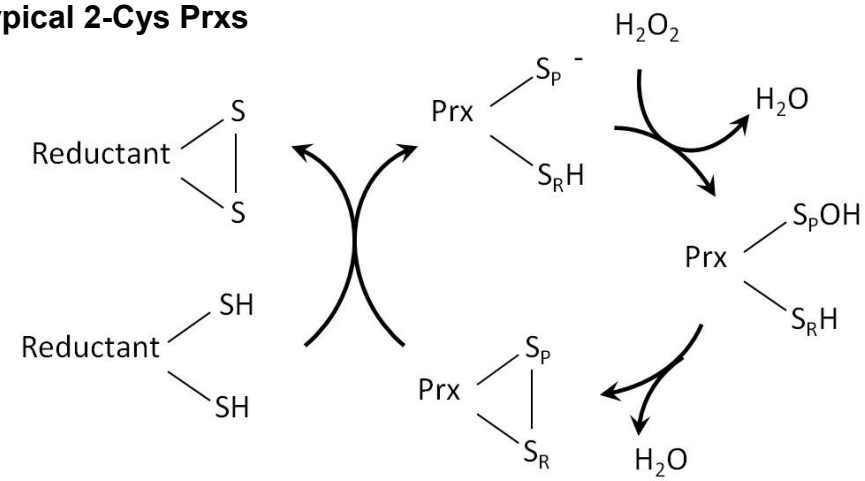

Figure 1-1. 1-Cys (A), typical 2-Cys (B), and atypical 2-Cys (C) peroxiredoxin mechanisms. The first phase of Prx-mediated catalysis is the production of sulfenic acid at the peroxidatic cysteine. (A) After sulfenic acid formation, 1-Cys Prxs are reduced by reducing substrates and cycled back to their active form. (B) In typical 2-Cys Prxs, sulfenic acid is resolved with the formation of a disulfide bond between the peroxidatic and resolving cysteine where the red S_R represents a resolving cysteine on another subunit, forming an inter-subunit disulfide bond. Typical 2-Cys Prxs function as dimers. (C) In atypical 2-Cys Prxs, the resolving cysteine comes from the same subunit.

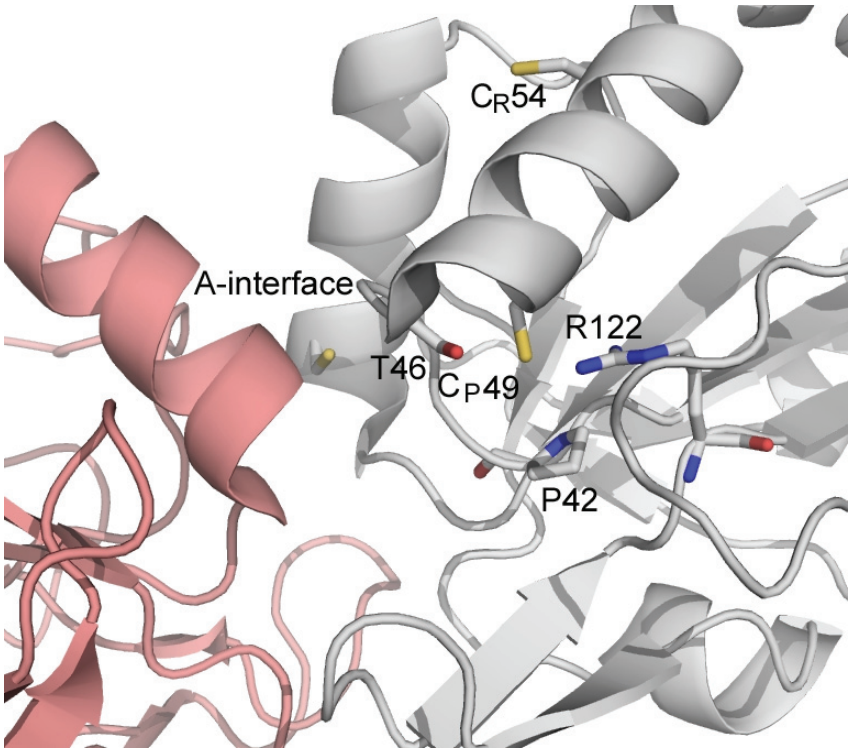
C_R54
A-interface
R122
T46
C_P49
P42

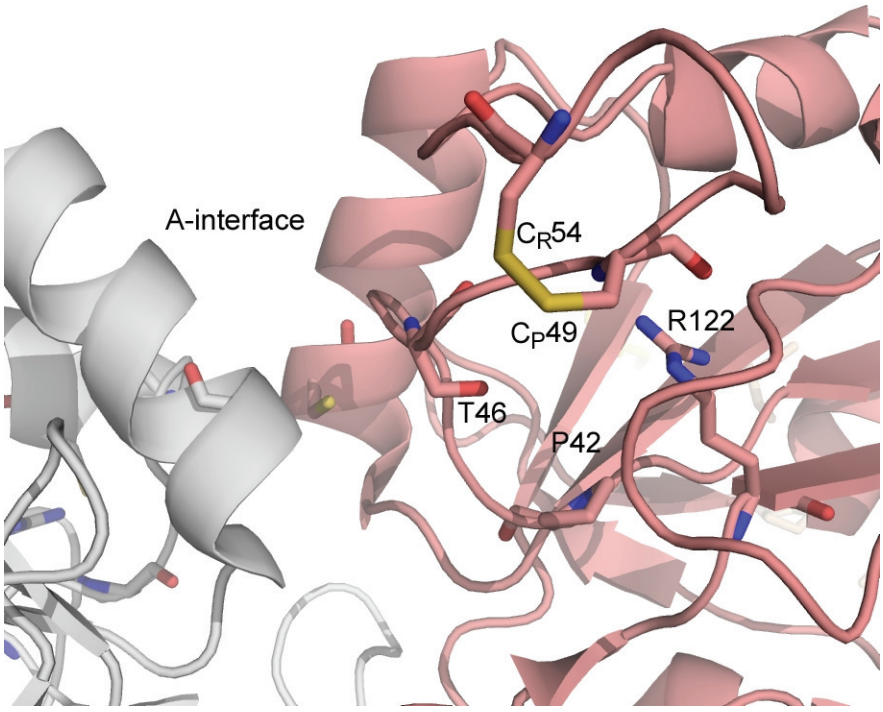
A-interface
C_R54
C_P49
R122
T46
P42

Figure 1-2. Location of residues conserved across all Prx subfamilies. The structure of *Aeropyrum pernix* BCP (PDB identifier 2CX4) is shown in the A-interface (discussed later) with the highly conserved active site residues (Pro42, Thr46, Cys49, and Arg122) highlighted. The C_R (Cys54) in *A. pernix* BCP is located in the same helix as the C_P (C49) in a C_PXXXXC_R motif. Monomer A, shown in gray, is in the fully folded, reduced structure and monomer B, shown in pink, is in the locally unfolded, disulfide bonded conformation. This figure was made using Pymol (http://sourceforge.net/projects/pymol/).

A local unfolding of the active site loop-helix region is necessary during the first phase of catalysis. During unfolding, a C_P-loop is formed housing the C_P residue from the partially unraveled α2 helix (Wood *et al.*, 2003). Local conformational changes in atypical 2-Cys Prxs involve either helix-to-loop or loop-to-helix unfolding (Choi, 2003). This unfolding is a universal Prx attribute. In the absence of disulfide bond formation, a second equivalent of peroxide substrate can oxidize the sulfenic acid to its sulfinic acid form (SO_2H), inactivating the enzyme. The hydroxyl group of Thr forms a hydrogen bond with the free thiol(ate) of C_P. This bond makes the thiol susceptible to proton abstraction by an active site base. The activated S^- is then able to attack and ultimately reduce its hydroperoxide substrate; the cysteine attacks the -O-O- bond of its peroxide (ROOH) substrate creating sulfenic acid (Cys-SOH) on the Prx and the reduced ROH product.

After sulfenic acid formation, 1-Cys Prxs are reduced by external thiols and thus cycled back to their active form. However, in typical and atypical 2-Cys Prxs, sulfenic acids are resolved with the formation of a disulfide bond between C_P and C_R. The C_R of typical 2-Cys Prxs resides on a second subunit, thus forming intersubunit disulfide bonds. Atypical 2-Cys Prxs, in contrast, generally form intrasubunit disulfide bonds between C_P and C_R. Choi *et al* (2003) further classified atypical 2-Cys Prxs based specifically on the "location" of the resolving cysteine. The atypical 2-Cys resolving cysteine is capable of residing in 1 of 4 places within the protein (α2, α3, α5, and the C-terminal tail) (Choi, 2003, Copley *et al.*, 2004, Hall *et al.*, 2011). It is important to note that each of these regions

are capable of undergoing a conformational change, causing some scientists to propose that resolving cysteines evolved independently and may potentially reside in any region possessing the ability to locally unfold (Copley *et al.*, 2004, Hall *et al.*, 2010). After disulfide formation occurs in the oxidized Prx, it must be reduced by combined action of a flavoprotein disulfide reductase and a dithiol protein containing a CXXC active site motif (Poole & Ellis, 1996, Poole *et al.*, 2000, Dietz, 2003). The reductant uses a thiol(ate) to form a mixed disulfide bond with the Prx, after which the mixed disulfide bond is resolved by the second Cys in the CXXC active site of the reductant, *e.g.* Trx. The freshly reduced Prx is capable of completing another round of peroxide removal, while the reductant must ultimately be regenerated by NADH or NADPH through action of the flavin-containing disulfide reductase. The ability of the active site cysteines of Prxs to reversibly form disulfide bonds with the proper reductants allows these proteins to play a role in disulfide exchange reactions and help demonstrate the versatility of the peroxidase mechanisms utilized by the peroxiredoxins.

Peroxiredoxin Structure and Subfamilies. Since Human PrxVI was crystalized in 1998, 73 additional Prx structures have been deposited in the Protein Data Bank (PDB) spanning all six Prx subfamilies: Prx1/AhpC, Prx5, Prx6, Tpx, AhpE, and BCP/PrxQ (Choi *et al.*, 1998, Declercq *et al.*, 2001, Wood *et al.*, 2003, Sarma *et al.*, 2005, Clarke *et al.*, 2009, Hall *et al.*, 2009, Horta *et al.*, 2010). Prxs are structurally similar with variations in loop lengths, oligomeric conformations, and N- and C-terminal conformations; hence structures are able to serve as blueprints for other similar Prxs for which no structure has been

determined. The scientific community received its first look at the crystal structure of a Prx in 1998 (Choi *et al.*, 1998). Structurally, all peroxiredoxins possess a core of 7 β-strands and 5 α-helices and a universal Trx fold. The Trx fold present in Prxs consist of a four-stranded β-sheet and three flanking α-helices (Martin, 1995). Proteins with Trx-like folds exhibit reactivity differences based on relatively tiny variations in their overall fold and respective active sites (Pan & Bardwell, 2006).

Prxs exist in a variety of documented quaternary structures, such as monomers, dimers, octamers, decamers, and dodecamers (Kim *et al.*, 2003, Guimaraes *et al.*, 2005, Li *et al.*, 2005, Clarke *et al.*, 2010). In non-monomeric Prxs, homodimerization and multimerization are the result of 2 types of interfaces (A-type and B-type) occuring between different subunits. The A-type (or "ancestral") interface is widespread among bacterial Prxs and forms as the result of a tip-to-tip association with α3 helices from both subunits (Fig 1-2); while the B-type (or "beta-sheet") interface occurs as result of beta strand association, forming an extended beta-sheet (Choi *et al.*, 1998, Wood *et al.*, 2002, Choi, 2003, Sarma *et al.*, 2005, Echalier *et al.*, 2008). Octameric, decameric, and dodecameric Prxs; found in the Prx1/AhpC and Prx6 subfamilies, form dimers via B-type interfaces and higher ordered structures through A-type interfaces (Hall *et al.*, 2010). These structures can be affected or disrupted in some instances by disulfide bond formation, pH, and ionic strength (Schroder & Ponting, 1998, Kitano *et al.*, 1999, Kristensen *et al.*, 1999, Schroder *et al.*, 2000, Chauhan & Mande, 2001, Wood *et al.*, 2002, Guimaraes *et al.*, 2005, Papinutto *et al.*, 2005).

The original nomenclature for Prx classification was mechanism based which led to confusion because multiple mechanisms can be used by members of each of the subfamilies. Hence, a more comprehensive and coherent classification system has been developed that segregates Prxs into 6 subfamilies (Prx1/AhpC, Prx6, Prx5, Tpx, BCP/PrxQ, and AhpE) based on sequence and structural similarities (Table III; (Hall *et al.*, 2010, Nelson *et al.*, 2011).

The Prx1/AhpC subfamily, also known as group "A" or "typical 2-Cys", (Hofmann *et al.*, 2002, Trivelli *et al.*, 2003) are found in archaea, bacteria, and eukaryotes, and include yeast TSA proteins, plant Prxs, tryparedoxin peroxidases, AhpC, and human Prx I – IV. To date, there are 22 known structures in databases from 13 different Prxs. The Prx1/AhpC subfamily is comprised of 2-Cys Prxs (~96%) in B-type dimers, with most forming A-type interface decamers. The resolving cysteine is located in the C-terminal extension of members of this subfamily.

The Prx5 subfamily, also known as group "D", is named after human Prx5 (HsPrxV) (Declercq *et al.*, 2001). Prx5 proteins are found in bacteria, fungi, mammals, and higher plants (Hofmann *et al.*, 2002). Members of the Prx5 subfamily utilize both 1-Cys (most prevalent) and 2-Cys mechanisms (Copley *et al.*, 2004, Nelson *et al.*, 2011). Members of this subfamily form A-type dimers and only 17% are 2-Cys proteins with the C_R in the α5 helix. Unique features of this subfamily include some members which have fused Grx and Prx

Table 1-III: Summary of Prx Subfamilies

Subfamily	**Canonical subfamily members**	**Phylogenetic Distribution**	**Typical Location of C_R When Present** [a]
Prx1/AhpC	*Salmonella typhimurium* AhpC, *Homo sapiens* Prx1 through Prx4	Archae, Bacteria, Plants, Unicellular & Multicellular Eukaryotes	C-terminus' (>96%)[b]
BCP/PrxQ	*Escherichia coli* bacterioferritin comigratory protein, plant PrxQ	Bacteria, Plants	Helix α2 (~50%) or α3 (~7%) [c]
Prx5	*H. sapiens* Prx5 *Populus trichocarpa* PrxD plant type II Prxs, bacterial glutaredoxin-Prx5 fusion proteins	Bacteria, Eukaryotes	Helix α5 (~17%) [c]
Prx6	*H. sapiens* Prx6 *A. thaliana* 1-Cys Prx	Archae, Bacteria, Plants, Unicellular & Multicellular Eukaryotes	No C_R [a]
Tpx	*E. coli* Tpx *Helicobacter pylori* scavengase p20	Bacteria	Helix α3 (>96%) [c]
AhpE	*Mycobacterium tuberculosis* AhpE	Bacteria	Unknown [d]

[a] If no C_R is present, resolving thiol must come from another protein or small molecule.

[b] Near the C-terminus of the partner subunit within the homodimer; upon oxidation, intersubunit disulfide forms between the C_P and the C_R of the two chains.

[c] Intrasubunit disulfide formed in oxidized protein (so-called "atypical" 2-Cys Prxs).

[d] Canonical member contains no C_R, but >50% of sequences include a potential C_R in α2, like *E. coli* BCP.

domains (~16% of all Prx5 proteins, all bacterial). Interestingly, the members lacking the Grx fusion utilize Trx as a preferred reductant. The 12 known structures from this subfamily represent 5 different Prxs.

The Prx6 subfamily, also known as group “B”, can be found in archaea, bacteria, and eukaryotes. There are 15 known structures from 4 different Prxs. They are almost all 1-Cys (~98%) with B-type dimers and in some cases A-type interface-containing decamers. The Prx6 subfamily shares some sequence conservation with the Prx1/AhpC subfamily and they also share in common an extended C-terminal extension that is even longer in the Prx6 subfamily (50 – 80 residues) than the Prx1/AhpC subfamily (15 – 40 residues). By some criteria, they have been classified as members of the same subfamily (Copley *et al.*, 2004). The rare 2-Cys members (~2%) of this subfamily possess a potential resolving cysteine in the C-terminal extension (Deponte & Becker, 2005, Nelson *et al.*, 2011).

Members of the Tpx subfamily, also known as group “E” or p20, function through an atypical 2-Cys mechanism, with ~99% of subfamily members containing a C_R on the C-terminal turn of the α3 helix. Thus, essentially all Prxs found in the Tpx family are classified as atypical 2-Cys. Catalytic turnover of members of this subfamily requires local unfolding of the helices containing the peroxidatic cysteine and the resolving cysteine, α2 and α3, respectively (Hall *et al.*, 2009, Hall *et al.*, 2010). The 13 known structures of this subfamily represent 7 different Prxs. All structurally characterized Tpx members exist as A-type

dimers. This subfamily possesses a unique feature; it is an N-terminal β-hairpin that forms a hydrophobic collar around the active site pocket (Hall *et al.*, 2009).

The AhpE subfamily includes the fewest representatives, with only 25 members (Nelson *et al.*, 2011). They are found in mycobacterial and other closely related bacteria species. AhpE members react favorably with peroxynitrite (10^7 M^{-1} s^{-1} second order rate of reaction) as opposed to H_2O_2 (10^5 M^{-1} s^{-1}). Only 2 structures exist from this subfamily and both are from *Mycobacterium tuberculosis*. AhpE members are A-type dimers that share ~30% sequence identity with Prx1/AhpC members and ~25% identity with BCP/PrxQ subfamily members.

The sixth and final Prx subfamily, BCP/PrxQ (also known as group "C"), are largely bacterial (some archaeal), but some exist in lower eukaryotes like yeast and plants (Konig *et al.*, 2003, Nelson *et al.*, 2011). The lack of a universally conserved resolving cysteine resulted in the initial classification of BCP-like peroxiredoxins as either 1-Cys or 2-Cys (Chae *et al* 1994) with the C_R either lacking altogether, or located in one of two places, within a C_PXXXXC_R motif, or, in ~7% of members, within α3 (like Tpx) (Jeong *et al.*, 2000, Wakita *et al.*, 2007).

Presently, a search of the PDB database yields 9 crystal structures of BCP representing 6 organisms; *Sulfolobus tokodaii*, *Sulfolobus solfataricus*, *Xanthomonas campestris*, *Xylella fastidiosa*, *Aeropyrum pernix*, and *Saccharomyces cerevisiae* (Dot5p) *(D'Ambrosio et al., 2009, Liao et al., 2009, Horta et al., 2010, Limauro et al., 2010)*. Generally, members of the BCP family

were believed to exist as monomers, but the dimeric crystal structures of *A. pernix* BCP (2CX4) and *S. tokodaii* BCP (2ywn) have challenged this notion. It must be noted that these structures have not been published in peer reviewed journal articles, and the structure of *E. coli* BCP has not been determined. Although structural data exists for the BCP/PrxQ subfamily, there is much remaining to be elucidated by future structural information regarding active site pocket accessibility, local unfolding, and substrate docking interactions.

E. coli Peroxiredoxins. The oxidative stress defense system in *E. coli* includes 3 Prxs: AhpC, Tpx, and BCP. AhpC is reduced by AhpF in a NADH-AhpF linked reducing system (Poole, 1996, Poole *et al.*, 2000, Poole, 2005), but demonstrated limited capability utilizing Trx as a reductant (Poole 1996). *E. coli* knockout strains of the *ahp* genes resulted in increased sensitivity and cytotoxicity toward reactive oxygen species, *i.e.* cumene hydroperoxide (Storz *et al.*, 1989). Based on ROS sensitivity, a V_{max}/K_m in the range of 10^7 for H_2O_2, and a micromolar K_m for H_2O_2, (Seaver & Imlay, 2001) demonstrated AhpC to be the primary *E. coli* Prx responsible for the reduction of endogenously-generated hydrogen peroxide AhpC also reduces organic hydroperoxides (e.g., cumene and t-butyl hydroperoxides), and reactive nitrogen species; although it prefers H_2O_2 as a peroxide substrate (Jacobson *et al.*, 1989, Poole, 1996, Chen *et al.*, 1998, Bryk *et al.*, 2000, Seaver & Imlay, 2001, Parsonage *et al.*, 2008).

E. coli Tpx was once thought to be periplasmic until recent studies reported cytoplasmic localization of the enzyme (Jacobson *et al.*, 1989, Tao, 2008). *E. coli* Tpx reduced H_2O_2 in kinetic studies, but demonstrated higher

specificity for the bulkier, hydrophobic cumene hydroperoxide, with K_m values of 1.7 mM and 9 μM, respectively, for H_2O_2 and CHP (Baker, 2003). Tpx was not induced by oxidative stress, although researchers determined it to be critical for peroxide defense under anaerobic conditions (Cha *et al.*, 2004).

Escherichia coli BCP. If Tpx acts as an organic hydroperoxide peroxidase and AhpC efficiently removes low levels of H_2O_2 from the cytoplasm, what role does BCP play in oxidative stress defense (Poole *et al.*, 1997, Cha *et al.*, 2004)? We sought to understand the role of *Ec*BCP through elucidation of its mechanism, specificity, and any other contributions or protective role it may play.

The peroxiredoxin central to my research studies, *Ec*BCP, is among those responsible for catalyzing the reduction of hydrogen peroxide and alkyl hydroperoxides. Discovered in 1983, BCP receives its name from the protein bacterioferritin, because at the time of its discovery the unknown protein co-migrated with bacterioferritin in SDS/PAGE analysis (Neidhardt *et al.*, 1983). *Ec*BCP possesses 3 cysteine residues (Cys45, Cys50, Cys99) and only mutations of the absolutely conserved cysteine (Cys45) resulted in complete loss of thiol peroxidase activity (Jeong *et al.*, 2000), thus cementing *Ec*BCP as member of the Prx family (Chae *et al.*, 1994, Ellis & Poole, 1997, Chen, 2000, Flohe, 2002). It is comprised of 156 amino acids, has a mass of 18.11 kDa, and possesses a C_PXXXXC_R active site. The importance of BCP's presence in the cell can be seen in studies conducted on the pathogenic bacterium, *Helicobacter pylori*. In the *H. pylori* studies, the oxidative stress resistance and the host colonization ability of wild type and *bcp* knockout *H. pylori* strains was tested.

The study pointed to the significance of BCP in both colony survival and colony size within the host (Wang *et al.*, 2005).

Real Time-PCR was used to measure BCP gene expression under varying oxidative stresses in *Desulfovibrio vulgaris* Hildenborough, a ubiquitous gram-negative bacterium. BCP was upregulated following oxygen exposure (Fournier *et al.*, 2006). BCP null mutants in *D. vulgaris* also demonstrated hypersensitivity to oxidants, with sensitivity lessened by *bcp* gene expression, further supporting BCP's defensive role against peroxides and oxidative stress (Fournier *et al.*, 2006).

In peroxidase activity studies, BCP exhibited very low activity rates when assayed in a linked Trx system and demonstrated a 5-fold higher affinity for reducing linoleic acid hydroperoxide than for hydrogen peroxide or t-butyl hydroperoxide (Jeong *et al.*, 2000). The relatively low rate calls into question BCP's ability to act as a hydroperoxide scavenger. Kinetics and substrate specificity experiments are important because they provide insights into possible physiological roles and functions. The peroxidase mechanism of *Ec*BCP has been investigated by several different groups, utilizing (in our opinion) limited kinetic assays. Previous peroxidase assays used similar BCP and Trx concentrations (or substituted DTT for Trx) (Jeong *et al.*, 2000, Clarke *et al.*, 2009, Clarke *et al.*, 2010) and typically used a fixed amount of reductant and varying amounts of peroxide substrate. Under these conditions for *Ec*BCP, true V_{max} and K_m values cannot be obtained because BCP interacts with 2 substrates, a situation that requires a full bisubstrate kinetic analysis for proper evaluation.

In those previous assays, several peroxide substrates were investigated, with Trx serving as the electron donor to *Ec*BCP, during which K_m values of 47.8, 37.4, and 11.7 μM were observed for H_2O_2, t-butyl hydroperoxide (t-BHP), and linoleic acid hydroperoxide, respectively. The V_{max} values were 7.0, 1.93, and 8.23 min^{-1} for H_2O_2, t-butyl hydroperoxide (t-BHP), lipid hydroperoxide, respectively. These results yielded a V_{max}/K_m value of 2.45 x 10^3 M^{-1} s^{-1} with H_2O_2. Other kinetically characterized subfamily members, the PrxQ proteins from *Xylella fastidiosa* and *Populus tremula* x *Populus tremuloides* (poplar), exhibit values of around 10^4 M^{-1} s^{-1} (Rouhier, 2004, Horta *et al.*, 2010). The limiting conditions of previous assays along with greater reported V_{max}/K_m values from other subfamily members led us to believe that even higher activity levels were possible for *Ec*BCP under optimized conditions. While the multicomponent assay used above is technically straightforward and uses relatively small amounts of materials to determine what does and doesn't show activity, determination of the kinetic parameters (k_{cat} and K_m) of BCP is difficult or impossible with this approach.

Previous studies utilized SDS-PAGE analysis to investigate the oligomeric state of *Ec*BCP, although this method tests only for covalent linkage of subunits (Jeong *et al.*, 2000). Recently, high resolution mass spectometry was used to demonstrate the formation of two disulfide-bonded forms of *Ec*BCP, the expected form with an intrasubunit disulfide bond (from experiments with the wild type enzyme), and a dimeric species (perhaps artifactual) with an intersubunit disulfide bond (from experiments with C50S, lacking the C_R). Both forms were reportedly capable of being reduced by Trx after incubation of the proteins for

several minutes (Clarke *et al.*, 2009). The mass spectrometry results, as well as the appearance in the PDB of dimeric forms of BCP/PrxQ subfamily members, encouraged our use of analytical ultracentrifugation to accurately determine the molecular weight of reduced and oxidized *E. coli* BCP in solution.

Based on recent mass spectrometry results, Clarke and coworkers categorized *Ec*BCP as an atypical 2-Cys Prx. These studies also confirmed Cys45 as the C_P and Cys50 as the C_R using top-down fragmentation of the protein in the mass spectrometer to locate SO_2H and disulfide bonds within the protein (Clarke *et al.*, 2009). The main deficiency in the experiments performed to date with *Ec*BCP, however, is in the lack of information about the catalytic competence of each of the redox forms of *Ec*BCP. Past experience tells us that the presence and location of cysteine residues is simply not enough information to accurately classify peroxidase mechanisms in Prxs. For example, *Plasmodium falciparum* Antioxidant protein (AOP) was discovered to contain a second cysteine but to use a 1-Cys Prx mechanism (Sarma *et al.*, 2005). Other striking disparities between mechanistic properties of homologues thought in advance to be 1-Cys or 2-Cys Prxs have also been reported. In *Toxoplasma gondii*, a Prx6 subfamily protein named TgPrx2 exhibits a typical 2-Cys Prx mechanism by utilizing a cysteine (Cys209) that is apparently unique to TgPrx2 when compared to other homologous 1-Cys peroxiredoxins (Deponte & Becker, 2005). In the case of poplar PrxQ, the wild type is active in turnover with peroxides only in the presence of Trx; the C51S mutant (lacking C_R) remains

active with Trx, but also gains activity with Grx, suggesting that both 1-Cys and 2-Cys Prx mechanisms can be operative with this protein (Rouhier, 2004).

BCP Reducing Systems and Pathways. Trx is the physiological reductant for many cellular enzymes, including (but not limited to) ribonucleotide reductase I, PAPS reductase, methionine sulfoxide reductase, OxyR, and many Prxs (Holmgren, 1976, Krone *et al.*, 1990, Poole & Ellis, 1996, Aslund & Beckwith, 1999, Kim *et al.*, 2002, Baker, 2003, Comtois, 2003, Weissbach *et al.*, 2005, Gon & Beckwith, 2006). The Trx reducing system is comprised of a reduced pyridine nucleotide (NADPH), a flavoprotein disulfide reductase (TrxR), and a CXXC-containing Trx protein (Figure 1-3) (Poole *et al.*, 2000, Hofmann *et al.*, 2002, Wood *et al.*, 2003).

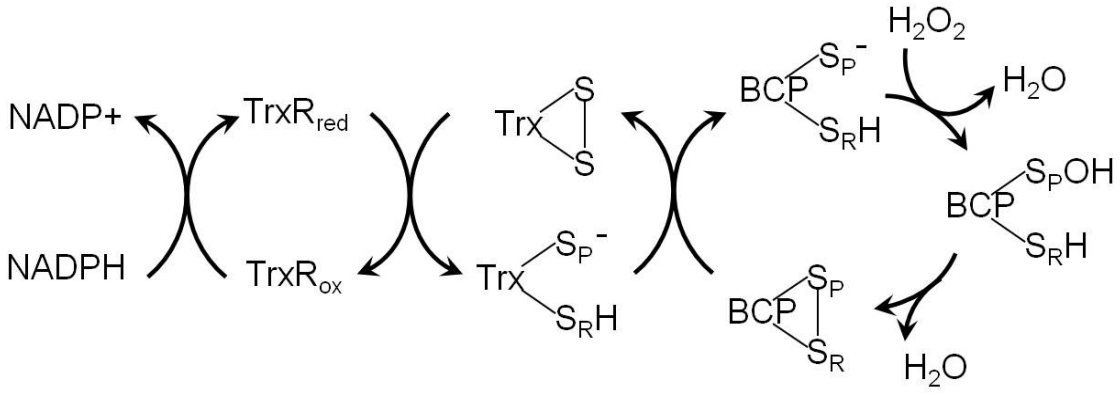

Figure 1-3. Thioredoxin (Trx) reducing system. When Prxs react with peroxide substrates, the active site becomes oxidized. The Trx reducing system is responsible for reductively recycling oxidized intermediates of Prxs formed during turnover. The system is composed of Trx, Trx reductase, and NADPH. Electrons flow from NADPH to oxidized BCP.

In acting as a protein reductant, the first cysteine in the active site of Trx acts as a nucleophile and attacks disulfide bonds within proteins. This attack results in a mixed disulfide between Trx and the targeted protein. The resolution of this disulfide bond is done by the C-terminal cysteine in Trx, resulting in oxidized Trx and a reduced protein substrate (Holmgren, 1985). Several residues surrounding the active site CXXC in Trx1, in particular Asp26 and Lys57, form hydrogen bonds with the active site Cys residues, lowering the pK_a of the N-terminal cysteine; a pK_a value of approximately 7.5 was calculated for the N-terminal Cys in the Trx CXXC motif, whereas the C-terminal Cys has a pK_a of approximately 9.2 (Kallis & Holmgren, 1980, Holmgren & Fagerstedt, 1982, Dyson *et al.*, 1991, Chivers *et al.*, 1997, Dyson *et al.*, 1997). Trx1 has been identified as a reductant of a number of Prxs, among them is *Ec*BCP (Jeong *et al.*, 2000, Clarke *et al.*, 2009). Trx was also identified as the (or a) physiological reductant of *H. pylori* BCP. In *H. pylori*, a functional Trx system is needed for oxidative stress resistance; however viability is not dependent on this system (Comtois, 2003).

E. coli has several proteins similar to Trx1, including Trx2, Grx1, Grx2, Grx3, and Grx4 (Table II). In studies conducted on the plant homologue of BCP, poplar Prx Q, a Trx homologue more closely related to Trx2 than Trx1 of *E. coli*, Trx-h1, was an effective reductant (Rouhier, 2004). Trx2 (encoded by *trxC*) in *E. coli* shares a 30% amino acid sequence identity with Trx-h1 (28% sequence identity between Trx-h1 and *E. coli* Trx1), making *E. coli* Trx2 a candidate as a reductant of *Ec*BCP *in vivo*. Trx2 contains a WCGPC active site motif that is

identical to the active site of Trx1. Trx2 is constitutively expressed under normal growing conditions and is strongly upregulated in response to oxidative stress by OxyR activation (Miranda-Vizuete *et al.*, 1997). In the absence of a peroxide stressor, Trx2 concentrations are 5-fold less than Trx1, but its concentration increases 20-fold in response to oxidative stress (Miranda-Vizuete *et al.*, 1997, Ritz *et al.*, 2000).

The glutaredoxin system transfers electrons from NADPH to glutathione reductase (GR), then to glutathione, and lastly to Grxs 1, 2, and 3 (Figure 1-4) (Aslund, 1994, Holmgren & Aslund, 1995, Vlamis-Gardikas *et al.*, 2002). As described above, wild type PrxQ from poplar was unable to use Grx1 as a reductant; however, mutant PrxQ (C51S) did exhibit significant peroxidase activity in the presence of Grx1. In fact, peroxidase activity was higher for the C51S mutant than for wild type PrxQ in the presence of either Trx-h1 or Grx1, suggesting a possible efficient 1-Cys mechanism utilized by an otherwise 2-Cys Prx (Rouhier, 2004). A 41% amino acid sequence identity between *Ec*BCP and PrxQ implies structural similarities and suggests that *Ec*BCP may also exhibit robust 1-Cys and 2-Cys mechanisms using Grx and/or or Trx proteins (Trx1 and Trx2).

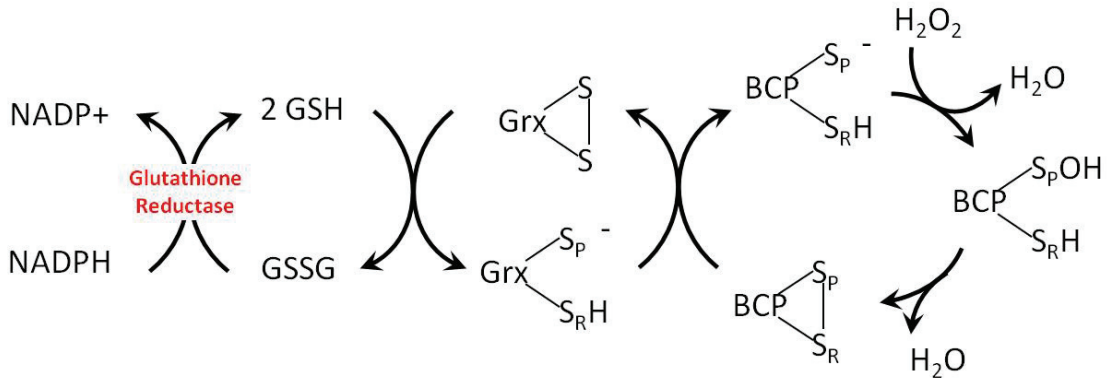

Figure 1-4. Glutaredoxin (Grx) reducing system. Peroxiredoxins like BCP react with peroxide substrates leading to oxidation of the active site. Grx may reductively recycle oxidized BCP directly, receiving its electrons in turn from glutathione (GSH). Oxidized glutathione (GSSG) is recycled by glutathione reductase using electrons derived from NADPH.

STATEMENT OF PURPOSE

The experiments conducted and data presented in this manuscript provide a detailed analysis of *Ec*BCP enzyme kinetics, specificity, and overall peroxidase mechanisms in order to better understand the physiological role of BCP *in vivo*. Chapter 2 describes the construction, expression, and purification of a novel fluorescent, redox–sensitive Grx1 mutant that has allowed us to test the role of Grx1 as an electron donor for *Ec*BCP. Chapter 3 describes detailed kinetic and thermodynamic analyses of *Ec*BCP and the insights that have been gained regarding its versatility in function. Chapter 4 addresses the role of the putative resolving cysteine on peroxidase mechanism and substrate specificity. Chapter 5 is a summary of the conclusions derived from these data, focusing on the overall role of BCP in *E. coli* oxidative stress defense and how it compares to other peroxiredoxins in its subfamily.

REFERENCES

Arenas, F. A., Covarrubias, P. C., Sandoval, J. M., Perez-Donoso, J. M., Imlay, J. A., and Vasquez, C. C. (2011) The *Escherichia coli* BtuE protein functions as a resistance determinant against reactive oxygen species, *PLoS One 6*, e15979.

Arenas, F. A., Diaz, W. A., Leal, C. A., Perez-Donoso, J. M., Imlay, J. A., and Vasquez, C. C. (2010) The *Escherichia coli btuE* gene, encodes a glutathione peroxidase that is induced under oxidative stress conditions, *Biochem Biophys Res Commun 398*, 690-694.

Aslund, F. (1994) Two additional glutaredoxins exist in *Escherichia coli*: Glutaredoxin 3 is a hydrogen donor for ribonucleotide reductase in a Thioredoxin/Glutaredoxin 1 double mutant, *Proc Natl Acad Sci U S A 91*, 9813-9817.

Aslund, F., and Beckwith, J. (1999) The thioredoxin superfamily: redundancy, specificity, and gray-area genomics, *J Bact 181*, 1375-1379.

Baker, L. M. S. (2003) Catalytic mechanism of thiol peroxidase from *Escherichia coli*. Sulfenic acid formation and overoxidation of essential Cys61, *J Biol Chem 278*, 9203-9211.

Bannister, J. V., Bannister, W. H., and Rotilio, G. (1987) Aspects of the structure, function, and applications of superoxide dismutase, *CRC Crit Rev Biochem 22*, 111-180.

Beckman, J. S., Beckman, T. W., Chen, J., Marshall, P. A., and Freeman, B. A. (1990) Apparent hydroxyl radical production by peroxynitrite: implications for endothelial injury from nitric oxide and superoxide, *Proc Natl Acad Sci U S A 87*, 1620-1624.

Berkner, L. V., and Marshall, L. C. (1965) On the origin and rise of oxygen concentration in the Earth's atmosphere, *J Atmospheric Sci 22*, 225-261.

Bryk, R., Griffin, P., and Nathan, C. (2000) Peroxynitrite reductase activity of bacterial peroxiredoxins, *Nature 407*, 211-215.

Cha, M. K. (2004) *Escherichia coli* periplasmic thiol peroxidase acts as lipid hydroperoxide peroxidase and the principal antioxidative function during anaerobic growth, *J Biol Chem 279*, 8769-8778.

Cha, M. K., Kim, H. K., and Kim, I. H. (1995) Thioredoxin-linked "thiol peroxidase" from periplasmic space of *Escherichia coli*, *J Biol Chem 270*, 28635-28641.

Cha, M. K., Kim, W. C., Lim, C. J., Kim, K., and Kim, I. H. (2004) *Escherichia coli* periplasmic thiol peroxidase acts as lipid hydroperoxide peroxidase and the principal antioxidative function during anaerobic growth, *J Biol Chem 279*, 8769-8778.

Chae, H. Z., Chung, S. J., and Rhee, S. G. (1994) Thioredoxin-dependent peroxide reductase from yeast, *J Biol Chem 269*, 27670-27678.

Chae, H. Z., Kim, H. J., Kang, S. W., and Rhee, S. G. (1999) Characterization of three isoforms of mammalian peroxiredoxin that reduce peroxides in the presence of thioredoxin, *Diabetes Res Clin Pract 45*, 101-112.

Chauhan, R., and Mande, S. C. (2001) Characterization of the *Mycobacterium tuberculosis* H37Rv alkyl hydroperoxidase AhpC points to the importance of ionic interactions in oligomerization and activity, *Biochem J 354*, 209-215.

Chen, J. W. (2000) 1-Cys peroxiredoxin, a bifunctional enzyme with glutathione peroxidase and phospholipase A2 activities, *J of Biol Chem 275*, 28421-28427.

Chen, L., Xie, Q. W., and Nathan, C. (1998) Alkyl hydroperoxide reductase subunit C (AhpC) protects bacterial and human cells against reactive nitrogen intermediates, *Mol Cell 1*, 795-805.

Chivers, P. T., Prehoda, K. E., Volkman, B. F., Kim, B. M., Markley, J. L., and Raines, R. T. (1997) Microscopic pKa values of *Escherichia coli* thioredoxin, *Biochemistry 36*, 14985-14991.

Choi, H. J., Kang, S. W., Yang, C. H., Rhee, S. G., and Ryu, S. E. (1998) Crystal structure of a novel human peroxidase enzyme at 2.0 A resolution, *Nat Struct Biol 5*, 400-406.

Choi, J. (2003) Crystal Structure of *Escherichia coli* thiol peroxidase in the oxidized state: Insights into intramolecular disulfide formation and substrate binding in atypical 2-Cys peroxiredoxins, *J of Biol Chem 278*, 49478-49486.

Choi, J., Choi, S., Cha, M. K., Kim, I. H., and Shin, W. (2005) Crystallization and preliminary X-ray analysis of a truncated mutant of yeast nuclear thiol peroxidase, a novel atypical 2-Cys peroxiredoxin, *Acta Crystallogr Sect F Struct Biol Cryst Commun 61*, 659-662.

Clarke, D. J., Mackay, C. L., Campopiano, D. J., Langridge-Smith, P., and Brown, A. R. (2009) Interrogating the molecular details of the peroxiredoxin activity of the *Escherichia coli* bacterioferritin comigratory protein using high-resolution mass spectrometry, *Biochemistry 48*, 3904-3914.

Clarke, D. J., Ortega, X. P., Mackay, C. L., Valvano, M. A., Govan, J. R., Campopiano, D. J., Langridge-Smith, P., and Brown, A. R. (2010) Subdivision of the bacterioferritin comigratory protein family of bacterial peroxiredoxins based on catalytic activity, *Biochemistry 49*, 1319-1330.

Cloud, P. (1972) A working model of the primitive Earth, *Am J Sci 272*, 537-548.

Comtois, S. L. (2003) Role of the thioredoxin system and the thiol-peroxidases Tpx and Bcp in mediating resistance to oxidative and nitrosative stress in *Helicobacter pylori*, *Microbiology 149*, 121-129.

Copley, S. D., Novak, W. R., and Babbitt, P. C. (2004) Divergence of function in the thioredoxin fold suprafamily: evidence for evolution of peroxiredoxins from a thioredoxin-like ancestor, *Biochemistry 43*, 13981-13995.

Cotgreave, I. A., and Gerdes, R. G. (1998) Recent trends in glutathione biochemistry--glutathione-protein interactions: a molecular link between

oxidative stress and cell proliferation?, *Biochem Biophys Res Commun 242*, 1-9.

Cox, A. G., Winterbourn, C. C., and Hampton, M. B. (2010) Mitochondrial peroxiredoxin involvement in antioxidant defence and redox signalling, *Biochem J 425*, 313-325.

Czapski, G. (1984) [24] Reaction of ·OH, In *Methods Enzymol* (Lester, P., Ed.), pp 209-215, Academic Press.

D'Ambrosio, K., Limauro, D., Pedone, E., Galdi, I., Pedone, C., Bartolucci, S., and De Simone, G. (2009) Insights into the catalytic mechanism of the Bcp family: Functional and structural analysis of Bcp1 from *Sulfolobus solfataricus*, *Proteins 76*, 995-1006.

Declercq, J. P., Evrard, C., Clippe, A., Stricht, D. V., Bernard, A., and Knoops, B. (2001) Crystal structure of human peroxiredoxin 5, a novel type of mammalian peroxiredoxin at 1.5 A resolution, *J Mol Biol 311*, 751-759.

Deponte, M., and Becker, K. (2005) Biochemical characterization of *Toxoplasma gondii* 1-Cys peroxiredoxin 2 with mechanistic similarities to typical 2-Cys Prx, *Mol Biochem Parasitol 140*, 87-96.

Dietz, K.-J. (2003) Plant Peroxiredoxins, *Ann Rev of Plant Bio 54*, 93-107.

Dyson, H. J., Jeng, M. F., Tennant, L. L., Slaby, I., Lindell, M., Cui, D. S., Kuprin, S., and Holmgren, A. (1997) Effects of buried charged groups on cysteine thiol ionization and reactivity in *Escherichia coli* thioredoxin: structural and functional characterization of mutants of Asp 26 and Lys 57, *Biochemistry 36*, 2622-2636.

Dyson, H. J., Tennant, L. L., and Holmgren, A. (1991) Proton-transfer effects in the active-site region of *Escherichia coli* thioredoxin using two-dimensional 1H NMR, *Biochemistry 30*, 4262-4268.

Echalier, A., Brittain, T., Wright, J., Boycheva, S., Mortuza, G. B., Fulop, V., and Watmough, N. J. (2008) Redox-linked structural changes associated with the formation of a catalytically competent form of the diheme cytochrome c peroxidase from Pseudomonas aeruginosa, *Biochemistry 47*, 1947-1956.

Eisenstark, A. (1989) Bacterial genes involved in response to near-ultraviolet radiation, *Adv Genet 26*, 99-147.

Ellis, H. R., and Poole, L. B. (1997) Roles for the two cysteine residues of AhpC in catalysis of peroxide reduction by alkyl hydroperoxide reductase from *Salmonella typhimurium*, *Biochemistry 36*, 13349-13356.

Fahey, R. C., Brown, W. C., Adams, W. B., and Worsham, M. B. (1978) Occurrence of glutathione in bacteria, *J Bact 133*, 1126-1129.

Farr, S. B., and Kogoma, T. (1991) Oxidative stress responses in *Escherichia coli* and *Salmonella typhimurium*, *Microbiol. Mol. Biol. Rev. 55*, 561-585.

Ferguson, G. P., and Booth, I. R. (1998) Importance of glutathione for growth and survival of *Escherichia coli* cells: detoxification of methylglyoxal and maintenance of intracellular K+, *J Bact 180*, 4314-4318.

Ferguson, G. P., McLaggan, D., and Booth, I. R. (1995) Potassium channel activation by glutathione-S-conjugates in *Escherichia coli*: protection against methylglyoxal is mediated by cytoplasmic acidification, *Mol Microbiol 17*, 1025-1033.

Flatley, J., Barrett, J., Pullan, S. T., Hughes, M. N., Green, J., and Poole, R. K. (2005) Transcriptional responses of *Escherichia coli* to S-nitrosoglutathione under defined chemostat conditions reveal major changes in methionine biosynthesis, *J Biol Chem 280*, 10065-10072.

Flint, D. H., Tuminello, J. F., and Emptage, M. H. (1993) The inactivation of Fe-S cluster containing hydro-lyases by superoxide, *J Biol Chem 268*, 22369-22376.

Flohe, L. (2002) Tryparedoxin Peroxidase of *Leishmania donovani*: Molecular Cloning, Heterologous Expression, Specificity, and Catalytic Mechanism, *Arch Biochem Biophys 397*, 324-335.

Fournier, M., Aubert, C., Dermoun, Z., Durand, M. C., Moinier, D., and Dolla, A. (2006) Response of the anaerobe *Desulfovibrio vulgaris* Hildenborough to oxidative conditions: proteome and transcript analysis, *Biochimie 88*, 85-94.

Freeman, B. (1994) Free radical chemistry of nitric oxide. Looking at the dark side, *Chest 105*, 79S-84S.

Fridovich, I. (1978) The biology of oxygen radicals, *Science 201*, 875-880.

Fridovich, I. (1983) Superoxide dismutases: regularities and irregularities, *Harvey Lect 79*, 51-75.

Fridovich, I. (1983) Superoxide radical: an endogenous toxicant, *Annu Rev Pharmacol Toxicol 23*, 239-257.

Gardner, P. R., and Fridovich, I. (1991) Superoxide sensitivity of the *Escherichia coli* 6-phosphogluconate dehydratase, *J Biol Chem 266*, 1478-1483.

Gardner, P. R., and Fridovich, I. (1991) Superoxide sensitivity of the *Escherichia coli* aconitase, *J Biol Chem 266*, 19328-19333.

Garrels, R. M. (1978) The History of the Earth's Environment, *Science 201*, 247-248.

Gon, S., and Beckwith, J. (2006) Ribonucleotide reductases: influence of environment on synthesis and activity, *Antioxid Redox Signal 8*, 773-780.

Greenberg, J. T., Monach, P., Chou, J. H., Josephy, P. D., and Demple, B. (1990) Positive control of a global antioxidant defense regulon activated by superoxide-generating agents in *Escherichia coli*, *Proc Natl Acad Sci U S A 87*, 6181-6185.

Guimaraes, B. G., Souchon, H., Honore, N., Saint-Joanis, B., Brosch, R., Shepard, W., Cole, S. T., and Alzari, P. M. (2005) Structure and mechanism of the alkyl hydroperoxidase AhpC, a key element of the *Mycobacterium tuberculosis* defense system against oxidative stress, *J Biol Chem 280*, 25735-25742.

Haas, A., and Goebel, W. (1992) Cloning of a superoxide dismutase gene from Listeria ivanovii by functional complementation in *Escherichia coli* and characterization of the gene product, *Mol Gen Genet 231*, 313-322.

Haber, F., and Weiss, J. (1934) The catalytic decomposition of hydrogen peroxide by iron salts, *Proc Royal Soc London. Series A, Math and Phys Sci 147*, 332-351.

Hall, A., Nelson, K., Poole, L. B., and Karplus, P. A. (2011) Structure-based Insights into the Catalytic Power and Conformational Dexterity of Peroxiredoxins, *Antioxid Redox Signal* 15, 795-815

Hall, A., Parsonage, D., Horita, D., Karplus, P. A., Poole, L. B., and Barbar, E. (2009) Redox-dependent dynamics of a dual thioredoxin fold protein: evolution of specialized folds, *Biochemistry 48*, 5984-5993.

Hall, A., Parsonage, D., Poole, L. B., and Karplus, P. A. (2010) Structural evidence that peroxiredoxin catalytic power Is based on transition-state stabilization, *J Mol Biol 402*, 194-209.

Hall, A., Sankaran, B., Poole, L. B., and Karplus, P. A. (2009) Structural changes common to catalysis in the Tpx peroxiredoxin subfamily, *J Mol Biol 393*, 867-881.

Halliwell, B. (2007) Biochemistry of oxidative stress, *Biochem Soc Trans 35*, 1147-1150.

Halliwell, B., and Gutteridge, J. M. (1984) Oxygen toxicity, oxygen radicals, transition metals and disease, *Biochem J 219*, 1-14.

Hancock, J. T., Desikan, R., and Neill, S. J. (2001) Role of reactive oxygen species in cell signalling pathways, *Biochem Soc Trans 29*, 345-350.

Hassett, D. J. (1989) The Role of Hydroxyl Radical in Chromosomal and Plasmid Damage in *Neisseria gonorrhoeae in vivo*, *Free Radic Res 7*, 83.

Heimberger, A., and Eisenstark, A. (1988) Compartmentalization of catalases in *Escherichia coli*, *Biochem Biophys Res Commun 154*, 392-397.

Hillar, A., Peters, B., Pauls, R., Loboda, A., Zhang, H., Mauk, A. G., and Loewen, P. C. (2000) Modulation of the activities of catalase-peroxidase HPI of *Escherichia coli* by site-directed mutagenesis, *Biochemistry 39*, 5868-5875.

Hofmann, B., Hecht, H. J., and Flohé, L. (2002) Peroxiredoxins, *Biol Chem 383*, 347-364.

Hogg, N., Darley-Usmar, V. M., Wilson, M. T., and Moncada, S. (1992) Production of hydroxyl radicals from the simultaneous generation of superoxide and nitric oxide, *Biochem J 281 (Pt 2)*, 419-424.

Holland, H. D. (1972) The geologic history of sea water--an attempt to solve the problem, *Geochimica et Cosmochimica Acta 36*, 637-651.

Holland, H. D. (2002) Volcanic gases, black smokers, and the great oxidation event, *Geochim Cosmochim Acta 66*, 3811-3826.

Holmgren, A. (1976) Hydrogen donor system for *Escherichia coli* ribonucleoside-diphosphate reductase dependent upon glutathione, *Proc Natl Acad Sci U S A 73*, 2275-2279.

Holmgren, A. (1979) Glutathione-dependent synthesis of deoxyribonucleotides. Purification and characterization of glutaredoxin from *Escherichia coli*, *J Biol Chem 254*, 3664-3671.

Holmgren, A. (1985) Thioredoxin, *Annu Rev Biochem 54*, 237-271.

Holmgren, A., and Aslund, F. (1995) Glutaredoxin, *Methods Enzymol 252*, 283-292.

Holmgren, A., and Fagerstedt, M. (1982) The in vivo distribution of oxidized and reduced thioredoxin in *Escherichia coli*, *J Biol Chem 257*, 6926-6930.

Hopkins, F. G. (1921) On an autoxidisable constituent of the cell, *Biochem J 15*, 286-305.

Horta, B. B., de Oliveira, M. A., Discola, K. F., Cussiol, J. R. R., and Netto, L. E. S. (2010) Structural and biochemical characterization of peroxiredoxin Q from Xylella fastidiosa: Catalytic mechanism and high reactivity, *J Biol Chem 285*, 16051-16065.

Imai, H., and Nakagawa, Y. (2003) Biological significance of phospholipid hydroperoxide glutathione peroxidase (PHGPx, GPx4) in mammalian cells, *Free Radic Biol Med 34*, 145-169.

Imlay, J., and Linn, S. (1987) Mutagenesis and Stress Responses Induced in *Escherichia coli* by Hydrogen Peroxide, *J Bact 169*, 2967-2976.

Imlay, J. A., Chin, S. M., and Linn, S. (1988) Toxic DNA damage by hydrogen peroxide through the Fenton reaction in vivo and in vitro, *Science 240*, 640-642.

Imlay, J. A., and Fridovich, I. (1991a) Assay of metabolic superoxide production in *Escherichia coli*, *J Biol Chem 266*, 6957-6965.

Imlay, J. A., and Fridovich, I. (1991b) Superoxide production by respiring membranes of *Escherichia coli*, *Free Radic Res Commun 12-13 Pt 1*, 59-66.

Imlay, J. A., and Fridovich, I. (1992) Suppression of oxidative envelope damage by pseudoreversion of a superoxide dismutase-deficient mutant of *Escherichia coli*, *J Bact 174*, 953-961.

Imlay, J. A., and Linn, S. (1988) DNA damage and oxygen radical toxicity, *Science 240*, 1302-1309.

Jacobson, F. S., Morgan, R. W., Christman, M. F., and Ames, B. N. (1989) An alkyl hydroperoxide reductase from *Salmonella typhimurium* involved in the defense of DNA against oxidative damage. Purification and properties, *J Biol Chem 264*, 1488-1496.

Jeong, W., Cha, M. K., and Kim, I. H. (2000) Thioredoxin-dependent hydroperoxide peroxidase activity of bacterioferritin comigratory protein (BCP) as a new member of the thiol-specific antioxidant protein (TSA)/Alkyl hydroperoxide peroxidase C (AhpC) family, *J Biol Chem 275*, 2924-2930.

Justino, M. C., Vicente, J. B., Teixeira, M., and Saraiva, L. M. (2005) New genes implicated in the protection of anaerobically grown *Escherichia coli* against nitric oxide, *J Biol Chem 280*, 2636-2643.

Kallis, G. B., and Holmgren, A. (1980) Differential reactivity of the functional sulfhydryl groups of cysteine-32 and cysteine-35 present in the reduced form of thioredoxin from *Escherichia coli*, *J Biol Chem 255*, 10261-10265.

Kang, S. W., Rhee, S. G., Chang, T. S., Jeong, W., and Choi, M. H. (2005) 2-Cys peroxiredoxin function in intracellular signal transduction: therapeutic implications, *Trends Mol Med 11*, 571-578.

Keele, B. B., Jr., McCord, J. M., and Fridovich, I. (1970) Superoxide dismutase from *Escherichia coli* B. A new manganese-containing enzyme, *J Biol Chem 245*, 6176-6181.

Kim, H. S., Manevich, Y., Feinstein, S. I., Pak, J. H., Ho, Y. S., and Fisher, A. B. (2003) Induction of 1-cys peroxiredoxin expression by oxidative stress in lung epithelial cells, *Am J Physiol Lung Cell Mol Physiol 285*, L363-369.

Kim, S. Y., Kim, E. J., and Park, J. W. (2002) Yeast thioredoxin peroxidase expression enhances the resistance of *Escherichia coli* to oxidative stress induced by singlet oxygen, *Redox Rep 7*, 79-84.

Kitano, K., Niimura, Y., Nishiyama, Y., and Miki, K. (1999) Stimulation of peroxidase activity by decamerization related to ionic strength: AhpC protein from *Amphibacillus xylanus*, *J Biochem 126*, 313-319.

Konig, J., Lotte, K., Plessow, R., Brockhinke, A., Baier, M., and Dietz, K. J. (2003) Reaction mechanism of plant 2-Cys peroxiredoxin. Role of the C terminus and the quaternary structure, *J Biol Chem 278*, 24409-24420.

Kosower, E. M., and Kosower, N. S. (1969) Lest I forget thee, glutathione, *Nature 224*, 117-120.

Kristensen, P., Rasmussen, D. E., and Kristensen, B. I. (1999) Properties of thiol-specific anti-oxidant protein or calpromotin in solution, *Biochem Biophys Res Commun 262*, 127-131.

Krone, F. A., Westphal, G., Meyer, H. E., and Schwenn, J. D. (1990) PAPS-reductase of *Escherichia coli*. Correlating the N-terminal amino acid sequence with the DNA of gene cys H, *FEBS Lett 260*, 6-9.

Kuo, C. F., and Fridovich, I. (1988) Stimulation of the activity of horseradish peroxidase by nitrogenous compounds, *J Biol Chem 263*, 3811-3817.

Lee, J., Spector, D., Godon, C., Labarre, J., and Toledano, M. B. (1999) A new antioxidant with alkyl hydroperoxide defense properties in yeast, *J Biol Chem 274*, 4537-4544.

Li, M., Huang, W., Yang, Q., Liu, X., and Wu, Q. (2005) Expression and oxidative stress tolerance studies of glutaredoxin from cyanobacterium Synechocystis sp. PCC 6803 in *Escherichia coli*, *Protein Expr Purif 42*, 85-91.

Liao, S. J., Yang, C. Y., Chin, K. H., Wang, A. H., and Chou, S. H. (2009) Insights into the alkyl peroxide reduction pathway of *Xanthomonas campestris* bacterioferritin comigratory protein from the trapped intermediate-ligand complex structures, *J Mol Biol 390*, 951-966.

Limauro, D., D'Ambrosio, K., Langella, E., De Simone, G., Galdi, I., Pedone, C., Pedone, E., and Bartolucci, S. (2010) Exploring the catalytic mechanism

of the first dimeric Bcp: Functional, structural and docking analyses of Bcp4 from *Sulfolobus solfataricus*, *Biochimie 92*, 1435-1444.

Link, A. J., Robison, K., and Church, G. M. (1997) Comparing the predicted and observed properties of proteins encoded in the genome of *Escherichia coli* K-12, *Electrophoresis 18*, 1259-1313.

Liochev, S. I., and Fridovich, I. (1993) Modulation of the fumarases of *Escherichia coli* in response to oxidative stress, *Arch Biochem Biophys 301*, 379-384.

Loewen, P. C. (1979) Levels of glutathione in *Escherichia coli*, *Can J Biochem 57*, 107-111.

Loewen, P. C. (1984) Isolation of catalase-deficient *Escherichia coli* mutants and genetic mapping of katE, a locus that affects catalase activity, *J Bact 157*, 622-626.

Loewen, P. C., and Triggs, B. L. (1984) Genetic mapping of katF, a locus that with katE affects the synthesis of a second catalase species in *Escherichia coli*, *J Bact 160*, 668-675.

Loewen, P. C., Triggs, B. L., George, C. S., and Hrabarchuk, B. E. (1985) Genetic mapping of katG, a locus that affects synthesis of the bifunctional catalase-peroxidase hydroperoxidase I in *Escherichia coli*, *J Bact 162*, 661-667.

Martin, J. L. (1995) Thioredoxin--a fold for all reasons, *Structure 3*, 245-250.

Massey, V., Strickland, S., Mayhew, S. G., Howell, L. G., Engel, P. C., Matthews, R. G., Schuman, M., and Sullivan, P. A. (1969) The production of superoxide anion radicals in the reaction of reduced flavins and flavoproteins with molecular oxygen, *Biochem Biophys Res Commun 36*, 891-897.

McCord, J. M., and Fridovich, I. (1969) Superoxide dismutase. An enzymic function for erythrocuprein (hemocuprein), *J Biol Chem 244*, 6049-6055.

McCord, J. M., and Fridovich, I. (1969) The utility of superoxide dismutase in studying free radical reactions. I. Radicals generated by the interaction of sulfite, dimethyl sulfoxide, and oxygen, *J Biol Chem 244*, 6056-6063.

McCord, J. M., and Fridovich, I. (1978) The biology and pathology of oxygen radicals, *Ann Intern Med 89*, 122-127.

Meister, A. (1982) Metabolism and function of glutathione: an overview, *Biochem Soc Trans 10*, 78-79.

Meister, A. (1983) Transport and metabolism of glutathione and gamma-glutamyl amino acids, *Biochem Soc Trans 11*, 793-794.

Meister, A. (1991) Glutathione deficiency produced by inhibition of its synthesis, and its reversal; applications in research and therapy, *Pharmacol Ther 51*, 155-194.

Meister, A., and Anderson, M. E. (1983) Glutathione, *Annu Rev Biochem 52*, 711-760.

Miller, R., and Britigan, B. E. (1997) Role of oxidants in Microbial Pahophysiology, *Clin Microbiol Rev* 10, 1-18.

Miranda-Vizuete, A., Damdimopoulos, A. E., Gustafsson, J., and Spyrou, G. (1997) Cloning, expression, and characterization of a novel *Escherichia coli* thioredoxin, *J Biol Chem 272*, 30841-30847.

Moncada, S., and Higgs, A. (1993) The L-arginine-nitric oxide pathway, *N Engl J Med 329*, 2002-2012.

Moncada, S., and Martin, J. F. (1993) Evolution of nitric oxide, *Lancet 341*, 1511.

Montemartini, M., Kalisz, H. M., Hecht, H. J., Steinert, P., and Flohe, L. (1999) Activation of active-site cysteine residues in the peroxiredoxin-type tryparedoxin peroxidase of *Crithidia fasciculata*, *Eur J Biochem 264*, 516-524.

Mukhopadhyay, P., Zheng, M., Bedzyk, L. A., LaRossa, R. A., and Storz, G. (2004) Prominent roles of the NorR and Fur regulators in the *Escherichia coli* transcriptional response to reactive nitrogen species, *Proc Natl Acad Sci U S A 101*, 745-750.

Neidhardt, F. C., Vaughn, V., Phillips, T. A., and Bloch, P. L. (1983) Gene-protein index of *Escherichia coli* K-12, *Microbiol Rev 47*, 231-284.

Nelson, K. J., Knutson, S. T., Soito, L., Klomsiri, C., Poole, L. B., and Fetrow, J. S. (2011) Analysis of the peroxiredoxin family: using active-site structure and sequence information for global classification and residue analysis, *Proteins 79*, 947-964.

Niederhoffer, E. C., Naranjo, C. M., Bradley, K. L., and Fee, J. A. (1990) Control of *Escherichia coli* superoxide dismutase (sodA and sodB) genes by the ferric uptake regulation (fur) locus, *J Bact 172*, 1930-1938.

Pacelli, R., Wink, D. A., Cook, J. A., Krishna, M. C., DeGraff, W., Friedman, N., Tsokos, M., Samuni, A., and Mitchell, J. B. (1995) Nitric oxide potentiates hydrogen peroxide-induced killing of *Escherichia coli*, *J Exp Med 182*, 1469-1479.

Pan, J. L., and Bardwell, J. C. A. (2006) The origami of thioredoxin-like folds, *Protein Science 15*, 2217-2227.

Papinutto, E., Windle, H. J., Cendron, L., Battistutta, R., Kelleher, D., and Zanotti, G. (2005) Crystal structure of alkyl hydroperoxide-reductase (AhpC) from *Helicobacter pylori*, *Biochim Biophys Acta - Proteins & Proteomics 1753*, 240-246.

Park, S. G., Cha, M. K., Jeong, W., and Kim, I. H. (2000) Distinct physiological functions of thiol peroxidase isoenzymes in *Saccharomyces cerevisiae*, *J Biol Chem 275*, 5723-5732.

Parsonage, D., Karplus, P. A., and Poole, L. B. (2008) Substrate specificity and redox potential of AhpC, a bacterial peroxiredoxin, *Proc Natl Acad Sci U S A 105*, 8209-8214.

Poole, L. B. (1996) Flavin-dependent alkyl hydroperoxide reductase from *Salmonella typhimurium*. 2. Cystine disulfides involved in catalysis of peroxide reduction, *Biochemistry 35*, 65-75.

Poole, L. B. (2005) Bacterial defenses against oxidants: mechanistic features of cysteine-based peroxidases and their flavoprotein reductases, *Arch Biochem Biophys 433*, 240-254.

Poole, L. B. (2007) The catalytic mechanism of peroxiredoxins, *Subcell Biochem 44*, 61-81.

Poole, L. B., Chae, H. Z., Flores, B. M., Reed, S. L., Rhee, S. G., and Torian, B. E. (1997) Peroxidase activity of a TSA-like antioxidant protein from a pathogenic amoeba, *Free Radic Biol Med 23*, 955-959.

Poole, L. B., and Ellis, H. R. (1996) Flavin-dependent alkyl hydroperoxide reductase from *Salmonella typhimurium*. 1. Purification and enzymatic activities of overexpressed AhpF and AhpC proteins, *Biochemistry 35*, 56-64.

Poole, L. B., Karplus, P. A., and Claiborne, A. (2004) Protein Sulfenic Acids in Redox Signaling, *Ann Rev Pharm Tox 44*, 325-347.

Poole, L. B., and Nelson, K. J. (2008) Discovering mechanisms of signaling-mediated cysteine oxidation, *Curr Opin Chem Biol 12*, 18-24.

Poole, L. B., Reynolds, C. M., Wood, Z. A., Karplus, P. A., Ellis, H. R., and Li Calzi, M. (2000) AhpF and other NADH:peroxiredoxin oxidoreductases, homologues of low Mr thioredoxin reductase, *Eur J Biochem 267*, 6126-6133.

Powell, C. S., and Jackson, R. M. (2003) Mitochondrial complex I, aconitase, and succinate dehydrogenase during hypoxia-reoxygenation: modulation of enzyme activities by MnSOD, *Am J Physiol Lung Cell Mol Physiol 285*, L189-198.

Radi, R., Beckman, J. S., Bush, K. M., and Freeman, B. A. (1991) Peroxynitrite-induced membrane lipid peroxidation: the cytotoxic potential of superoxide and nitric oxide, *Arch Biochem Biophys 288*, 481-487.

Radi, R., Beckman, J. S., Bush, K. M., and Freeman, B. A. (1991) Peroxynitrite oxidation of sulfhydryls. The cytotoxic potential of superoxide and nitric oxide, *J Biol Chem 266*, 4244-4250.

Ritz, D., Patel, H., Doan, B., Zheng, M., Aslund, F., Storz, G., and Beckwith, J. (2000) Thioredoxin 2 is involved in the oxidative stress response in *Escherichia coli*, *J Biol Chem 275*, 2505-2512.

Rockett, K. A., Awburn, M. M., Cowden, W. B., and Clark, I. A. (1991) Killing of *Plasmodium falciparum* in vitro by nitric oxide derivatives, *Infect Immun 59*, 3280-3283.

Ross, D., Albano, E., Nilsson, U., and Moldéus, P. (1984) Thiyl radicals - formation during peroxidase-catalyzed metabolism of acetaminophen in the presence of thiols, *Biochem Biophys Res Comm 125*, 109-115.

Rouhier, N. (2002) Glutaredoxin-dependent peroxiredoxin from Poplar. Protein-protein interaction and catalytic mechanism, *J Biol Chem 277*, 13609-13614.

Rouhier, N. (2004) Poplar Peroxiredoxin Q. A Thioredoxin-linked chloroplast antioxidant functional in pathogen defense, *Plant Physiol 134*, 1027-1038.

Russel, M., Model, P., and Holmgren, A. (1990) Thioredoxin or glutaredoxin in *Escherichia coli* is essential for sulfate reduction but not for deoxyribonucleotide synthesis, *J Bact 172*, 1923-1929.

Sarma, G. N., Nickel, C., Rahlfs, S., Fischer, M., Becker, K., and Karplus, P. A. (2005) Crystal structure of a novel *Plasmodium falciparum* 1-Cys peroxiredoxin, *J Mol Biol 346*, 1021-1034.

Sarma, G. N., Nickel, C., Rahlfs, S., Fischer, M., Becker, K., and Karplus, P. A. (2005) Crystal structure of a novel *Plasmodium falciparum* 1-Cys peroxiredoxin, *J Mol Biol 346*, 1021-1034.

Schroder, E., Littlechild, J. A., Lebedev, A. A., Errington, N., Vagin, A. A., and Isupov, M. N. (2000) Crystal structure of decameric 2-Cys peroxiredoxin from human erythrocytes at 1.7 A resolution, *Structure 8*, 605-615.

Schroder, E., and Ponting, C. P. (1998) Evidence that peroxiredoxins are novel members of the thioredoxin fold superfamily, *Protein Sci 7*, 2465-2468.

Seaver, L. C., and Imlay, J. A. (2001) Alkyl hydroperoxide reductase Is the primary scavenger of endogenous hydrogen peroxide in *Escherichia coli*, *J Bact 183*, 7173-7181.

Segal, A. W. (2005) How neutrophils kill microbes, *Annu Rev Immunol 23*, 197-223.

Segal, A. W. (2006) How superoxide production by neutrophil leukocytes kills microbes, *Novartis Found Symp 279*, 92-98; discussion 98-100, 216-109.

Stark, J. M., and Jackson, S. K. (1990) Sensitivity to endotoxin is induced by increased membrane fatty-acid unsaturation and oxidant stress, *J Med Microbiol 32*, 217-221.

Storz, G., Jacobson, F. S., Tartaglia, L. A., Morgan, R. W., Silveira, L. A., and Ames, B. N. (1989) An alkyl hydroperoxide reductase induced by oxidative stress in *Salmonella typhimurium* and *Escherichia coli*: genetic characterization and cloning of ahp, *J Bact 171*, 2049-2055.

Storz, G., Tartaglia, L. A., and Ames, B. N. (1990) Transcriptional regulator of oxidative stress-inducible genes: direct activation by oxidation, *Science 248*, 189-194.

Tao, K. (2008) Subcellular localization and in vivo oxidation-reduction kinetics of thiol peroxidase in *Escherichia coli*, *FEMS Microbiol Lett 289*, 41-45.

Triggs-Raine, B. L., and Loewen, P. C. (1987) Physical characterization of katG, encoding catalase HPI of *Escherichia coli*, *Gene 52*, 121-128.

Trivelli, X., Krimm, I., Ebel, C., Verdoucq, L., Prouzet-Mauleon, V., Chartier, Y., Tsan, P., Lauquin, G., Meyer, Y., and Lancelin, J. M. (2003) Characterization of the yeast peroxiredoxin Ahp1 in its reduced active and overoxidized inactive forms using NMR, *Biochemistry 42*, 14139-14149.

Trujillo, M. (2006) The mycobacterial thioredoxin peroxidase can act as a 1-cysteine Peroxiredoxin, *J Biol Chem 281*, 20555-20566.

Veal, E. A., Day, A. M., and Morgan, B. A. (2007) Hydrogen peroxide sensing and signaling, *Mol Cell 26*, 1-14.

Vlamis-Gardikas, A., Potamitou, A., Zarivach, R., Hochman, A., and Holmgren, A. (2002) Characterization of *Escherichia coli* null mutants for glutaredoxin 2, *J Biol Chem 277*, 10861-10868.

Wakita, M., Masuda, S., Motohashi, K., Hisabori, T., Ohta, H., and Takamiya, K. (2007) The significance of type II and PrxQ peroxiredoxins for antioxidative stress response in the purple bacterium Rhodobacter sphaeroides, *J Biol Chem 282*, 27792-27801.

Wang, G., Olczak, A. A., Walton, J. P., and Maier, R. J. (2005) Contribution of the *Helicobacter pylori* thiol peroxidase bacterioferritin comigratory protein

to oxidative stress resistance and host colonization, *Infect Immun 73*, 378-384.

Weiss, J. (1986) Oxygen, Ischemia and Inflammation, *acta physiol scand 548*, 9-37.

Weissbach, H., Resnick, L., and Brot, N. (2005) Methionine sulfoxide reductases: history and cellular role in protecting against oxidative damage, *Biochim Biophys Acta 1703*, 203-212.

Winterbourn, C. C., and Hampton, M. B. (2008) Thiol chemistry and specificity in redox signaling, *Free Radic Biol Med 45*, 549-561.

Wood, Z. A., Poole, L. B., Hantgan, R. R., and Karplus, P. A. (2002) Dimers to doughnuts: redox-sensitive oligomerization of 2-cysteine peroxiredoxins, *Biochemistry 41*, 5493-5504.

Wood, Z. A., Poole, L. B., and Karplus, P. A. (2003) Peroxiredoxin evolution and the regulation of hydrogen peroxide signaling, *Science 300*, 650-653.

Wood, Z. A., Schroder, E., Robin Harris, J., and Poole, L. B. (2003) Structure, mechanism and regulation of peroxiredoxins, *Trends Biochem Sci 28*, 32-40.

Yost, F. J., Jr., and Fridovich, I. (1973) An iron-containing superoxide dismutase from *Escherichia coli*, *J Biol Chem 248*, 4905-4908.

Chapter 2: Engineering a Fluorescent Reporter into Glutaredoxin 1

This chapter is excerpted and adapted from a paper published in 2010 in *Methods of Enzymology*. Development of the following methods came out of the need to measure substrate interactions of *Escherichia coli* BCP (*Ec*BCP) and Grx1 directly. Stylistic differences reflect the format used by *Methods in Enzymology*. All work with *E. coli* Grx1 and *Ec*BCP described in this chapter was completed by Stacy Reeves, while Dr. Derek Parsonage conducted assays and experiments pertaining to *Salmonella typhimurium* AhpF and AhpC.

ABSTRACT

The rate of electron transfer through multicomponent redox systems is often monitored by following the absorbance change due to the oxidation of the upstream pyridine nucleotide electron donor (NADPH or NADH) that initiates the process. Such coupled assay systems are powerful, but because of problems regarding the rate limiting step, they sometimes limit the kinetic information that can be obtained about individual components. For peroxiredoxins, such assays have led to widespread underestimates of their catalytic power. We show here how this problem can be addressed by a protein engineering strategy inspired by some bacterial and eukaryotic thioredoxins for which a significant fluorescence signal is generated during oxidation that provides a highly sensitive tool to directly measure electron transfers into and out of these domains. For *Escherichia coli* glutaredoxin 1 (Grx1) and the N-terminal domain of AhpF (a flavoprotein disulfide reductase), two cases not having such fluorescence signals, we have successfully added “sensor” tryptophan residues using the positions of tryptophan residues in thioredoxins as a guide. These tools have fundamentally changed our understanding of the catalytic power of peroxiredoxin systems and should also be widely applicable for improving quantitative assay capabilities in other electron transfer systems.

Reactive cysteine-containing redox centers within proteins are important to cellular metabolic and signaling processes and are often found within the CXXC-related motif of the thioredoxin (Trx)-like fold common to a broad range of redox proteins [e.g., Trx, Grx, glutathione-S-transferase (GST), peroxiredoxin (Prx) and glutathione peroxidase (Gpx) families] (Atkinson and Babbitt, 2009). In some members of this group, including *E. coli* Trx, tryptophan (Trp) residues are sufficiently close and appropriately oriented to act as sensitive fluorescent reporters of the active site redox state (Holmgren, 1972). In these cases, Trp fluorescence provides a powerful way to conduct kinetic studies focused on one or a few steps of reaction, without having to rely on linked spectral assays (e.g., by including NADPH and Trx reductase with Trx-dependent assays). However in many proteins in the group, the conversion between disulfide and dithiol forms is spectrally silent or minimally detectable so such assays cannot be used.

As described herein, sensitive fluorescent reporters of redox activity can be engineered into redox domains by utilizing mutation to introduce strategically-located Trp residues. While these approaches may not be successful in all enzymes, they have been quite successful in the bacterial peroxiredoxin systems that are the focus of this chapter. In the case of *S. typhimurium* AhpC, the fluorescence-based assays not only allowed insight into mechanistic details, but also transformed perceptions in the field by showing that this enzyme had an intrinsic activity 100 times greater than had been previously appreciated.

Peroxiredoxins (Prxs) are a widespread class of thiol-dependent peroxidases with roles in the control of damaging and signaling-relevant reactive

oxygen species such as hydrogen peroxide, organic hydroperoxides and peroxynitrite (Hall *et al.*, 2009a). Structurally, they are Trx fold proteins with insertions and modifications that support their peroxidase functions, and include conserved Arg, Pro and Thr residues in addition to the peroxidatic cysteine (Karplus and Hall, 2007). The catalytic cycle of Prx enzymes is initiated with the nucleophilic attack of the thiolate from the peroxidatic Cys on the peroxide substrate, forming the alcohol (or water), which is released, and a sulfenic acid at the active site Cys (R-SOH) (Poole, 2007). The resolution and reductive recycling of the Cys-sulfenic acid back to the thiol form for further catalysis differs in various Prx enzymes. Formation of a disulfide bond with a second, resolving Cys residue occurs in 2-Cys Prx, whereas 1-Cys enzymes form an intermolecular disulfide with a redox donor such as Trx, Grx or glutathione.

The most widespread and well-characterized category of Prxs is the typical 2-Cys Prx group, where the resolving Cys is positioned near the C-terminus of a second monomer, hence a dimeric (or higher order) form of the enzyme is required for activity. Trx is the typical cellular reductant of this class of Prx in eukaryotes, whereas in prokaryotes a gene encoding a specialized flavoprotein disulfide reductase, AhpF, is typically found downstream of the gene for AhpC-like Prx proteins (Wood *et al.*, 2003). Plant Prx proteins may in some cases use Grxs as electron donors (Rouhier *et al.*, 2002). With each of these reductive recycling systems, reduction of the Prx is linked to the cellular reductants NADPH or NADH through a flavoprotein (i.e., Trx reductase, AhpF, or

glutathione reductase); the coupled oxidation of NAD(P)H at 340 nm is followed to measure the catalytic activity of these Prx enzymes.

The question: Can Escherichia coli BCP efficiently use Grx1 as a reductant? Previous studies by Jeong *et al*. (2000) used only DTT and Trx as reductants of BCP. It has since been realized that a group of plant peroxiredoxins that are expressed in chloroplasts, called PrxQ proteins, are also relatives of BCP (Copley *et al* 2004). PrxQ from *Populus tremula* was shown to use a Grx protein, as well as Trx, as the reductant in turnover assays with peroxides (Rouhier *et al* 2004), suggesting that BCP, sharing 40% amino acid sequence identity with PrxQ, may also accept electrons from Grx. Attempts to demonstrate that Grx1 could function as a reducing substrate for BCP in the presence of hydrogen peroxide using a coupled assay with glutathione, glutathione reductase, and NADPH were not informative because of a high background rate in the absence of BCP arising from the nonenzymatic reaction between reduced glutathione and hydrogen peroxide. Another assay was developed that included BCP in high amounts as the terminal electron acceptor and left out peroxide altogether; this assay was used to confirm that Grx1 was able to reduce BCP, avoiding the problematic background reaction (Figure 2-1).

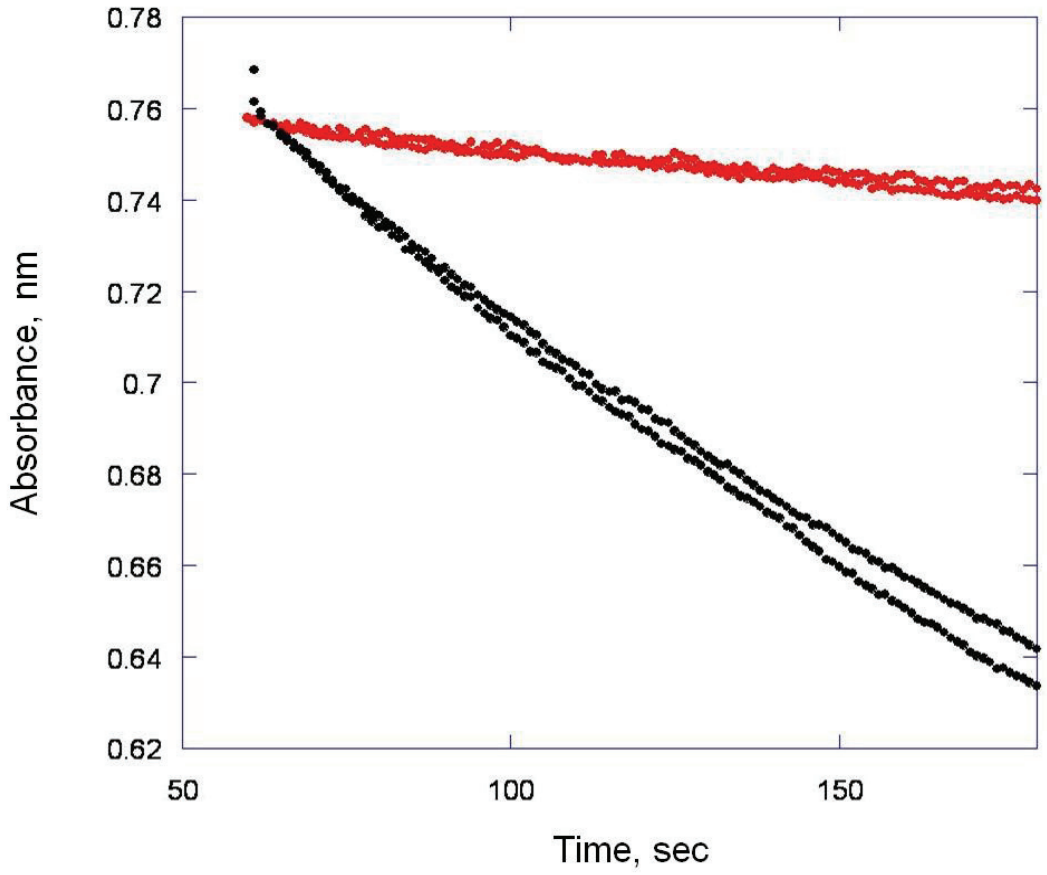

Figure 2-1. Reduction by glutaredoxin (Grx) of oxidized *E. coli* BCP. Using a Grx and glutathione-containing recycling system, assays to monitor reduction of BCP were conducted in the absence of hydrogen peroxide to circumvent the peroxidase activity of GSH towards hydrogen peroxide. Consequently, reduced (red) and oxidized (black) *Ec*BCP served as the terminal electron acceptor in duplicate assays. The assay was monitored at 340 nm and conducted in 50 mM Hepes-NaOH (pH 7.0), 1 mM EDTA, 150 μM NADPH, 1 U/ml glutathione reductase, 1 mM GSH, 2.5 μM Grx1, and 100 μM preoxidized *Ec*BCP.

The problem: Low sensitivity and improperly rate-limited assays for redox functions of bacterial peroxiredoxin systems. In the case of AhpC from *Salmonella typhimurium*, using multicomponent assays (e.g., including NADH, AhpF, AhpC and peroxide), measurements of the enzymatic activity of AhpC revealed no variations in rate for a wide range of concentrations of different hydroperoxide substrates (Parsonage *et al.*, 2008; Parsonage *et al.*, 2005; Poole and Ellis, 1996). The rates obtained were shown to be limited by the ability of AhpF to reduce the disulfide form of AhpC (Poole *et al.*, 2000b). This provided accurate V_{max} and K_m values for the AhpF-AhpC electron transfer interaction (Poole *et al.*, 2000b), but underestimated the reactivity of AhpC with peroxide substrates, promoting the view that Prx proteins are poor enzymes in comparison with heme-dependent peroxidases and catalases (Dietz *et al.*, 2006; Hofmann *et al.*, 2002). Usually, where the coupling enzyme is rate limiting, the solution is to increase the concentration of the coupling enzyme in the assay. In this case of AhpF, however, the assay is complicated by the high NADH oxidase activity of AhpF, whereby the FAD non-covalently bound to the enzyme is reduced by NADH and subsequently reacts directly with molecular oxygen to produce hydrogen peroxide and oxidized NAD^+ (Niimura *et al.*, 1995; Poole and Ellis, 1996). It is possible to carry out these activity measurements under anaerobic conditions to obviate this problem, but only at the expense of making these assays very time-consuming. For these and issues of better sensitivity, a more direct assay to assess catalytic turnover of bacterial *Ec*BCP and AhpC was sought.

The solution: Engineering of fluorescent redox reporters into E. coli Grx1 and the N-terminal domain of AhpF. Unlike Trx, which displays an increase in intrinsic Trp fluorescence when the enzyme is reduced, Grx1 shows no corresponding redox-dependent fluorescence changes. The reason for this is apparent in Figure 2-2, which shows an alignment of the amino acid sequences surrounding the CXXC motif of Grx1, Trx and several other redox-active Trx-like proteins. A Trp residue is found preceding the CXXC active site in both prokaryotic and eukaryotic Trxs, as well as protein disulfide isomerase (Pdi) and several extracytoplasmic Trx-like proteins (Tlps). A second Trp residue is also located three residues upstream of the first in prokaryotic Trxs and Tlps; in *Escherichia coli Trx*, these residues are Trp28 and Trp31. Mutagenesis of these residues in *E. coli* Trx identified Trp31 as the major contributor to fluorescence of oxidized Trx (Krause and Holmgren, 1991), whereas the fluorescence of reduced Trx is dominated by the emission from Trp28 (Slaby *et al.*, 1996). Prokaryotic and eukaryotic Trxs differ in the extent to which their Trp fluorescence increases when they are reduced; *E. coli* Trx undergoes a greater than 3-fold increase in fluorescence, whereas mammalian and yeast enzymes display only a 50-70% increase (Merola *et al.*, 1989).

```
TrxA     FDTDVLKADG AILVDFWAEW CGPCKMIAPI LDEIADEYQG---
TrxC     TLDKLLKDDL PVVIDFWAPW CGPCRNFAPI FEDVAQERSG---
ResA     RIELSDLKGK GVFLNFWGTW CEPCKKEFPY MANQYKHFKS---
TlpA     PKKLSDFRGK TLLVNLWATW CVPCRKEMPA LDELQGKLSG---
DspE     FDQSVLKDGK PLLLNVWATW CPTCRAEHQY LNSLAAQGVR---
Pdi      FESVALDKSK SVLVEFYAPW CGHCKQLAPI YDQLAEKYKD---
HsTrx1   QEALDAAGDK LVVVDFSATW CGPCKMIKPF FHSLSEKYSN---
HsTrx2   FQDRVVNSET PVVVDFHAQW CGPCKILGPR LEKMVAKQHG---
DsbA     TTLEKPVAGA PQVLEFFSFF CPHCYQFEEV LHISDNVKKK---
AhpF     LEQIRDIDGD FEFETYYSLS CHNCPDVVQA LNLMAVLNPR---

HsGrx    QEFVNCKIQP GKVVVFIKPT CPYCRRAQEI LSQLPIKQGL---
Grx1     ---------- MQTVIFGRSG CPYCVRAKDL AEKLSNERDD---
Grx2     ---------- -MKLYIYDH CPYCLKARMI FGLKNIPVEL---
Grx3     ---------M ANVEIYTKET CPYCHRAKAL LSSKGVSFQE---
```

Figure 2-2. Sequence alignment of thioredoxin (Trx)-fold proteins. Partial sequences surrounding the active CXXC motif of Trx and related redox-active proteins were aligned using CLUSTAL (Larkin *et al* 2007) showing the position of Trp residues upstream of the CXXC motif (in bold font). The representative structure above the sequences indicates the β–strand (arrow), turn (inverted U), and α-helix (zig-zag) of the *E. coli* Trx 1 structure. Sequences shown are for: TrxA, *E. coli* Trx 1 (THIO_ECOLI); TrxC, *E. coli* Trx 2 (THIO2_ECOLI); ResA, a Trx-like protein involved in cytochrome c maturation in Bacillus subtilis (RESA_BACSU); TlpA, a membrane-anchored protein thiol:disulfide oxidoreductase essential for cytochrome aa3 maturation in Bradyrhizobium japonicum (TLPA_BRAJA); DspE, an *E. coli* protein required for cytochrome c maturation (DSBE_ECOLI); Pdi, the protein diulfide isomerase from Drosophila melanogaster (PDI_DROME); HsTrx1 and HsTrx2, two human thioredoxins (THIO_HUMAN and THIOM_HUMAN); and AhpF from *Salmonella typhimurium*, the flavoprotein reductase for AhpC (AHPF_SALTY). Also shown are the sequences of one human and three *E. coli* dithiol-containing glutaredoxins of (GLRX1_HUMAN; GLRX1_ECOLI; GLRX2_ECOLI; and GLRX3_ECOLI).

Another redox-active enzyme with a Trx fold structure, DsbA (the key prokaryotic enzyme responsible for formation of disulfide bonds in periplasmic proteins) (Kadokura *et al.*, 2003), also exhibits redox-dependent changes in fluorescence. Although DsbA lacks Trp residues adjacent to the CXXC motif or within the Trx-like domain, two Trp residues are present within a second α-helical domain inserted into the Trx fold. Communication between the disufide of the oxidized active site and Trp76 is mediated by Phe26, resulting in quenching of the Trp fluorescence by the disulfide through an intramolecular, dynamic quenching process (Hennecke *et al.*, 1997). This is responsible for the 3-fold increase in Trp fluorescence when the active-site disulfide of DsbA is reduced (Wunderlich and Glockshuber, 1993).

As seen in Figure 2-3, placing a Trp residue in *E. coli* Grx1 corresponding to Trp31 of *E. coli* Trx would involve replacing the smallest possible amino acid (Gly) with the largest (Trp). Because this position is adjacent to the redox center, it is possible that this Gly contributes to the specificity of each of these redox domains for given substrates. As an alternative, we chose to mutate a nearby site in Grx1, adjacent to the location of Trp28 in *E. coli* Trx, which already includes a bulky, aromatic residue, creating the F6W mutant of Grx1 (Figure 2-3b). Described in this chapter are the characterization and use of this mutant to very sensitively and accurately measure *Ec*BCP activity.

As another potential electron donor to Prx proteins, the NTD of AhpF of *S. typhimurium* was also of interest and was under investigation as reductant of another bacterial Prx, AhpC. Amino acid sequence analysis of AhpF revealed

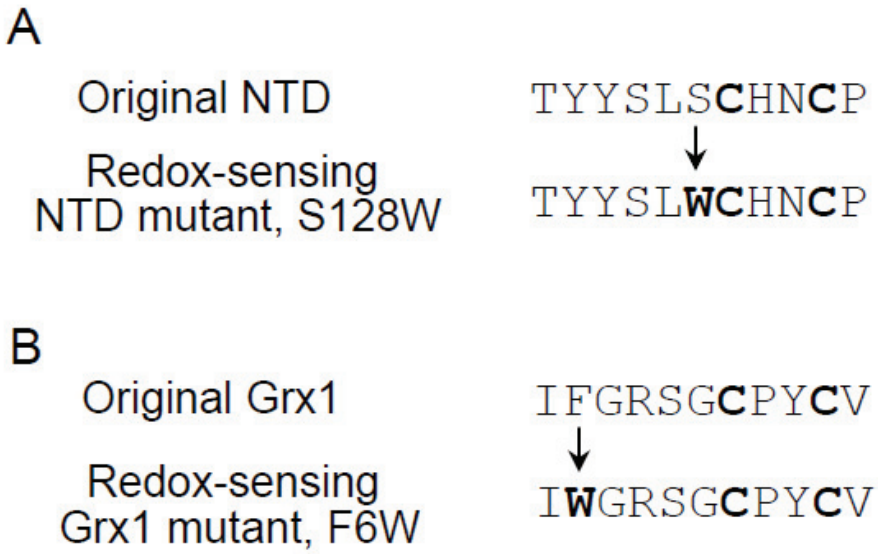

Figure 2-3. Strategies for introducing Trp residues as fluorophores into electron transferring proteins. Shown are the original sequences surrounding the active site cysteine residues for the N-terminal domain (NTD) of *S. typhimurium* AhpF (A) and *E. coli* Grx1 (B) as well as their respective mutated forms used to provide redox-sensitive fluorophores near the active site, S128W NTD and $Grx1_{F6W}$, respectively.

that this protein contains C-terminal domains homologous with those of prokaryotic Trx reductase and an N-terminal domain homologous to Trx, fused into one polypeptide (Poole *et al.*, 2000a). These two fragments of AhpF could be separated by limited proteolysis using trypsin (Poole, 1996), or separately expressed and purified as distinct Trx reductase- and Trx-like fragments (Poole *et al.*, 2000a). The fold of the N-terminal domain (NTD) of AhpF is, in fact, a tandem duplication of Trx folds in which only the second repeat retains the characteristic CXXC redox active dithiol motif (Hall *et al.*, 2009b; Wood *et al.*, 2001). The overall AhpC reductase activity of AhpF could be reconstituted, albeit much less efficiently, by mixing the two fragments (Poole *et al.*, 2000a). This structural homology of AhpF to Trx and Trx reductase was later confirmed by solution of the three-dimensional structure of AhpF by X-ray crystallography (Wood *et al.*, 2001). In order to use the AhpF NTD in fluorescence-monitored assays of AhpC-dependent peroxidase activities, we mutated the NTD (comprised of residues 1-202 of AhpF) to contain the equivalent of *E. coli* Trx1 Trp31, generating S128W NTD (Figure 2-3a) (Parsonage *et al.*, 2005).

Both Grx1 F6W and AhpF S128W constructs were successful in yielding highly active, CXXC-containing redox domains that could be used to directly monitor electron transfer reactions in simple, three component (donor – Prx – peroxide) assays conducted using a stopped-flow spectrofluorometer, as described in detail below.

MATERIALS

Solutions

25 mM Potassium phosphate, pH 7.0, 1 mM EDTA (standard buffer)

50 mM Potassium phosphate, pH 7.0, 0.5 mM EDTA, 100 mM ammonium sulfate (AhpC reaction buffer)

50 mM H_2O_2 (approximately 456 µl 30% solution in 100 ml H_2O)

100 mM Cumene hydroperoxide (concentrate diluted approximately 60-fold into dimethyl sulfoxide)

100 mM *t*-Butyl hydroperoxide

~30 mM NADH or NADPH (~2.5 mg per 100 µl 50 mM Tris-HCl, pH 8.0, stored at 4 °C in the dark for < 1 day)

100 mM 1,4-Dithio-DL-threitol (DTT), 154.2 g/mole (aliquots stored at –80 °C)

Glutathione, reduced

Hydroxyethyldisulfide (HED) (disulfide-bonded form of 2-mercaptoethanol)

Chemical Modification Agents

5,5'-Dithiobis(2-nitrobenzoic acid) (DTNB), 396.4 g/mole

2-Nitro-5-thiobenzoic acid (TNB) solution, equimolar DTNB and dithiothreitol mixed) (Poole and Ellis, 2002)

Proteins

S. typhimurium AhpC purified essentially as described previously (Parsonage *et al.*, 2008). Aliquots were stored at -80 °C at a concentration of 10 mg/ml.

S. typhimurium AhpF purified essentially as described previously (Poole and Ellis, 1996). Aliquots were stored at -80 °C at a concentration of 10 mg/ml. N-terminal domain (NTD) of *S. typhimurium* AhpF, and S128W mutant of the NTD, were purified as described previously (Poole *et al.*, 2000a). The S128W mutant was created using a QuikChange mutagenesis kit (Parsonage *et al.*, 2005). Aliquots of purified protein were stored at 10 mg/ml at -80 °C.

E. coli Grx 1 and the F6W mutant of Grx1 were expressed as His-tagged versions, purified first using a His-trap chelating column (GE Healthcare), cleaved with biotinylated-thrombin (Novagen), then further purified by gel filtration chromatography as described previously (Yamamoto *et al.*, 2008). The F6W mutant was generated and expressed essentially as described previously for S128W NTD, and purified by the same method as wild-type Grx1.

E. coli BCP was expressed in an *ahpC*-lacking *E. coli* strain (TA4315) and purified by a combination of QSepharose, Superose 12 prep grade and ceramic hydroxyapatite columns (see Chapter 3 for details).

Glutathione reductase from baker's yeast was purchased from Sigma.

METHODS and RESULTS

***Generation and testing of the F6W mutant of E. coli Grx1 as an electron donor to E. coli BCP*.** Generation of the pure, mutated Grx1 protein was straightforward. The F6W mutant Grx1 ($Grx1_{F6W}$) was created using the QuikChange method; mutant and wild-type Grx1 were expressed and purified as described previously (Yamamoto *et al*, 2007). Briefly, the protein was expressed from a T7 expression vector with a N-terminal His tag. After purification on a His-Trap chelating column, the His-tag was removed by cleaving with thrombin, followed by gel filtration. As had been intended, the F6W mutant displays higher overall fluorescence than wild-type Grx1; in addition, $Grx1_{F6W}$ shows a nearly 2-fold increase in fluorescence upon reduction (Figure 2-4). This allows a dramatic increase in the sensitivity in assays where the redox state of Grx1 is monitored.

To evaluate functional features of the new mutant protein, the catalytic activities of wild-type and $Grx1_{F6W}$ were compared using an assay based upon the ability of Grx to catalyze the reduction of a mixed disulfide formed between glutathione and the small molecule hydroxyethyldisulfide (HED) (Holmgren and Åslund, 1995). The resulting oxidized glutathione is reduced by glutathione reductase, allowing the reaction to be monitored by oxidation of NADPH measured spectrophotometrically at 340 nm. The activities of wild-type and F6W mutant Grx1 using this assay were found to be essentially identical (Figure 2-5). Additionally, $Grx1_{F6W}$ activity with *Ec*BCP was confirmed using a modified version of the previously described NADPH-linked assay with CHP serving as the final electron acceptor instead of oxidized *Ec*BCP (Figure 2-6).

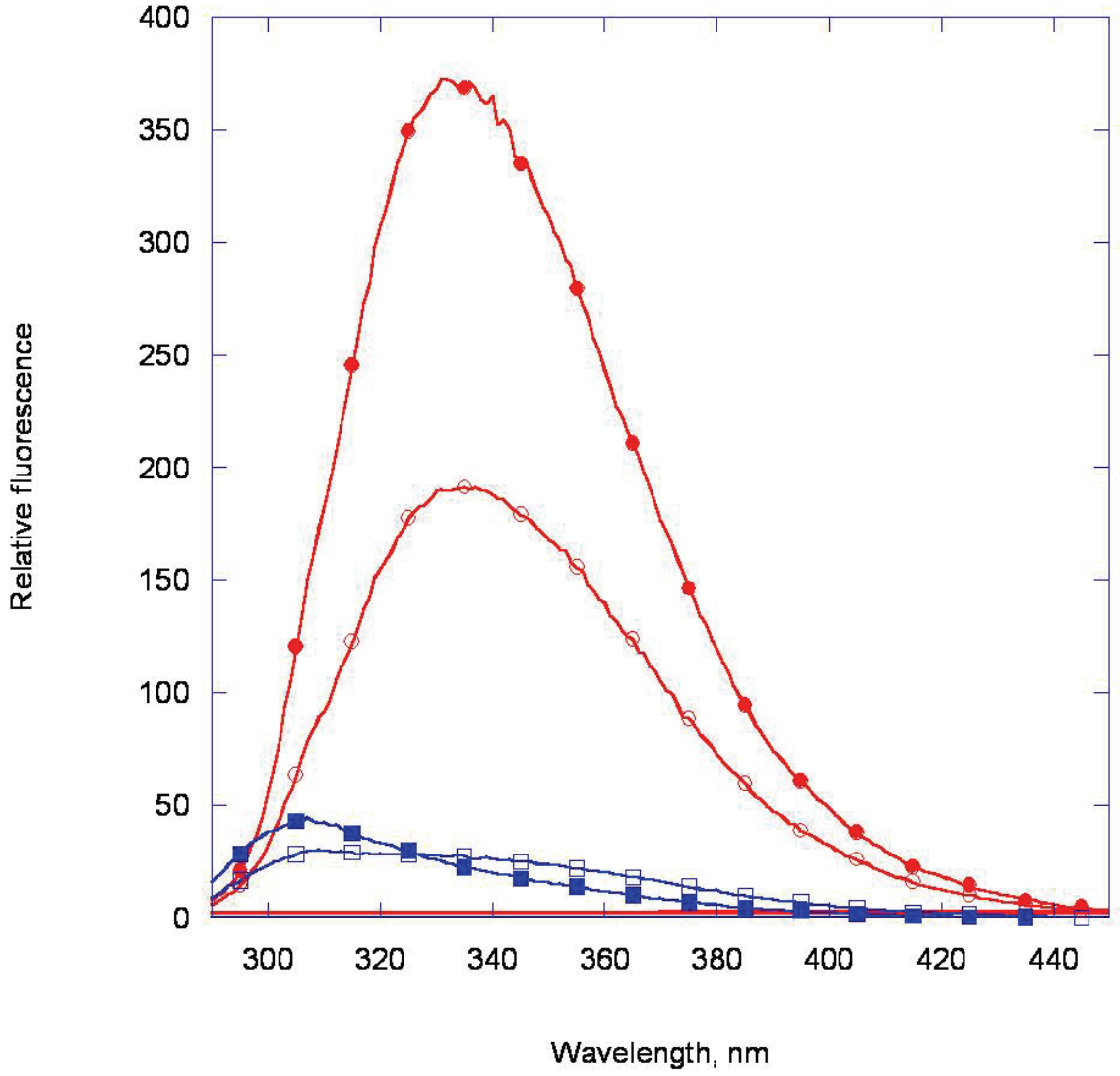

Figure 2-4. Fluorescence emission spectra of oxidized and reduced forms of *E. coli* Grx1 and $Grx1_{F6W}$. Fluorescence intensity was measured with excitation at 280 nm using a Varian Cary Eclipse fluorescence spectrophotometer. Proteins in 50 mM potassium phosphate buffer (pH 7) with 1 mM EDTA included 10 μM each oxidized (open blue squares) or reduced (closed blue squares) Grx1, and oxidized (open red circles) or reduced (closed red circles) $Grx1_{F6W}$.

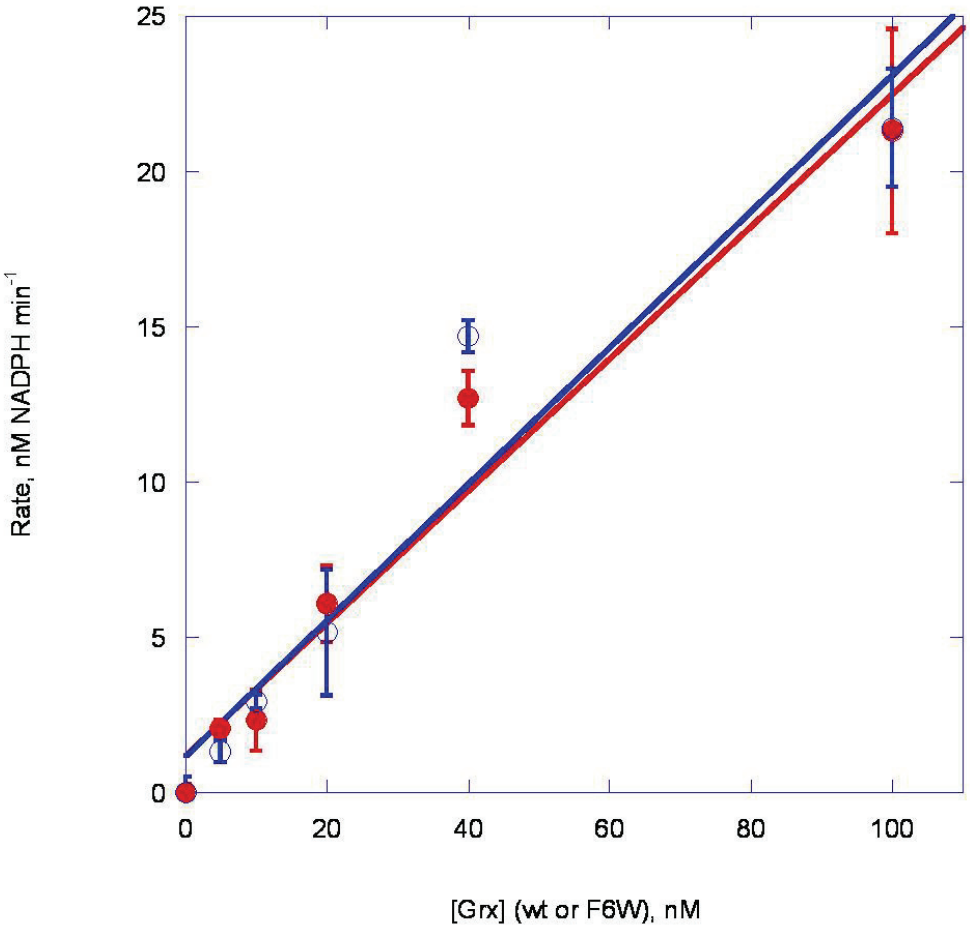

Figure 2-5. Grx1 and $Grx1_{F6W}$ activity comparision utilizing β-hydroxyethylene disulfide. A comparison of activity of Grx1 and $Grx1_{F6W}$ with GSH in the GSH-dependent disulfide reductase assay with hydroxyethyldisulfide (HED) indicates tha $Grx1_{F6W}$ is as active as wild-type Grx1. The HED assay (Holmgren and Åslund, 1995) couples the reduction of a glutathione-linked mixed disulfide to oxidation of NADPH, monitored by the decrease in 340 nm absorbance. The reaction mixture (0.5 mL) contained 100 mM Tris-Cl pH 8.0 buffer with 2 mM EDTA, 0.7 mM HED, 1 mM GSH, 0.2 mM NADPH, 0.1 mg/ml BSA, 0.12 μM glutathione reductase, and 5-100 nM wild-type Grx1 (open circles, blue line) or $Grx1_{F6W}$ (closed circles,, red line).

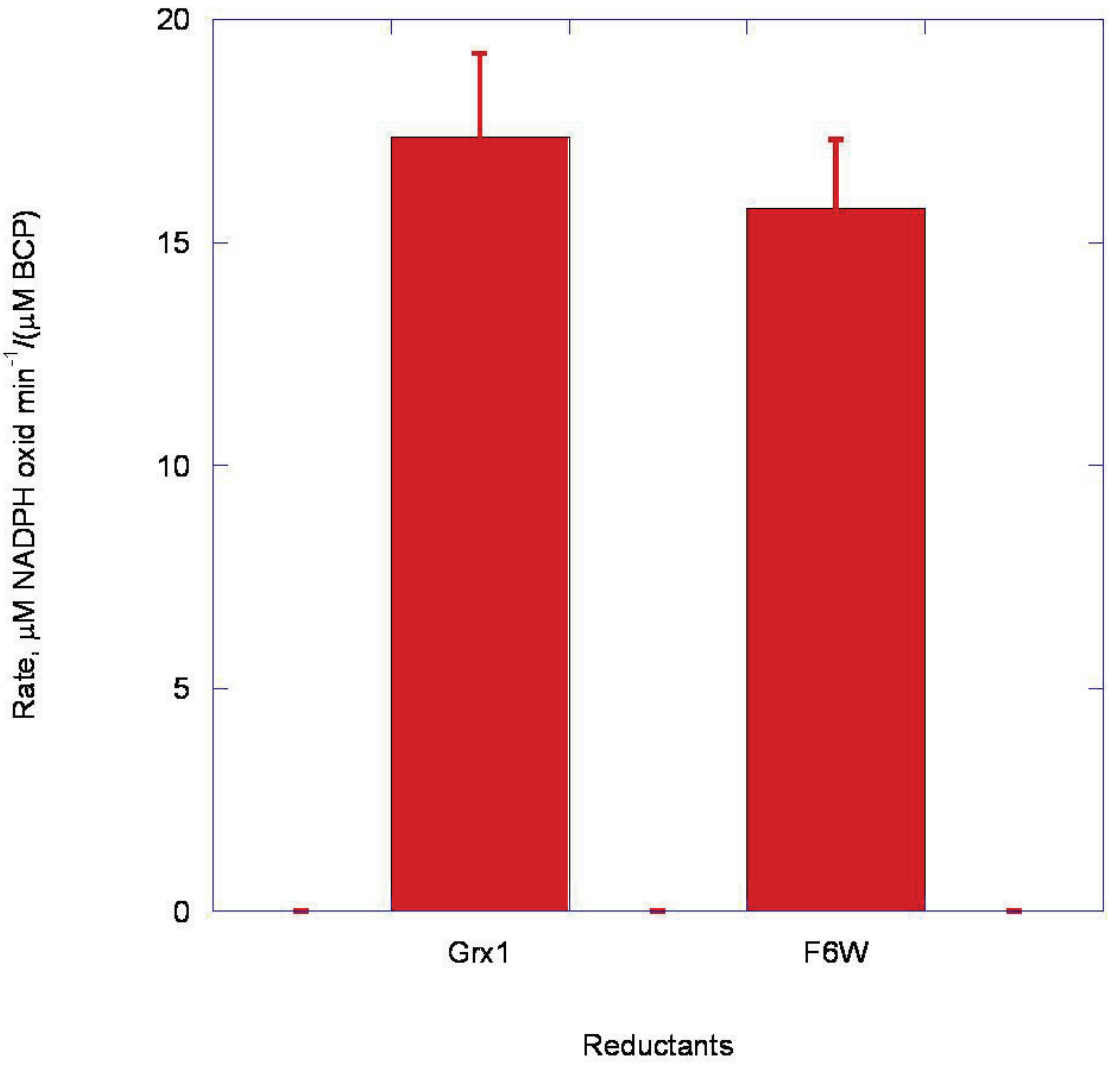

Figure 2-6. A comparison of activity of Grx1 and $Grx1_{F6W}$ in a NADPH-linked assay with cumene hydroperoxide. The glutathione reductase (GR)/GSH system was used to compare glutaredoxin as a reductant. The reaction mixture was similar to the previously described method in chapter 3 with 150 μM NADPH, 1 U/ml of GR, 1 mM GSH, and 10 μM of one of the following reductants: Grx1 or $Grx1_{F6W}$. Activity was measured by following the oxidation of NADPH at A_{340}.

Fluorescence-based peroxidase activity assays of EcBCP with $Grx1_{F6W}$ using stopped-flow analysis. For a bisubstrate kinetic characterization of *Ec*BCP, reaction rates have to be determined over varying concentrations of both reductant ($Grx1_{F6W}$) and hydroperoxide. As there is no regeneration of the reductant, it is necessary to use a stopped-flow spectrofluorometer to measure this reaction as the initial rates are only linear for the first few seconds of the reaction. Solutions containing reduced $Grx1_{F6W}$ and *Ec*BCP in one syringe are mixed with solutions of different concentrations of hydroperoxide (including hydrogen peroxide, ethyl hydroperoxide, cumene hydroperoxide and *t*-butyl hydroperoxide).

For the stopped-flow experiments shown in this chapter, solutions contained 10 μM concentrations of the prereduced $Grx1_{F6W}$ along with 0.5 μM *Ec*BCP. The solutions used in the stopped flow are all prepared in 50 mM phosphate buffer. Typically, using an Applied Photophysics stopped flow instrument, 5 to 7 ml is sufficient to determine the rate of reaction at one concentration of $Grx1_{F6W}$ and a range of peroxide substrate concentrations. If the *Ec*BCP has been stored in a buffer containing a component that will interfere with the reaction assay, DTT for example, a small desalting column should be used to transfer the enzyme into peroxidase reaction buffer, or a compatible buffer if necessary. Care should be taken to minimize changes in buffer composition during the measurements. Four to five sets of experiments with each set at a different concentration of $Grx1_{F6W}$ can be carried out in a normal working day.

The solutions containing a range of peroxide concentrations are prepared from the 50 mM stock or a dilution of the stock in peroxidase reaction buffer. The initial 50 mM dilution is freshly prepared and made in water or DMSO in the case of cumene hydroperoxide; further dilutions are made using 50 mM phophate buffer. Sufficient volumes of each dilution are made for all the sets of experiments to be carried out on that day. Aliquots of each concentration are removed to load into the drive syringes for each rate determination, then discarded. This minimizes any possible contamination of the peroxide solutions with enzyme. It is important to remember that stopped flow instruments usually mix equal volumes of reactants, so that all solutions need to be made twice the final concentration.

For best performance, the stopped flow instrument should be allowed to warm up in order to stabilize the lamp output, photomultiplier detectors and the temperature of the mixing chamber. The stopped flow spectrophotometer is set up to measure fluorescence with excitation at 280 nm and emission monitored at 90° and at wavelengths >320 nm using an emission filter. The solution of $Grx1_{F6W}$ and *Ec*BCP is first mixed in the stopped flow with 50 mM phosphate buffer and the photomultiplier voltage is set to give 80% of maximum signal. The signal should be monitored to ensure that the fluorescence signal is stable in the absence of any reaction. The buffer is then replaced by a peroxide solution of concentration higher than $Grx1_{F6W}$, and after temperature equilibration (~5 min) mixed with the solution of enzymes. The reaction is followed until no further change occurs. After extrapolating the signal back to time = 0 s, the total change

in fluorescence is calculated; this is defined as the change in fluorescence (signal voltage) caused by the oxidation of the known amount of $Grx1_{F6W}$. Hence, the rates measured in V/s can now be converted to rates in terms of μM $Grx1_{F6W}$ oxidized s^{-1} μM^{-1} BCP. This determination should be carried out at least in duplicate. The initial rate of fluorescence change for each assay is observed for the first 5 s. This reaction is repeated until at least 3 consistent traces are obtained. The next concentration of peroxide substrate is loaded into the drive syringe and allowed to thermally equilibrate while the previously obtained traces are averaged and the initial linear rate calculated by linear regression. This is repeated until rates have been measured with all the different peroxide solutions or fail to further increase with higher peroxide concentrations. At this point, the next concentration of $Grx1_{F6W}$ with *Ec*BCP is loaded into the drive syringe, and the photomultiplier voltage adjusted and the calibration of the fluorescence signal carried out as before. Examples of the resulting fluoresence changes are shown in Figure 2-7 with varying amounts of hydrogen peroxide.

The first step in analyzing the data is to determine the appropriate kinetic mechanism to apply. This is done by plotting the data using a linearized form of the Michaelis-Menten equation, for example the Hanes plot (Cornish-Bowden, 2004). An example of a Hanes plot of data obtained with wild-type AhpC and *t*-butyl hydroperoxide in shown in Figure 2-8. The intersection of the lines at the y-axis indicates a substituted enzyme (ping-pong) mechanism for AhpC. Consequently, all the rate data obtained for one peroxide substrate can be fit to

Equation 1:

$$\text{Rate} = \frac{k_{cat} \cdot [\text{S128W}] \cdot [\text{ROOH}]}{(K_m\ \text{S128W} \cdot [\text{ROOH}] + K_m\ \text{ROOH} \cdot [\text{S128W}] + [\text{ROOH}] \cdot [\text{S128W}])} \quad \text{Eq. 1}$$

using the multiple-function nonlinear regression capability of Sigmaplot (Systat Software, Inc. San Jose, CA) to calculate a global fit for k_{cat} and K_m of the two substrates (Figure 2-8). Kinetic analyses of a range of hydroperoxide substrates and AhpC mutants have been conducted using these approaches (Parsonage *et al.*, 2008; Parsonage *et al.*, 2005).

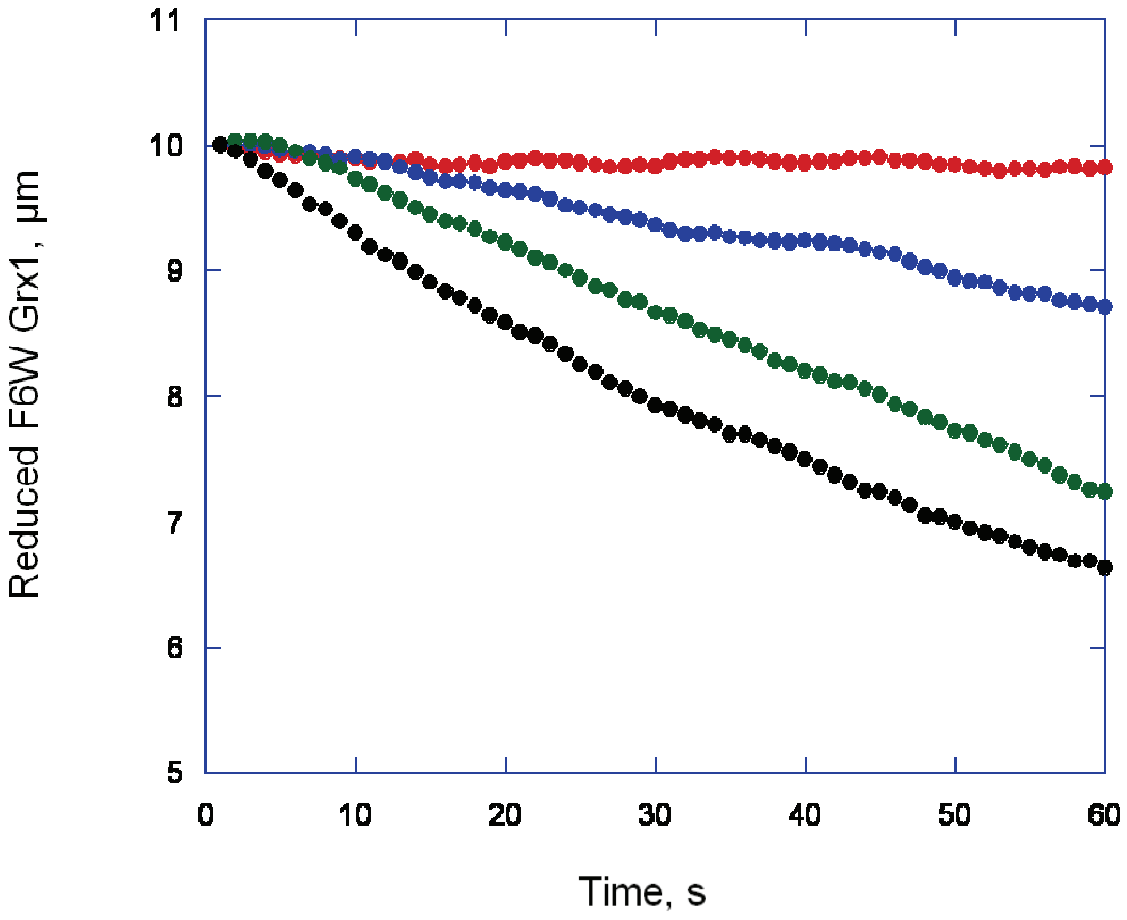

Figure 2-7. Reaction of BCP with hydrogen peroxide, monitored by $Grx1_{F6W}$ fluorescence. BCP (0.5 µM) and 10 µM $Grx1_{F6W}$ were combined with 0 (red), 5 (blue), 20 (green), or 200 (black) µM hydrogen peroxide (in order of increasing downward slope) in a stopped flow spectrofluorometer. The buffer in both syringes was 50 mM potassium phosphate, 0.5 mM EDTA at 25 °C. Fluorescence excitation was at 280 nm, with emission measured at >320 nm.

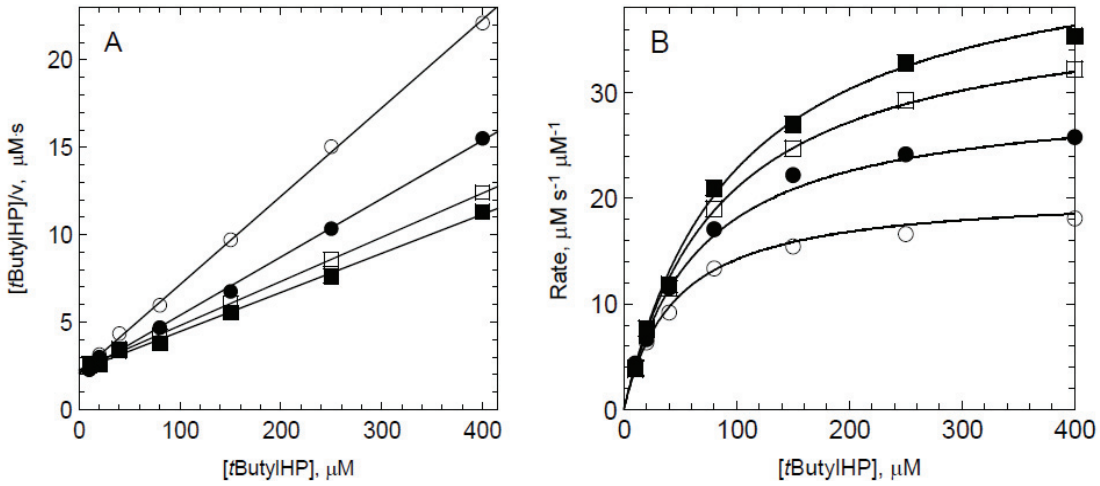

Figure 2-8. Kinetics of *t*-butyl hydroperoxide reduction by AhpC. S128W NTD (pre-reduced by dithiothreitol) and 100 nM AhpC were mixed with 10-400 μM *t*-butyl hydroperoxide in a stopped-flow spectrophotometer at 25 °C. All concentrations are after mixing. The buffer was 50 mM potassium phosphate pH 7.0, 0.5 mM EDTA and 100 mM ammonium sulfate. The reaction rate was measured by monitoring the fluorescence change of S128W NTD with excitation at 280 nm, and emission >320 nm. The fixed concentrations of S128W NTD in assays over a range of t-butyl hydroperoxide were 2.5 μM (○), 5 μM (●), 10 μM (□) and 20 μM (■). A Hanes plot of the data (panel A) shows that lines drawn through the data points intersect on the y-axis, indicating that AhpC is following a substituted enzyme mechanism. The rate data with global non-linear regression fits to the data are plotted in panel B with calculated values for K_m (tButylHP) of 119 ± 4 μM, K_m (S128W) of 4.1 ± 0.2 μM, and k_{cat} of 55 ± 1 s^{-1}.

Characterization of the fluorescence and activity of the S128W mutant of the NTD of S. typhimurium AhpF. The S128W mutant of the independently-expressed NTD of *S. typhimurium* AhpF was highly overexpressed from a T7 promoter using several *E. coli* strains, and was readily purified in large amounts (Parsonage *et al.*, 2005). Introduction of a third Trp into the NTD was expected to increase the 280 nm extinction coefficient, so the 280 nm absorbance of a solution of S128W NTD was compared to the protein content measured by the microbiuret assay. This gave an experimentally determined extinction coefficient of 21,250 M^{-1} cm^{-1} at 280 nm for S128W NTD, higher than the value of 15,100 M^{-1} cm^{-1} for wild-type NTD.

Comparison of the fluorescence of equal concentrations of reduced and oxidized S128W NTD revealed that the reduced form was 12% more fluorescent than the oxidized form (excitation at 280 nm, emission peak at 343 nm). This is a smaller difference between redox states than is seen with *E. coli* Trx, but was sufficient for the measurement of AhpC reacting with 0.5 μM H_2O_2 in the presence of 40 μM S128W (conditions exhibiting the smallest change in fluorescence measured). Therefore; the sensitive, redox-dependent fluorescence of S128W NTD can be utilized in stopped-flow spectrophotometric assays similar to those conducted with $Grx1_{F6W}$ and *Ec*BCP. Kinetic analyses of a range of hydroperoxide substrates and AhpC mutants conducted using these approaches have been published elsewhere (Parsonage *et al.*, 2008; Parsonage *et al.*, 2005).

SUMMARY

We have described two systems in which an amino acid near the redox-active CXXC motif has been mutated to Trp, mimicking the Trp(s) at the active site of Trx. The resultant redox-dependent changes in fluorescence of the introduced Trp allow the oxidation of the protein to be monitored directly. We have used these two systems to examine the kinetics of two different peroxiredoxin enzymes. These principles could be extended to other peroxiredoxins with non-Trx reductants, and also to other redox systems where there is little or no detectable spectral signal.

REFERENCES

Atkinson, H. J., and Babbitt, P. C. (2009). An atlas of the thioredoxin fold class reveals the complexity of function-enabling adaptations. *PLoS Comput Biol*. **5,** e1000541. Cornish-Bowden (2004). Fundamentals of Enzyme Kinetics. Portland Press Ltd., London.

Dietz, K. J., Jacob, S., Oelze, M. L., Laxa, M., Tognetti, V., de Miranda, S. M., Baier, M., and Finkemeier, I. (2006). The function of peroxiredoxins in plant organelle redox metabolism. *J Exp Bot*. **57,** 1697-709.

Ellis, H. R., and Poole, L. B. (1997). Roles for the two cysteine residues of AhpC in catalysis of peroxide reduction by alkyl hydroperoxide reductase from *Salmonella typhimurium*. *Biochemistry*. **36,** 13349-56.

Hall, A., Karplus, P. A., and Poole, L. B. (2009a). Typical 2-Cys peroxiredoxins - structures, mechanisms and functions. *Febs J*. **276,** 2469-77.

Hall, A., Parsonage, D., Horita, D., Karplus, P. A., Poole, L. B., and Barbar, E. (2009b). Redox dependent dynamics of a dual thioredoxin fold protein: evolution of specialized folds. *Biochemistry*. **48,** 5984-93.

Hennecke, J., Sillen, A., Huber-Wunderlich, M., Engelborghs, Y., and Glockshuber, R. (1997). Quenching of tryptophan fluorescence by the active-site disulfide bridge in the DsbA protein from *Escherichia coli* . *Biochemistry*. **36,** 6391-400.

Hofmann, B., Hecht, H.-J., and Flohé, L. (2002). Peroxiredoxins. *Biol. Chem.* **383,** 347-364.

Holmgren, A. (1972). Tryptophan fluorescence study of conformational transitions of the oxidized and reduced form of thioredoxin. *J Biol Chem*. **247,** 1992-8.

Holmgren, A., and Åslund, F. (1995). Glutaredoxin. *Methods Enzymol*. **252,** 283-92.

Jönsson, T. J., Ellis, H. R., and Poole, L. B. (2007). Cysteine reactivity and thiol-disulfide interchange pathways in AhpF and AhpC of the bacterial alkyl hydroperoxide reductase system. *Biochemistry*. **46,** 5709-21.

Kadokura, H., Katzen, F., and Beckwith, J. (2003). Protein disulfide bond formation in prokaryotes. *Annu Rev Biochem*. **72,** 111-35.

Karplus, P. A., and Hall, A., Structural Survey of the Peroxiredoxins. In: L. Flohé, J. R. Harris, Eds.), Peroxiredoxin Systems. Springer, New York, 2007, pp. 41-60.

Krause, G., and Holmgren, A. (1991). Substitution of the conserved tryptophan 31 in *Escherichia coli* thioredoxin by site-directed mutagenesis and structure-function analysis. *J Biol Chem*. **266,** 4056-66.

Larkin, M. A., Blackshields, G., Brown, N. P., Chenna, R., McGettigan, P. A., McWilliam, H., Valentin, F., Wallace, I. M., Wilm, A., Lopez, R., Thompson, J. D., Gibson, T. J., and Higgins, D. G. (2007). Clustal W and Clustal X version 2.0. *Bioinformatics*. **23,** 2947-8.

Merola, F., Rigler, R., Holmgren, A., and Brochon, J. C. (1989). Picosecond tryptophan fluorescence of thioredoxin: evidence for discrete species in slow exchange. *Biochemistry*. **28,** 3383-98.

Nelson, K. J., Parsonage, D., Hall, A., Karplus, P. A., and Poole, L. B. (2008). Cysteine pKa values for the bacterial peroxiredoxin AhpC. *Biochemistry*. **47,** 12860–12868.

Niimura, Y., Poole, L. B., and Massey, V. (1995). *Amphibacillus xylanus* NADH oxidase and *Salmonella typhimurium* alkyl-hydroperoxide reductase flavoprotein components show extremely high scavenging activity for both alkyl hydroperoxide and hydrogen peroxide in the presence of *S. typhimurium* alkyl-hydroperoxide reductase 22-kDa protein component. *J Biol Chem*. **270,** 25645-50.

Parsonage, D., Karplus, P. A., and Poole, L. B. (2008). Substrate specificity and redox potential of AhpC, a bacterial peroxiredoxin. *Proc Natl Acad Sci U S A*. **105,** 8209-14.

Parsonage, D., Youngblood, D. S., Sarma, G. N., Wood, Z. A., Karplus, P. A., and Poole, L. B. (2005). Analysis of the link between enzymatic activity and oligomeric state in AhpC, a bacterial peroxiredoxin. *Biochemistry*. **44,** 10583-92.

Poole, L. B. (1996). Flavin-dependent alkyl hydroperoxide reductase from *Salmonella typhimurium*. 2. Cystine disulfides involved in catalysis of peroxide reduction. *Biochemistry*. **35,** 65-75.

Poole, L. B., Flavin-linked redox components required for AhpC reduction in alkyl hydroperoxide reductase systems. In: S. Ghisla, *et al*., Eds.), Flavins and Flavoproteins. 1999. Agency for Scientific Publications, Berlin, 1999, pp. 195-202.

Poole, L. B. (2005). Bacterial defenses against oxidants: mechanistic features of cysteine-based peroxidases and their flavoprotein reductases. *Arch Biochem Biophys*. **433,** 240-54.

Poole, L. B., The Catalytic Mechanism of Peroxiredoxins. In: L. Flohé, J. R. Harris, Eds.), Peroxiredoxin Systems. Springer, New York, 2007, pp. 61-81.

Poole, L. B., and Ellis, H. R. (1996). Flavin-dependent alkyl hydroperoxide reductase from *Salmonella typhimurium*. 1. Purification and enzymatic activities of overexpressed AhpF and AhpC proteins. *Biochemistry*. **35,** 56-64.

Poole, L. B., and Ellis, H. R. (2002). Identification of cysteine sulfenic acid in AhpC of alkyl hydroperoxide reductase. *Methods Enzymol*. **348,** 122-36.

Poole, L. B., Godzik, A., Nayeem, A., and Schmitt, J. D. (2000a). AhpF can be dissected into two functional units: tandem repeats of two thioredoxin-like folds in the N-terminus mediate electron transfer from the thioredoxin reductase-like C-terminus to AhpC. *Biochemistry*. **39,** 6602-15.

Poole, L. B., Higuchi, M., Shimada, M., Calzi, M. L., and Kamio, Y. (2000b). *Streptococcus mutans* H2O2-forming NADH oxidase is an alkyl hydroperoxide reductase protein. *Free Radic Biol Med*. **28,** 108-20.

Riddles, P. W., Blakeley, R. L., and Zerner, B. (1979). Ellman's reagent: 5,5'-dithiobis(2-nitrobenzoic acid)--a reexamination. *Anal Biochem*. **94,** 75-81.

Rouhier, N., Gelhaye, E., and Jacquot, J. P. (2002). Glutaredoxin-dependent peroxiredoxin from poplar: protein-protein interaction and catalytic mechanism. *J Biol Chem*. **277,** 13609-14.

Slaby, I., Cerna, V., Jeng, M. F., Dyson, H. J., and Holmgren, A. (1996). Replacement of Trp28 in *Escherichia coli* thioredoxin by site-directed mutagenesis affects thermodynamic stability but not function. *J Biol Chem*. **271,** 3091-6.

Wood, Z. A., Poole, L. B., and Karplus, P. A. (2001). Structure of intact AhpF reveals a mirrored thioredoxin-like active site and implies large domain rotations during catalysis. *Biochemistry*. **40,** 3900-11.

Wood, Z. A., Schröder, E., Harris, J. R., and Poole, L. B. (2003). Structure, mechanism and regulation of peroxiredoxins. *Trends Biochem Sci*. **28,** 32-40.

Wunderlich, M., and Glockshuber, R. (1993). Redox properties of protein disulfide isomerase (DsbA) from *Escherichia coli* . *Protein Sci*. **2,** 717-26.

Yamamoto, Y., Ritz, D., Planson, A. G., Jonsson, T. J., Faulkner, M. J., Boyd, D., Beckwith, J., and Poole, L. B. (2008). Mutant AhpC Peroxiredoxins Suppress Thiol-Disulfide Redox Deficiencies and Acquire Deglutathionylating Activity. *Mol Cell*. **29,** 36-45.

Chapter 3: Kinetic and Thermodynamic Features Reveal That *E. coli* BCP Is an Unusually Versatile Peroxiredoxin

Stacy A. Reeves, Derek Parsonage, Kimberly J. Nelson, and Leslie B. Poole

This chapter was submitted to Biochemistry in June of 2011. Reeves performed the kinetic experiments, analytical ultracentrifugation studies, and pK_a analysis. Dr. Parsonage assisted Reeves with pK_a experiments. Dr. Nelson performed the bioinformatic analysis of BCP subfamily members. Dr. Poole is serving in an advisory and editorial capacity.

ABSTRACT

In *Escherichia coli*, bacterioferritin-comigratory protein (BCP) is a peroxiredoxin (Prx) which catalyzes the reduction of H_2O_2 and organic hydroperoxides. This protein, along with plant PrxQ, is a founding member of one of the least studied subfamilies of Prxs. Recent structural data have suggested that proteins in the BCP/PrxQ group can exist as monomers or dimers; we report here that, by analytical ultracentrifugation, both oxidized and reduced *E. coli* BCP behave as monomers in solution at concentrations as high as 200 μM. Unexpectedly, thioredoxin (Trx1)-dependent peroxidase assays conducted by stopped flow spectroscopy demonstrated that $V_{max,app}$ increases with increasing Trx1 concentrations, indicating a nonsaturable interaction (K_m > 100 μM). At a physiologically reasonable Trx1 concentration of 10 μM, the apparent K_m value for H_2O_2 is ~80 μM, and overall V_{max}/K_m for H_2O_2, which remains constant over the various Trx1 concentrations (consistent with a ping-pong mechanism), is about 1.3 x 10^4 M^{-1} s^{-1}. Our kinetic analyses demonstrated that BCP can utilize a variety of reducing substrates, including Trx1, Trx2, Grx1 and Grx3. BCP exhibited a high redox potential of -145.9 ± 3.2 mV, the highest to date observed for a Prx. Moreover, BCP exhibited a broad peroxide specificity, with comparable rates for H_2O_2 and cumene hydroperoxide. We determined a pK_a of ~5.8 for the peroxidatic cysteine (Cys45) using both spectroscopic and activity titration data. These findings support an important role for BCP in interacting with multiple substrates and remaining active under highly

oxidizing cellular conditions, potentially serving as a defense enzyme of last resort.

Like all aerobic bacteria, *Escherichia coli* must cope with damaging endogenous sources of reactive oxygen species (ROS) that result from autoxidation of components of the aerobic respiratory chain and byproducts of reactions with ferrous iron (Fenton chemistry) (Imlay, 2008). In addition, *E. coli* is exposed to endogenous ROS released from other bacteria to ward-off non-commensal intruders as well as macrophages and neutrophils, which release ROS as part of their microbicidal arsenals (Eschenbach *et al.*, 1989; Miller and Britigan, 1997; Ryan and Kleinberg, 1995). In response, *E. coli* employs a variety of antioxidant defense mechanisms including proteins such as superoxide dismutase and catalase and small molecules such as glutathione. Included among the defenses are a number of proteins that detoxify hydrogen peroxide and/or organic hydroperoxides, including KatG (HPI) and HPII (cytosolic and periplasmic catalases, respectively), BtuE (a glutathione peroxidase homologue), and three distinct members of the peroxiredoxin (Prx) family (Baker and Poole, 2003).

Prxs are fundamentally important, highly expressed, cysteine-dependent peroxidases found in nearly all organisms. Unlike catalase, which converts H_2O_2 to H_2O and O_2, Prxs convert H_2O_2 into two H_2O molecules with the reducing equivalents ultimately coming from NADPH or NADH. In all Prxs, the active site (or peroxidatic) Cys (denoted C_p) is located within a conserved ($PXXXTXXC_p$) motif (Nelson *et al.*, 2011). This active site Cys reacts with hydroperoxide substrates to generate a sulfenic acid [R-SOH, here denoted Cys(O)]. In many Prxs, a second Cys (the so-called resolving Cys, denoted C_r) reacts with the

Cys(O) to form a disulfide bond that prevents further damaging oxidation of the C_p and provides an accessible, disulfide-bonded substrate for recycling by Trx- or Trx-like redoxins (Jönsson *et al.*, 2007; Poole, 2005; Poole *et al.*, 2000b). Multiple Prxs are often expressed in a given organism, yet they cannot typically substitute for one another in knockout experiments. In eukaryotes, the role of Prxs clearly extends beyond simple detoxification into such complex phenomena as the regulation of cell signaling, resistance toward radiation treatment, and tumor suppression, though precise roles and mechanisms of these aspects are a major area of research in this field (Neumann *et al.*, 2003; Winterbourn, 2008; Wood *et al.*, 2003; Woolston *et al.*, 2011; Zhang *et al.*, 2009).

E. coli contains three Prxs from three different subfamilies: AhpC (Prx1/AhpC subfamily), Tpx (Tpx subfamily), and BCP (also known as bacterioferritin comigratory protein) from the BCP/PrxQ subfamily (Nelson *et al.*, 2011). AhpC is highly reactive with H_2O_2, with a k_{cat}/K_m of 1.4 x 10^7 $M^{-1}s^{-1}$. Although it is also able to reduce bulkier hydroperoxide substrates, the K_m for cumene hydroperoxide (CHP, 107 μM) and *t*-butyl hydroperoxide (*t*BHP, 238 μM) are significantly higher than for H_2O_2 (1.4 μM) (Parsonage *et al.*, 2008). AhpC and other Prx1/AhpC subfamily members form homodimers across the β sheet-extending B-interface, and these dimers further oligomerize into decamers across the A-type interface (for “ancestral” or “alternate”) in a redox-sensitive and concentration-dependent manner (Hall *et al.*, 2009; Hall *et al.*, 2011; Wood *et al.*, 2002). Reduced AhpC is present as a decamer, whereas disulfide-bonded AhpC can dissociate into dimers at lower protein concentrations (Wood *et al.*, 2002).

AhpF, the specialized reductant for AhpC, accepts electrons from NADH and delivers them to AhpC through three redox centers (FAD and two redox-active disulfide centers) within tethered Trx reductase-like and Trx-like domains (Jönsson *et al.*, 2007; Poole *et al.*, 2000a). In contrast, *E. coli* Tpx preferentially reduces the bulkier hydroperoxide, CHP [k_{cat}/K_m (for peroxide) = 7.7 x 10^6 M^{-1} s^{-1}], compared with H_2O_2 (k_{cat}/K_m = 4.4 x 10^4 M^{-1} s^{-1}) and forms stable dimers across the A-type interface in a non-redox sensitive manner (Baker and Poole, 2003). Previous studies have shown that *E. coli* Tpx is reduced by NADPH through thioredoxin reductase and Trx1 and is not reducible by Trx2, Grx1, or AhpF (Baker and Poole, 2003).

Much less is known about the substrates and function of BCP, the third *E. coli* Prx family member. The BCP/PrxQ subfamily is one of the least characterized Prx subfamilies overall that nonetheless is present across archaea, bacteria, and some eukaryotic organisms, including plants and *C. elegans*. (Horta *et al.*, 2010; Nelson *et al.*, 2011; Rouhier and Jacquot, 2005). Bioinformatic analyses of Prxs have been facilitated recently by the increasing amount of structural and sequence information available for these proteins and various studies have suggested that members of the BCP subfamily are most similar to the ancestral Prx protein (Copley *et al.*, 2004; Hall *et al.*, 2011; Nelson *et al.*, 2011). Within the BCP/PrxQ subfamily of proteins, the low redox potential PrxQ proteins of plant chloroplasts have been studied by several groups and have been shown to be important in maintaining photosynthesis within this organelle (Dietz, 2011). *E. coli* BCP reportedly exhibits low peroxidase activity

with Trx1, raising the question of whether this protein might be more active with other peroxide or reducing substrates (Jeong *et al.*, 2000). The functional importance of this protein has been demonstrated, at least in the human pathogen *Helicobacter pylori,* where it helps establish long term infections within the host's gastric mucosa (Wang *et al.*, 2005).

Interestingly, the C_r residue has been found in at least four different locations across all Prxs (in helices α2, α3, α5 and the C-terminal tail) and can involve either an intrasubunit or intersubunit linkage (Copley *et al.*, 2004; Hall *et al.*, 2011). The presence of a C_r is particularly variable in the BCP/PrxQ subfamily (Nelson *et al.*, 2011), with members possessing a C_r in helix α2 (54%) (Clarke *et al.*, 2009; D'Ambrosio *et al.*, 2009), α3 (like members of the Tpx subfamily, 7%) (Liao *et al.*, 2009), or lacking a C_r altogether ($\leq$39%). Where C_r is missing (in the so-called "1-Cys" enzymes), less is understood about the reductive recycling pathways, but small molecule thiols like glutathione, or thiol groups from other proteins like redoxins may be involved (Clarke *et al.*, 2010; Nelson *et al.*, 2011). *E. coli* BCP is representative of the largest group of BCP/PrxQ proteins, with the C_r located 5 residues after the C_p in helix α2 (Clarke *et al.*, 2009; Copley *et al.*, 2004). Reports to date have concluded that *E. coli* BCP is a monomeric protein, although the recent finding that BCP/PrxQ subfamily members can be dimeric suggests that more rigorous studies of the oligomeric state of this protein in solution are warranted (Hall *et al.*, 2011).

The present study was designed to gather detailed information about the peroxidatic function and biochemical underpinnings of the reactivity of *E. coli* BCP. Its oligomeric and kinetic properties, substrate preferences (for both hydroperoxide and reducing substrates), redox potential and pK_a for C_p were all investigated and found to support a broad substrate specificity and wide tolerance of varying cell conditions. For example, this enzyme is less dependent than the other two Prxs (AhpC and Tpx) on specific reducing pathways, which may be compromised under conditions that would render other oxidant defenses less active. As a high potential redoxin, it is also poised to remain reduced under highly oxidizing conditions that would likely compromise other defense systems within the cell.

METHODS

Cloning and Mutagenesis of BCP From E. coli. The BCP structural gene (GenBank accession number EU897604.1) was amplified by PCR from *E. coli* XL1-Blue cells. The resulting PCR product was purified from an agarose gel using the QIAquick gel extraction kit (QIAGEN) and ligated into the pCR-Blunt-TOPO PCR cloning vector (Invitrogen) following the manufacturer's protocol. The sequence and orientation of the insert was confirmed by plasmid sequencing. The resulting plasmid was digested with *Eco*RI and *Bam*HI, the digested fragments were gel purified and the BCP-encoding fragment was ligated into pTrc99A (Amersham Pharmacia Biotech Inc, Piscataway, NJ) to generate the wild-type BCP expression construct.

BCP mutagenesis (C45S, C50S, C99S, and C50S/C99S) was performed using the QuikChange II Site-Directed Mutagenesis Kit (Stratagene) following the manufacturer's protocol. All mutations were confirmed by sequencing of the entire BCP-encoding insert.

***Protein Expression and Purification*.** For all protein preparations, cells were lysed by passage through an Avestin EmulsiFlex-C5 and cell debris was removed by centrifugation at 40,000 $\times$ g for 40 min. Purification procedures were carried out at 4 ^{o}C, unless indicated otherwise. All chromatography, unless noted otherwise, was accomplished using an Akta Explorer 10S Air FPLC system (GE Healthcare).

Wild-type *E. coli* BCP was expressed from TA4315 cells, which lack AhpC, the major Prx of *E. coli* (Storz *et al.*, 1989); all BCP mutants were expressed and purified from *E. coli* strain JW2465, from the Keio collection, which has a confirmed knockout in BCP (Baba *et al.*, 2006). Cells were grown at 37 ^{o}C in 6 L of LB medium containing 100 µg/mL ampicillin to an A_{600} of 0.6, then induced for 18 h with 0.8 mM isopropyl-1-thio-β-D-galactopyranoside (IPTG). Cells were harvested and resuspended in 50 mM potassium phosphate with 1 mM EDTA at pH 7.0 (Buffer A) and lysed as described above. The nucleic acids were removed from the cleared lysate by the addition of 1% (w/v) streptomycin sulfate and centrifugation at 18,000 × g for 20 min. The resulting supernatant was applied to a Q-Sepharose HP (GE Healthcare) column equilibrated with Buffer A and eluted using a linear gradient from 0 to 1.0 M NaCl. Fractions were pooled, concentrated, and loaded onto a 250 mL Superose 12 prep grade (GE Healthcare) gel filtration column equilibrated with Buffer A (except lacking EDTA). Fractions were pooled and loaded onto a 10 mL CHT Ceramic Hydroxyapatite (Bio-Rad Laboratories) gravity-flow column equilibrated with 5 mM sodium phosphate at pH 7.0. The column was washed using a stepwise concentration gradient of 50 and 100 mM sodium phosphate, and BCP was eluted at 200 mM sodium phosphate. Fractions containing purified BCP (~180 mg) were pooled and stored as 10 mg/mL aliquots at -80 ^{o}C. Mutant BCP proteins were expressed and purified essentially as described for wild type, except that 2 mM dithiothreitol (DTT) was present during all steps of the purification, as previously

required to avoid oxidative damage for similar mutants of AhpC and Tpx lacking the resolving Cys (Baker and Poole, 2003; Nelson *et al.*, 2008).

To obtain pure Trx1, W3110 cells containing pDL59ΔT4 (Veine *et al.*, 1998), a Trx1-expressing, heat inducible plasmid, were grown at 30 ^{o}C in 6 L of 2×YT media in the presence of ampicillin (100 μg/mL) to an A_{600} of 0.6, then switched to growth at 42 ^{o}C for 18 h. Trx1 was purified as previously described (Lennon and Williams, 1995), except that the crude extract was heated at 65 °C for 20 min, and then centrifuged before chromatography with Q-Sepharose HP and Superose 12 prep grade columns. Purity was verified by SDS polyacrylamide gels and pure Trx1 was concentrated and stored as 10 mg/mL aliquots at -80 ^{o}C.

Grx1 was expressed with a removable, N-terminal His tag in *E. coli* BL21 (DE3) and purified as described previously (Yamamoto *et al.*, 2008). Briefly, the fusion protein was purified on a HiTrap Chelating HP column (GE Healthcare), cleaved with thrombin, and applied to a Superose 12 prep grade column . The F6W mutant of Grx1 ($Grx1_{F6W}$) was expressed and purified from C41 (DE3) *E. coli* cells as previously described (Parsonage *et al.*, 2010b).

Trx2 with an N-terminal His-tag was expressed in DHB4 *E. coli* cells transformed with plasmid DR1000 containing *trxC* in a pET15b vector (Ritz *et al.*, 2000). Cells were grown at 37 ^{o}C to an A_{600} of 0.6 and induced with 0.8 mM IPTG for 18 h. The Trx2 protein was purified and the His-tag was removed essentially as described above for Grx1.

Grx3 was expressed from pRO1 (*grxC* in a pBAD33-derived plasmid) (Ortenberg *et al.*, 2004) harbored within DHB4 *E. coli* and purified based on previous methods (Åslund *et al.*, 1994; Nordstrand *et al.*, 1999). Briefly, 6 L of cell culture induced for protein expression by addition of 0.02% arabinose were harvested, lysed and treated with streptomycin sulfate. Chromatographic separations used Q-Separose (equilibrated and eluted in Buffer A, except at pH 8) and Superose 12 columns (also using Buffer A at pH 8).

Expression of DsbA from *E. coli* XL1-Blue transformed with pBJ41 (Bardwell *et al.*, 1991) was induced by overnight growth at 37 °C after addition of 1 mM IPTG when A_{600} = 1. The harvested cells were treated with 300 µg/mL lysozyme in buffer containing 20 % sucrose, 20 mM Tris-Cl pH 8.0, and 2.5 mM EDTA. The resulting supernatant after centrifugation was dialyzed against 10 mM Tris-Cl containing 0.25 mM EDTA at pH 8.0, loaded onto a 55 mL Q Sepharose HP column equilibrated with the same buffer, and eluted with a 0-0.5 M NaCl gradient. Peak fractions containing DsbA were pooled, brought to 1 M in ammonium sulfate, and loaded onto a 75 mL Phenyl Sepharose HP column equilibrated with 1 M ammonium sulfate, 20 mM Tris-Cl pH 8.0, 0.1 M NaCl. DsbA was eluted using a 1 to 0 M ammonium sulfate gradient. Fractions containing pure protein were pooled, concentrated and frozen in aliquots at 10 mg/mL.

E. coli thioredoxin reductase (TrxR) was purified as previously described (Poole *et al.*, 2000a). Yeast glutathione reductase was purchased from Sigma.

Analytical Ultracentrifugation. Multiple concentrations of both oxidized and reduced BCP (25, 33, 50 66, 100, and 200 μM) were analyzed by sedimentation velocity experiments using an Optima XL-A analytical ultracentrifuge (Beckman Instruments, Palo Alto, CA) outfitted with absorbance optics. Before analysis, BCP was treated with 10 mM DTT for 30 to 60 min, then DTT was removed and the buffer was exchanged using a PD10 (GE Healthcare) column (reduced BCP sample). Oxidized BCP was prepared from the freshly reduced protein by addition of 10 mM H_2O_2 for 5 min and exchanged into fresh buffer without H_2O_2 using a PD10 column. Samples were analyzed at 20 °C in double-sectored cells in 25 mM potassium phosphate buffer, 1 mM EDTA, and 0.15 M NaCl at pH 7; reduced BCP buffers also contained 0.1 mM DTT. Sedimentation data at 280 nm were collected every 4 min at rotor speeds of 42,000 rpm and a radial step size of 0.003 cm. Values of 0.73445 and 0.73446 cm^3/g for the partial specific volumes of reduced and oxidized BCP, respectively, were calculated from their amino acid compositions (Laue *et al.*, 1992). The molecular weight was calculated using the Svedberg equation (Van Holde, 1971) after extrapolation to zero concentration of the corrected sedimentation coefficient ($s^0_{20,w}$) and the translational diffusion coefficient ($D^0_{20,w}$) obtained using SVEDBERG version 6.39 (www.jphilo.mailway.com) (Philo, 1997; Philo, 2000).

Kinetic Assays. Previous NADPH-dependent assays conducted by Jeong et al. (Jeong *et al.*, 2000) used a single concentration of Trx1 and amounts of BCP that were equivalent to or in excess of the concentration of Trx1; under these

conditions, BCP turnover is expected to be limited by the rate of reduction. We therefore adapted those assays to measure BCP's activity with various reductants so that each reductant was in 10-fold excess over BCP. Reactions were carried out at 25 ^{o}C in Buffer A containing 150 μM NADPH, 0.5 μM BCP, and 1 mM CHP; CHP rather than H_2O_2 was used because H_2O_2 gave a significant background rate of reaction with glutathione under these conditions, whereas CHP did not. Assays with 10 μM Trx1 or Trx2 contained 0.1 μM TrxR. Assays with 10 μM Grx1, $Grx1_{F6W}$, or Grx3 instead contained 1 mM glutathione and 1 U/mL glutathione reductase. Assay mixtures were first prepared without CHP, monitored for 1 – 2 min to establish the low background rate, then supplemented with CHP to start the BCP-dependent peroxidase reaction. A_{340} was followed for the first 2 min of the reaction on an Agilent 8453 diode array spectrophotometer, and initial linear rates were determined to calculate the rate of NADPH oxidation using an ε_{340} of 6220 M^{-1} cm^{-1}.

Bisubstrate kinetic analysis varying both Trx1 and hydrogen peroxide concentrations as well as studies to determine BCP specificity with H_2O_2, cumene hydroperoxide (CHP), or *t*-butyl hydroperoxide (*t*BHP) with both Trx1 and Grx1 were performed using an Applied Photophysics SX.18MV stopped-flow spectrophotometer. First, Trx1 (or $Grx1_{F6W}$) and BCP were prereduced by 10 mM DTT for 1 h, and excess DTT was removed by using a PD10 size exclusion column (GE Healthcare). Pre-reduced BCP was mixed in one syringe with either Trx1 or Grx1 and the reaction buffer (Buffer A, present in both syringes); peroxide was added to the second syringe. After mixing, the rate of reaction was

measured by monitoring the change in fluorescence of Trx as it is oxidized, with excitation at 280 nm and emission >320 nm (using an emission filter). Initial rates for the fluorescence changes at each Trx or Grx concentration were converted to μM peroxide reduced per second per μM BCP using Equation 1.

$$\text{Rate [}\mu\text{M peroxide s}^{-1}\text{ (}\mu\text{M BCP)}^{-1}\text{]} = \text{rate (V s}^{-1}\text{)} \cdot \frac{[\text{Trx1}]}{(\Delta F \cdot [\text{BCP}])}$$

[Trx1] and [BCP] are the final micromolar concentrations of these proteins, and ΔF is the maximum Trx1 fluorescence signal change (in V) in the presence of excess peroxide for the same Trx1 concentration as that being analyzed.

The initial rate of fluorescence decrease was determined by linear regression of the data during the first 2 seconds of the reaction. Reported rates are averages of three measurements in no less than 3 independent assays conducted at 25 ^{o}C.

Detemination of Midpoint Reduction (Redox) Potential. Reduced BCP (50 μM) was mixed with oxidized DsbA (50 μM) in 100 mM potassium phosphate, 1 mM EDTA, pH 7.0 and allowed to equilibrate for 6 h at room temperature (an equilibration time that was verified to be sufficient in preliminary experiments). Although we have previously used a rapid acidification of the sample followed by direct separation by HPLC, in this case an additional step of rapid alkylation with NEM had to be added to trap free thiol groups and improve separation on HPLC

of the reduced and oxidized species of BCP in the same gradient in which the two redox forms of DsbA were resolved. Thus, samples (50 µL) were quenched by adding 50 µL of 200 mM N-ethylmaleimide (NEM) for 2 min, followed by addition of a 10% volume of 1 M phosphoric acid, then aliquots were resolved using a 4.6 × 250-mm Vydac C4 HPLC column. Protein components were separated using a shallow gradient of acetonitrile (50 to 60% acetonitrile for 60 min, then 60 to 82% for another 102 min), with 0.08–0.1% trifluoroacetic acid in both solvents, at a flow rate of 0.5 mL/min and room temperature. The locations of the peaks for the reduced and oxidized species were determined using standards for each protein, and quantitation of the proteins was based on the peak area for each species. The redox potential was calculated by using a derivation of the Nernst equation (Equation 2) and a value of -110 mV (range -122 to -100 mV) for the DsbA redox potential (Hawkins and Freedman, 1991; Lundstrom and Holmgren, 1993; Wunderlich and Glockshuber, 1993) .

$$E_o' \text{ (BCP)} = E_o'\text{(DsbA)} + (RT/nF) \ln \left(\frac{[\text{DsbA}_{ox}] \cdot [\text{BCP}_{red}]}{[\text{DsbA}_{red}] \cdot [\text{BCP}_{ox}]} \right) \qquad \text{Equation 2}$$

In separate experiments, oxidized BCP was mixed with reduced DsbA and incubated for 12 and 24 h at room temperature to ensure complete equilibration of the two proteins (Parsonage *et al.*, 2008).

Stability and pK_a Analysis of BCP. The pK_a of BCP (wild type and mutant) was determined by measuring the change in the ε_{240} between pH 3 and 9, following

confirmation that the protein was stable across this pH range (retained full activity when shifted back to pH 7), essentially as previously described (Nelson *et al.*, 2008). For pK_a analysis, BCP was first reduced with 10 mM DTT for 10 min, then excess DTT was removed using a PD10 column pre-equilibrated with 5 mM potassium phosphate and 1 mM EDTA at pH 7. The concentration of reduced BCP was determined using an ε_{280} of 15,400 M^{-1} cm^{-1}. BCP was diluted to a final concentration of 25 µM into citrate-borate-phosphate (CBP) buffer containing 10 mM of each component (sodium citrate, boric acid, and sodium phosphate), 100 mM sodium chloride, and 0.1 mM diethylene triamine pentaacetic acid (DTPA) at various pH values between 3 and 9; the final pH value of each solution was determined after mixing. At each pH, the absorbance values at 240 and 280 nm were measured with an Agilent 8453 diode array spectrophotometer and the ε_{240} was calculated assuming that the ε_{280} value of 15,400 M^{-1} cm^{-1} remained constant across the pH range. The ε_{240} values were plotted versus pH and the pK_a was determined by direct fit to equation 3:

$$y = [(A \times 10^{pH}) + (B \times 10^{pKa})] / (10^{pKa} + 10^{pH}) \qquad \text{Equation 3}$$

where $y = \varepsilon_{240}$, A = the upper plateau at high pH (ε_{240} for the deprotonated form), and B = the lower plateau at low pH (ε_{240} for the protonated form).

The pK_a of BCP was also determined by measuring the pH dependence of BCP peroxidase activity. The rate of peroxide disappearance was measured

using the FOX assay to assess peroxide levels (Jaeger *et al.*, 1994). Pre-reduced BCP was diluted to 40 μM in 2X CBP buffer at various pH values between 4.5 and 8 and the assay was started by the addition of an equal volume of 80 μM H_2O_2, resulting in a final volume of 25 μL. The reaction was quenched at various times between 0 and 15 s by the addition of 1 mL FOX reagent (Jaeger *et al.*, 1994). The absorbance at 560 nm was determined using the Agilent spectrophotometer and the amount of peroxide remaining in the solution was calculated by comparison with standard solutions of H_2O_2.

RESULTS AND DISCUSSION

***E. coli* BCP Is a Monomer In Solution Even At Concentrations Up To 200 µM.** Of the six described subfamilies of Prx proteins, only the proteins within the BCP/PrxQ class of Prxs are described as monomeric. Although this was originally thought to be characteristic of the subfamily as a whole, recent crystallographic analyses have demonstrated that some members of the BCP/PrxQ group are indeed dimeric (Hall *et al.*, 2011). In fact, the oligomeric state of *E. coli* BCP in solution over a range of concentrations has not been rigorously tested, although intersubunit disulfide bond formation was ruled out by SDS polyacrylamide gel analysis and high resolution mass spectrometry (MS) (Clarke *et al.*, 2009; Jeong *et al.*, 2000). We therefore used analytical ultracentrifugation analyses to determine the oligomeric state of reduced and oxidized BCP in solution up to concentrations as high as 200 µM. As shown in Figure 3-1, both redox forms of BCP exhibit sedimentation coefficients around 2 Svedbergs; together with the diffusion coefficient measured from the same experiments, these data and the Svedberg equation yield shape-independent molecular masses of 19.4 and 22.2 kDa for reduced and oxidized BCP, respectively (given a theoretical mass for *E. coli* BCP of 17502.7 g/mol). No evidence of higher order species was observed. Thus, in either redox state, *E. coli* BCP remains monomeric in solution even at very high concentrations.

As alluded to above, of the structural representatives of the BCP/PrxQ subfamily characterized by X-ray crystallography to date, four were monomeric,

while two members crystallized as dimers (through the A-type interface commonly used to form PrxV and Tpx subfamily dimers). Unfortunately, no peer-reviewed publications have resulted from the dimeric structures of these *Aeropyrum pernix* (PDB codes 2cx3 and 2cx4) and *Sulfolobus tokadaii* BCP proteins (PDB code 2ywn), so limited information is available.

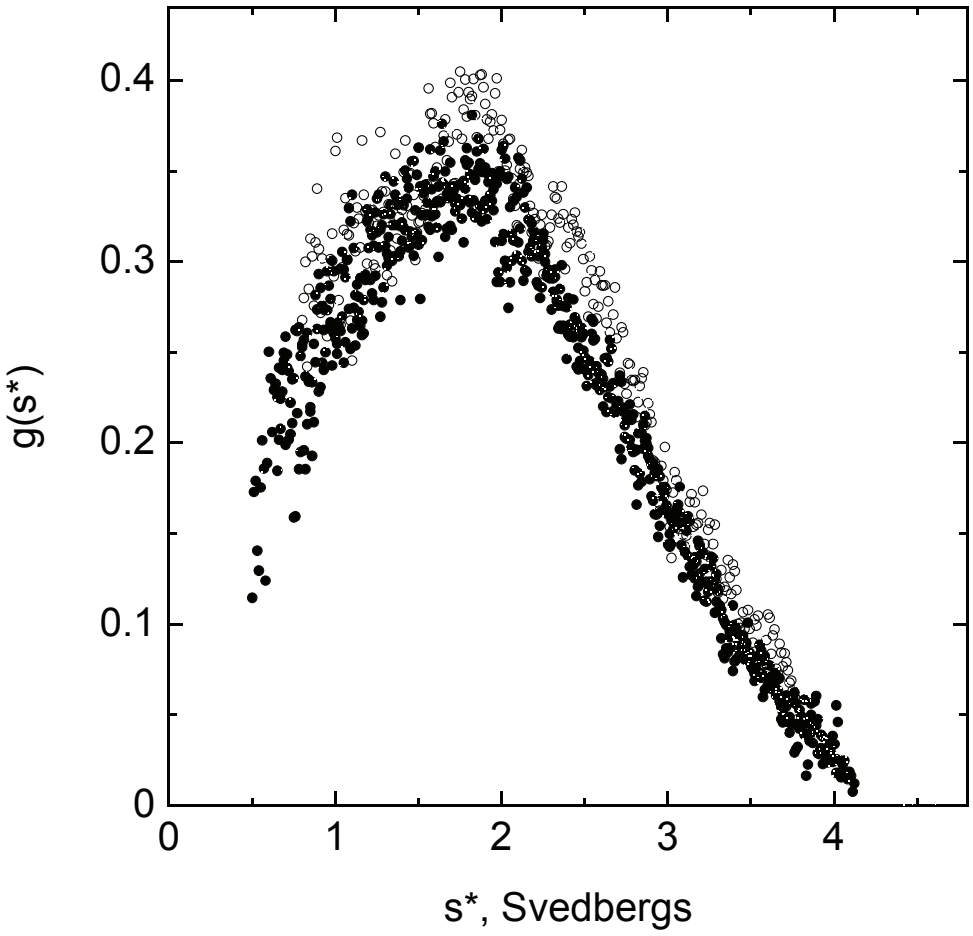

Figure 3-1. Sedimentation velocity studies of reduced and oxidized wild-type BCP. Analytical ultracentrifugation studies of BCP proteins were carried out by centrifugation at 42,000 rpm, 20 °C, and neutral pH as described in Experimental Procedures. Global analyses of the 280 nm data employed Svedberg software to give the g*(s) distributions for both the reduced and oxidized BCP. Data for reduced (open circles), and oxidized (closed circles) wild-type BCP at 50 μM were fit to a single-species model. Molecular weights derived from extrapolated and corrected s and D values the Svedberg equation were 19.4 kDa for reduced BCP and 22.2 kDa for oxidized BCP. Results show no evidence of the formation of dimers or higher multimers.

E. coli *BCP Exhibits Nonsaturable Interactions With Trx1 and Broad Specificity For Peroxide Substrates.* Previous assays conducted by Jeong et al. (Jeong *et al.*, 2000), which used a single concentration of Trx1 at 0.8 μM and amounts of BCP that were equivalent to or in excess of the concentration of Trx1, yielded apparent V_{max} values for BCP with H_2O_2 of 7 μM peroxide substrate reduced min^{-1} (μM BCP) $^{-1}$. Our initial assays of *E. coli* BCP with Trx1 in excess yielded rates higher than those previously reported; furthermore, rates with Trx1 concentrations up to 40 μM continued to increase, with no evidence of saturation (Table IV). A range of assays were therefore employed to better establish the kinetic attributes of this system.

As the BCP reaction can monitored directly by the loss of Trx1 fluorescence as it becomes oxidized, we carried out a bisubstrate kinetic analysis of BCP with H_2O_2 and Trx1 using a stopped-flow spectrofluorometer to monitor turnover. Under these conditions, an increase in $V_{max,app}$ and $K_{m,app}$ for H_2O_2 was observed with increasing Trx1 concentrations up to 80 μM, indicating an interaction between the reductant and BCP that is non-saturable under physiologically reasonable concentrations (Figure 3-2, a and b). Extrapolated values from global fits of all the data for the K_m for Trx and for V_{max} are far outside the range of the data, at about 500 μM and 64 s^{-1}, respectively. Nonetheless, Hanes-Woolf treatment of the data is consistent with a ping-pong mechanism (Figure 3-2c). This lack of saturation with Trx1 demonstrates a major difference between BCP and many other Trx-dependent Prxs including Tpx from *E. coli*; the latter protein interacts saturably with Trx1 during turnover with peroxide

Table 3-I. Steady-state Kinetic Parameters of BCP with varying [H_2O_2] and [Trx][a]

[Trx]	$V_{max, app}$	$K_{m, app}$ for H_2O_2	$(V_{max}/K_m)_{app}$
μM	*(μM/s)/ μM* BCP	*μM*	$M^{-1} s^{-1}$
10	1.31 ± 0.05[b]	92.2 ± 18.5[b]	1.42 x 10^4
	1.24 ± 0.02[c]	76.1 ± 3.9[c]	1.63 x 10^4
20	2.58 ± 0.10	226 ± 31	1.14 x 10^4
40	4.65 ± 0.10	332 ± 23	1.40 x 10^4
80	8.23 ± 0.23	633 ± 44	1.30 x 10^4

[a] Corresponding plot shown in Figure 3-2a.
[b] Kinetic parameters obtained at 10 μM Trx with this set of assays (Fig. 1), using 100 to 2000 μM H_2O_2.
[c] Kinetic parameters obtained at 10 μM Trx in the assays with varying peroxide substrates (Table IV), using 25 to 2000 μM H_2O_2.

A

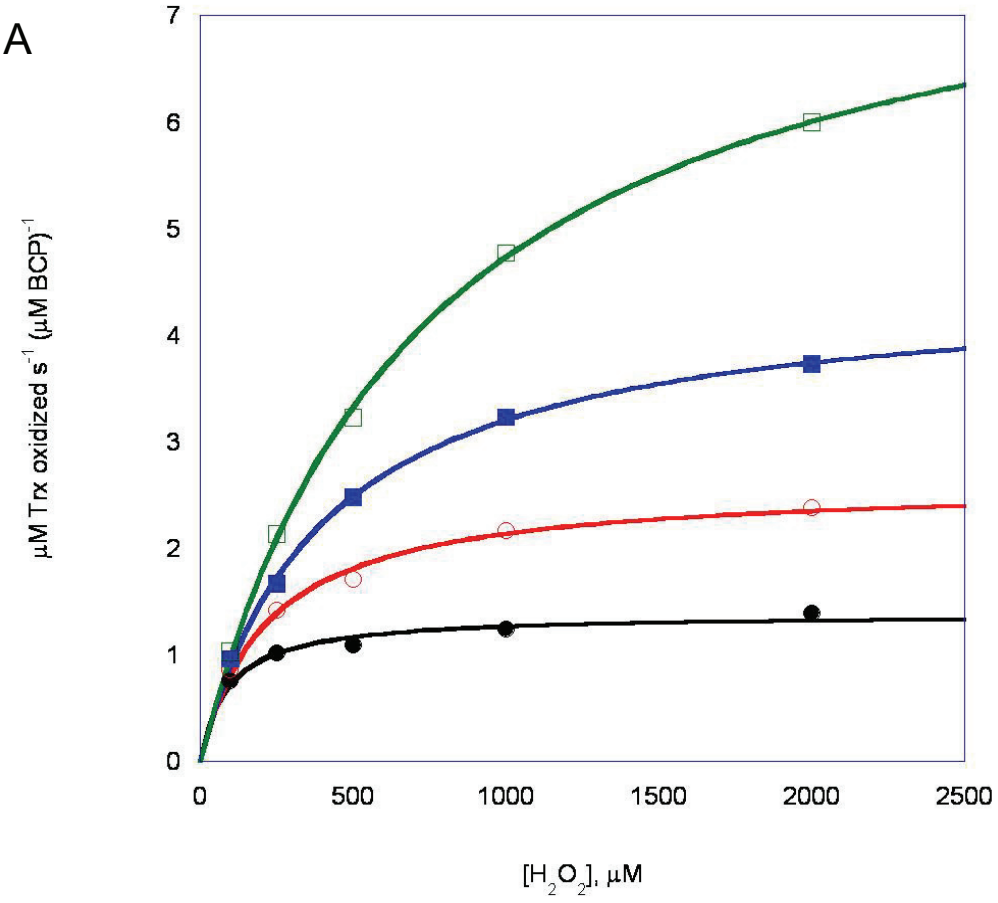
μM Trx oxidized s-1 (μM BCP)-1
0
1
2
3
4
5
6
7
0
500
1000
1500
2000
2500
[H2O2], μM

B

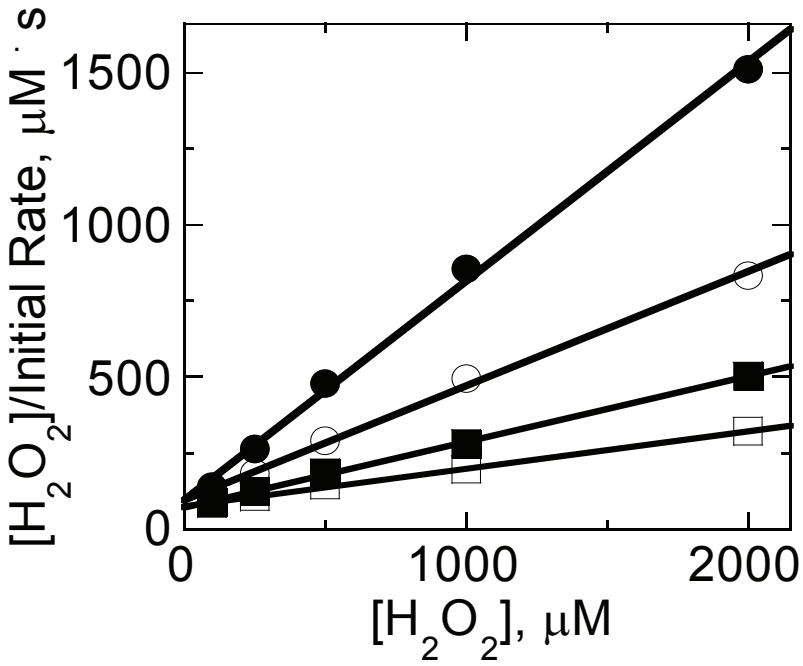
[H2O2]/Initial Rate, μM · s
0
500
1000
1500
0
1000
2000
[H2O2], μM

C

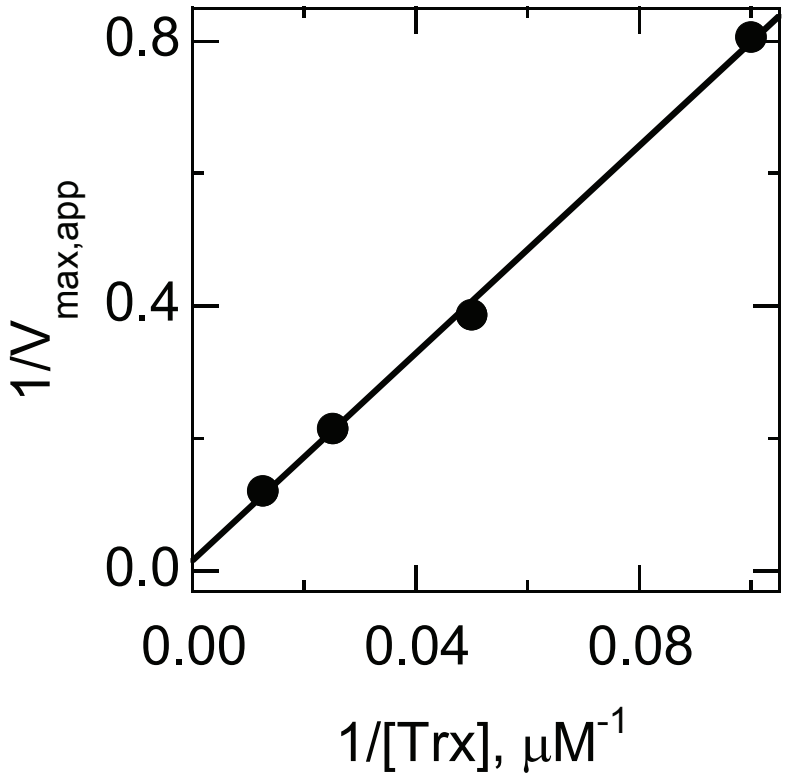

Figure 3-2. Steady state kinetic analyses of *E. coli* BCP with H_2O_2 and Trx1. Peroxidase activity was measured by mixing various concentrations of *E. coli* Trx1 (prereduced by DTT) and BCP (0.5 μM) in 50 mM potassium phosphate at pH 7.0 (with 0.5 mM EDTA) with various concentrations of H_2O_2 in a stopped-flow spectrophotometer at 25 °C. The decrease in Trx fluorescence due to oxidation was monitored using a stopped flow spectrofluorometer and converted to initial rates as described in Experimental Procedures. Fixed concentrations of Trx1 assayed over a range of H_2O_2 concentrations were 10 μM (closed circles), 20 μM (open circles), 40 μM (closed squares), and 80 μM (open squares). Data shown in A (plus or minus standard error) are the averages of three independent replicates. Lines through the points show the direct fits to the Michaelis-Menten equation for each Trx1 concentration. B. Hanes-Woolf plot of $v/[H_2O_2]$ vs. $[H_2O_2]$ from data shown in panel A and Table IV. Lines intersecting at the y-axis are consistent with a substituted (ping-pong) enzyme mechanism. C. Secondary plot of $1/V_{max,app}$ vs. 1/[Trx] from data shown in panel A and Table IV.

substrates (K_m for Trx1 ~ 25 μM) (Baker and Poole, 2003). Two other BCP/PrxQ subfamily members, from *Xylella fastidiosa* and poplar, were examined using similar kinetic approaches and also exhibited saturable interactions with both the reducing and oxidizing substrates (K_m of 7 and 1.5 μM for their Trx reductants, respectively) (Horta *et al.*, 2010; Rouhier *et al.*, 2004), indicating that saturability by Trx1 is at least sometimes observed for members of the BCP/PrxQ subfamily.

Although the values for $V_{max,app}$ and $K_{m,app}$ for H_2O_2 changed with the concentration of Trx1 used, the $(V_{max}/K_m)_{app}$ for H_2O_2 remained constant over the various Trx1 concentrations used as expected for a ping pong mechanism, giving an overall value of about 1.3 x 10^4 M^{-1} s^{-1} (Table IV). This matches well with the value of V_{max}/K_m for H_2O_2 obtained as the reciprocal of the y intercept in the Hanes Woolf plot (1.2 x 10^4 M^{-1} s^{-1}), an alternative way to analyze steady state kinetic data (Figure 3-2c). This value is in the same range as the values of about 4 x 10^4 M^{-1} s^{-1} and 8 x 10^3 M^{-1} s^{-1} obtained for the *X. fastidiosa* and poplar PrxQ proteins, respectively (Horta *et al.*, 2010; Rouhier *et al.*, 2004), and rather higher than the original estimate of 2.45 x 10^3 M^{-1} s^{-1} for *E. coli* BCP reported by Jeong et al. (Jeong *et al.*, 2000). This catalytic efficiency is somewhat modest when compared with k_{cat}/K_m values obtained for Trx-dependent Prxs from other subfamilies, which typically exhibit values for their best substrates as high as 10^7 or 10^8 M^{-1} s^{-1} (Ferrer-Sueta *et al.*, 2011; Parsonage *et al.*, 2008). Interestingly, *E. coli* Tpx, which reduces organic hydroperoxides much more efficiently, has a very high K_m for H_2O_2 (~ 1.7 mM) and consequently a very similar k_{cat}/K_m value for H_2O_2 (4.4 x 10^4 M^{-1} s^{-1}) compared with BCP (Baker and Poole, 2003).

In order to directly compare *E. coli* BCP activity with different peroxide substrates, a physiologically reasonable Trx1 concentration of 10 μM was chosen for these analyses [based on cellular concentrations of around 10 to 30 μM (Holmgren, 1981; Holmgren *et al.*, 1978)]. Using Trx1, the apparent K_m value for H_2O_2 is ~80 μM and similar to the value obtained for cumene hydroperoxide; the $V_{max,app}$ for these two substrates is also very similar (Table IV). A related hydroperoxide substrate lacking the aromatic ring, but with a methyl group in its place, *t*-butyl hydroperoxide, is a very poor substrate under these conditions (Table V and Figure 3-3). The similarity between H_2O_2 and cumene hydroperoxide as substrates, and the demonstration that *t*-butyl hydroperoxide is a worse substrate for *E. coli* BCP, is quite similar to the trend seen with the kinetically-characterized PrxQ enzymes from *X. fastidiosa* and poplar, although the differences between the two organic hydroperoxides were not so striking in those cases (Horta *et al.*, 2010; Rouhier *et al.*, 2004).

Table 3-II. Steady-state Kinetic Parameters of BCP Using 10 μM Trx1 or $Grx1_{F6W}$ and Varying Hydroperoxide Substrates Measured By Stopped Flow Fluorescence Analysis

Protein Reductant, at 10 *μM*	ROOH [a]	$V_{max, app}$	$K_{m, app}$ for ROOH	V_{max}/K_m
		(μM/s)/ μM BCP	*μM*	$M^{-1}\ s^{-1}$
Trx1	H_2O_2	1.24 ± 0.02	76.1 ± 3.9	1.6×10^4
	CHP	1.21 ± 0.02	99.5 ± 5.2	1.2×10^4
	t-BHP	(1.6 ± 2.2)[b]	(6800 ± 11000)[b]	2.3×10^2
$Grx1_{F6W}$	H_2O_2	0.104 ± 0.006	14.6 ± 4.9	7.1×10^3
	CHP	0.128 ± 0.002	21.6 ± 1.3	5.9×10^3
	t-BHP	0.124 ± 0.039	574 ± 294	2.2×10^2

[a] Abbreviations for hydroperoxide substrates are CHP for cumene hydroperoxide and *t*-BHP for *t*-butyl hydroperoxide.

[b] Because of a very high apparent K_m, these values are poorly determined; data gathered included *t*-BHP concentrations up to 2 mM.

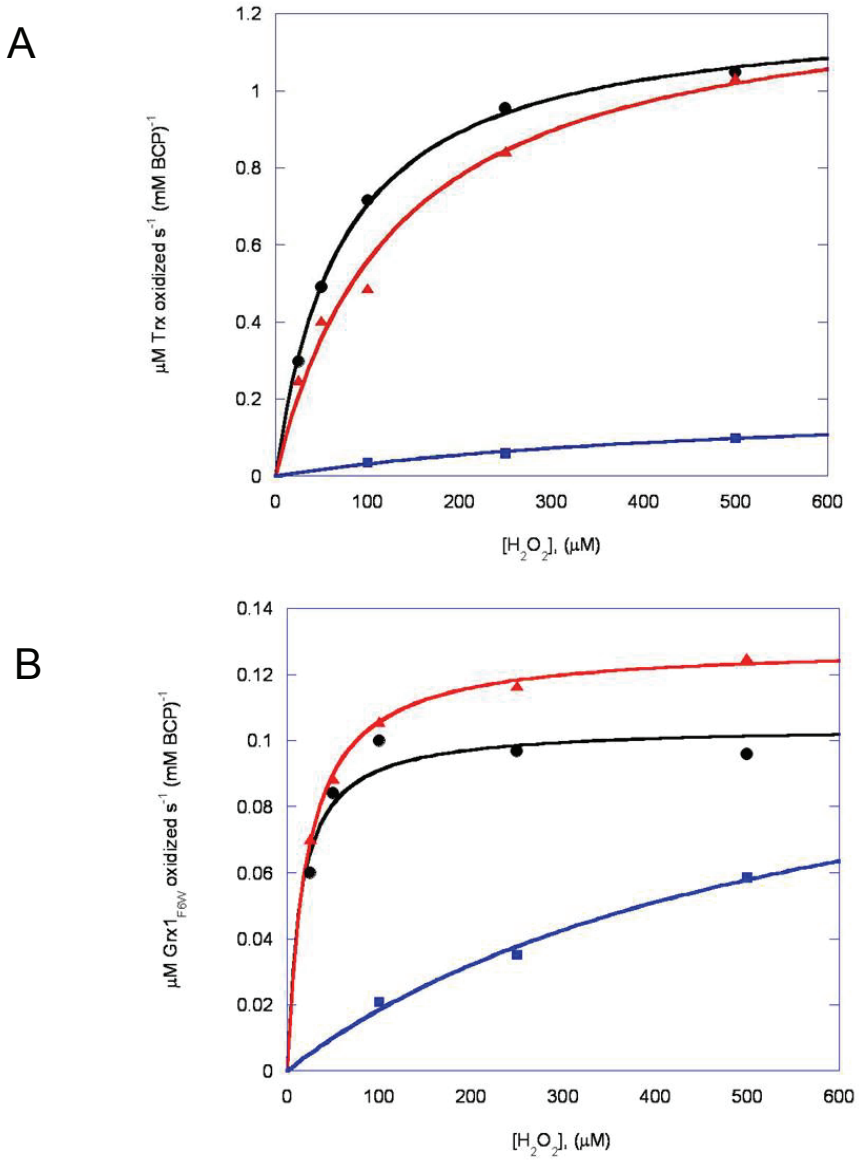

Figure 3-3. Stopped-flow spectral analysis of *E. coli* BCP peroxidase activity utilizing various ROOH and either Trx1 or $Grx1_{F6W}$ as reductant. The rates of reaction were measured by monitoring the change in fluorescence of oxidized Trx1 (panel A) or $Grx1_{F6W}$ (panel B) with excitation at 280 nm and emission > 320 nm. The reaction was initiated (with both syringe contents in 50 mM phosphate buffer with 1 mM EDTA) by mixing 10 µM of reductant (Trx1 or $Grx1_{F6W}$ plus 0.5 µM BCP in one syringe with varying concentrations of the hydroperoxide substrate in the other syringe (all concentrations given are after mixing). Shown are the initial rates (average ± standard error) plotted against the various peroxide substrate concentrations used for H_2O_2 (▲, 25-500 µM), cumene hydroperoxide (●, 25-500 µM), and *t*-butyl hydroperoxide (■,100-500 µM). The steady state parameters obtained from these plots are given in Table IV.

***Multiple Trx and Grx Proteins Are Functionally Relevant Reductants of* E. coli *BCP*.** Although most Prxs which use Trx substrates for reductive recycling do not show significant activity with Grx proteins (smaller, CXXC-containing Trx-fold proteins present in many organisms), some degree of overlapping substrate specificity between these reductants and specific Prxs has been observed, e.g. in a plant PrxII subgroup member from poplar phloem (in the PrxV subfamily) (Rouhier *et al.*, 2002; Rouhier *et al.*, 2001) and in members of the BCP/PrxQ subfamily (Clarke *et al.*, 2010; Rouhier *et al.*, 2004). Other cases where a Grx is or may be the physiological reductant of a Prx include the bacterial Prx-Grx hybrid proteins within the Prx5 subfamily (Kim *et al.*, 2003; Rouhier and Jacquot, 2003), and an unusual system from *Clostridium pasteurianum* where the Prx1/AhpC protein (denoted Cp20) is recycled by Trx reductase (Cp34) and Grx (Cp9) related proteins expressed from the same operon (Reynolds *et al.*, 2002). There is also a second Trx protein in *E. coli*, Trx2, which has distinct properties from Trx1 (El Hajjaji *et al.*, 2009) and has not previously been investigated as a potential BCP reductant. To quantitatively evaluate the specific contributions of Trx- and Grx-linked pathways to recycling of *E. coli* BCP during turnover with peroxides, we expressed and purified both Trx proteins (Trx1 and Trx2), as well as the two small, CXXC-containing Grx proteins from *E. coli* (Grx1 and Grx3). The two Grx proteins that were not evaluated were Grx2, which is much larger and more closely related to the glutathione S-transferases (Ladner *et al.*, 2004; Xia *et al.*, 2001), and Grx4, which is a "monothiol" Grx with CXXS at the active site instead of CXXC (Fernandes *et al.*,

2005). Multicomponent, NADPH-dependent assays were used, keeping conditions as nearly identical as possible. These assay mixtures all contained NADPH, a low amount of BCP (0.5 μM), 1 mM cumene hydroperoxide, and 10 μM of the reductant being tested; assays also included either TrxR (0.1 μM), or glutathione (1 mM) and glutathione reductase (1 U/mL), as the recycling systems for Trx and Grx, respectively. AhpF, the physiological reductant of AhpC, was also tested in similar assays but exhibited no detectable activity with BCP (not shown). Under these conditions, the most active reductant (Trx1) differed less than 6-fold from the least active (Grx3) in rate of turnover (Figure 3-4a). In order to get an idea of how much each reductant might be expected to contribute toward the reductive recycling of *E. coli* BCP *in vivo*, previously published data regarding the abundance of each reductant during exponential or stationary phases of growth (Potamitou *et al.*, 2002) were combined with these rates to estimate their relative contributions in *E. coli* (Figure 3-4b). Thus, because of its abundance, Grx3 is likely to contribute more toward BCP reduction than Grx1 even though it exhibits a more moderate rate of turnover with BCP (Figure 3-3a and b). This data treatment does not take into account, however, that under high oxidative stress conditions, when OxyR is activated and transcriptionally upregulating *trxC* (Trx2) expression, the level of Trx2 can actually rise to a point where it becomes more abundant than Trx1 (Ritz *et al.*, 2000), thus suggesting that all four of these reductants may contribute meaningfully to the cellular reducing power that sustains BCP peroxidase activity.

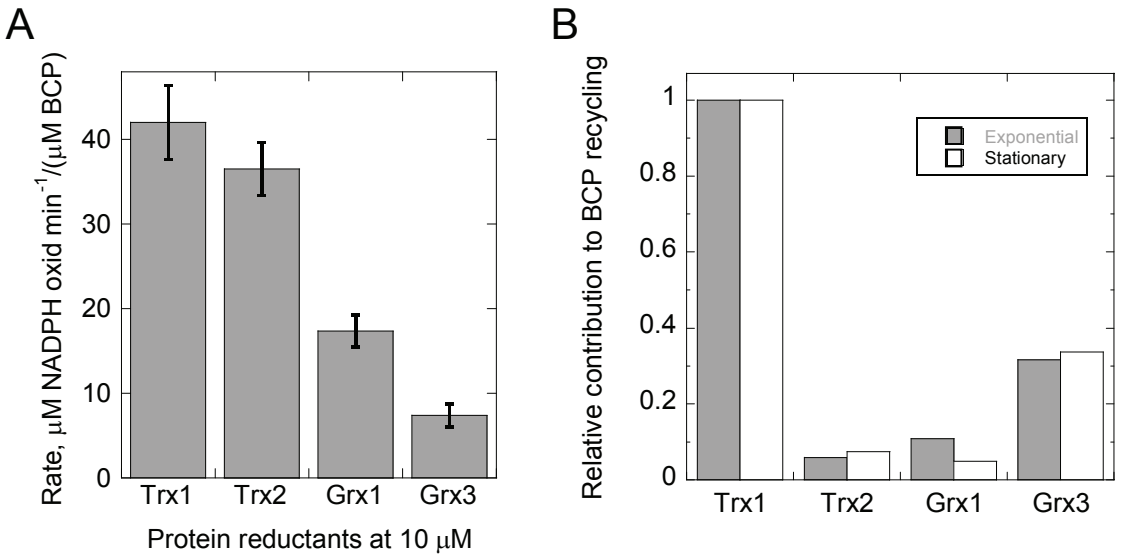

Figure 3-4. Reductants of *E. coli* BCP. Thioredoxin (Trx) and glutaredoxin (Grx) proteins from *E. coli* were assayed with BCP in a common buffer that differed only in the appropriate regeneration system for each (Trx reductase, or glutathione reductase and glutathione, respectively). Assays were conducted in 50 mM phosphate buffer (pH 7.0) with 1 mM EDTA, 150 μM NADPH, 0.5 μM BCP, 1 mM cumene hydroperoxide, and 10 μM Trx1, Trx2, Grx1 or Grx3. For Trx-linked assays, 0.3 μM *E. coli* Trx reductase was also added; the Grx-linked assays were supplemented instead with 1 mM reduced glutathione and 1 U/mL glutathione reductase. Activity was monitored spectrophotometrically at 340 nm and initial rates were used to calculate the amount of NADPH oxidized per min normalized to the amount of BCP added. Shown are averages from at least three experiments ± standard error. Also tested was a reductant system including NADH and AhpF in addition to the BCP and peroxide, but no activity was observed and thus this result is not included in the plot. In panel B, abundance in ng/mL for each protein (Potamitou *et al.*, 2002) was multiplied by the rate reported in panel A, and the product was normalized to 1.0 for Trx1.

As previously established in studies of AhpC and other Prxs, assays which utilize only one concentration of reductant and/or one concentration of peroxide may give somewhat deceptive results (Parsonage *et al.*, 2008). Therefore, we focused our efforts on conducting a full kinetic analysis with *E. coli* Grx1 varying both reductant and peroxide, as was done above for Trx1. Initial experiments established, however, that the low fluorescence emission of Grx1, in combination with a similar fluorescence signal being contributed by BCP, even at low concentration, obviated use of a similar approach to that used with Trx1 (Figure 3-2) (Parsonage *et al.*, 2010b). To circumvent this problem, we engineered a new fluorescent tryptophan into Grx1 in a position near the active site CXXC where a bulky residue was already present, creating the F6W mutant of this protein. This mutant is highly fluorescent, and the fluorescence changes substantially with redox state (Parsonage *et al.*, 2010b). As verified by the commonly used HED assays for Grx proteins, the mutant $Grx1_{F6W}$ exhibited equivalent activity compared with the wild type protein using this small molecule substrate (Parsonage *et al.*, 2010b). In an extension of these studies, the same multiprotein assays used above to compare the various Trx and Grx reductants (Figure 4-3) established that the mutation caused little, if any, change in activity in a full peroxidase assay with BCP and peroxide (15.8 ± 1.5 for the F6W mutant compared with 17.4 ± 1.9 μM s^{-1} (μM BCP)$^{-1}$ for the wild type Grx1). Using the full bisubstrate analysis of BCP with various concentrations of $Grx1_{F6W}$ and peroxides, we found that the catalytic efficiency (V_{max}/K_m) of BCP with H_2O_2 is within about two-fold of this value with Trx1 (7.1 x 10^3 M^{-1} s^{-1}), and the relative

reactivities with the different hydroperoxide substrates using Grx1 mirrors that with Trx1 (Table IV and Figure 3-2). Nonetheless, the $V_{max,app}$ and the $K_{m,app}$ values for peroxides are both lower with Grx1 than with Trx1; this may reflect a greater limitation in the reductive recycling of BCP by Grx1 than by Trx1, yielding an "artificially" lower $K_{m,app}$ value for H_2O_2 than would be observed with a better reductant or poorer peroxide substrate (supported by data in Table V).

Previous studies have demonstrated that the *E. coli* Prx with greatest activity on organic hydroperoxides, Tpx, is functional only with Trx1 and not Trx2 or Grx1 (Baker and Poole, 2003). To establish whether or not broad reductant specificity is unique (among the *E. coli* Prxs) to BCP, we also investigated the ability of *S. typhimurium* AhpC (closely related to the *E. coli* enzyme) to function with Trx1 and Grx1 as alternatives to its native reductant, AhpF. Although turnover with H_2O_2 can be observed with AhpC in the presence of *E. coli* Trx1, the interaction between these two proteins to support catalysis is non-saturable using Trx1 concentration up to 30 μM. Picking a single concentration of 10 μM for Trx1 and the S128W mutant of C-terminally truncated AhpF used in stopped flow assays with AhpC (Parsonage *et al.*, 2005), the apparent V_{max} with H_2O_2 is much lower with Trx1, at about 1.7% of the value with the AhpF derivative. The rate of reaction of AhpC with H_2O_2 in the presence of Grx1 is even lower.

The Midpoint Reduction Potential of BCP is Very High, Consistent With High Reactivity of This Protein Toward Multiple Reductants. The midpoint reduction (redox) potentials of the two Trx and two Grx proteins studied above vary widely (-198 mV for Grx3, -221 mV for Zn-replete Trx2, -233 mV for

Grx1 and -284 or -270 mV for Trx1) (Åslund *et al.*, 1997; El Hajjaji *et al.*, 2009), but all act as rather efficient reductants of BCP during turnover with peroxides. However, the only known redox potential for members of this Prx subfamily is for the poplar PrxQ protein, at -325 mV (Rouhier *et al.*, 2004), a very low redox potential that would hinder electron transfer from all but the most reducing of the Trx/Grx proteins. In the plant chloroplast, this redox potential is well suited to the role of Prxs in protection against oxidants where the Prx must be compatible with the unique, light-driven redox cycles of this photosynthetic organelle (Dietz, 2011; König *et al.*, 2002). As BCP functions, instead, in the cytoplasm of *E. coli*, it was important to determine the redox potential for *E. coli* BCP to better understand its functional attributes contributing to catalysis.

To determine the redox potential of BCP, we modified an approach used successfully in our hands to determine the redox potentials of two bacterial AhpC proteins (Parsonage *et al.*, 2010a; Parsonage *et al.*, 2008) in which a protein of unknown potential is equilibrated with another of known potential and the amount of oxidized and reduced species in the equilibrated mixtures can be used to calculate the redox potential of the unknown protein using a derivation of the Nernst equation (Åslund *et al.*, 1997). When BCP was equilibrated with Grx1, an approach that worked well for the two AhpC proteins, Grx1 was fully oxidized and BCP was fully reduced, indicating that the redox potential of the BCP was more than 50 mV higher than that of the test protein (data not shown). We then expressed and purified *E. coli* DsbA for the equilibration as it has a much higher redox potential (see Experimental Procedures). Briefly, reduced BCP and

oxidized DsbA at pH 7 and room temperature were mixed, equilibrated for 6 h (an equilibration time that was verified to be sufficient in preliminary experiments), quenched by addition of NEM followed by acid, then resolved by HPLC to quantify the respective redox forms of the two proteins (Figure 3-5, red). In three independent replicates, a value for the redox potential of BCP of -152.6 ± 1.2 mV was obtained. Similarly, three replicates of the reverse experiment (reduced DsbA mixed with oxidized BCP) yielded a redox potential of -139.2 ± 2.2 mV (Figure 3-5, blue). Averaging all values yielded a final redox potential value of -145.9 ± 3.2 mV for *E. coli* BCP. This value is the highest determined redox potential for a Prx to date, and strikingly different from the poplar PrxQ in the same subfamily, which is the lowest reported value among all Prxs studied so far (Dietz, 2011; Dietz *et al.*, 2006; Rouhier *et al.*, 2004). Like the values previously obtained for *T. pallidum* AhpC and *S. typhimurium* AhpC (-192 ± 2 and -178 ± 0.4 mV) (Parsonage *et al.*, 2010a; Parsonage *et al.*, 2008), this is a relatively high redox potential compared with those of many other redox disulfide-containing proteins, and is consistent with the reduction of BCP being thermodynamically favorable with a wide range of reductants.

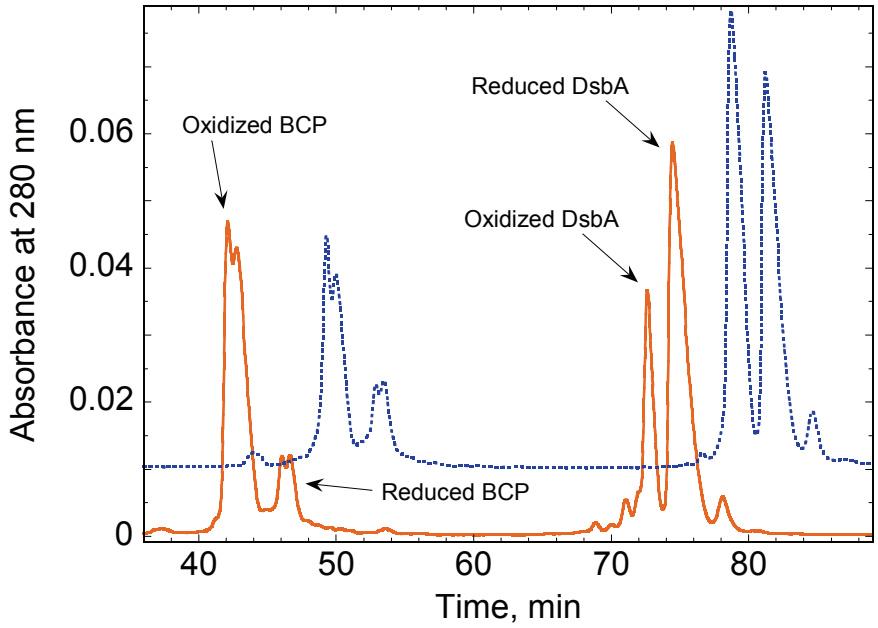

Figure 3-5. HPLC profile of the separation of equilibrated reduced and oxidized forms of *E. coli* BCP and DsbA to determine redox potential. Reduced and oxidized *Tp*AhpC and *E. coli* Grx1 (each at 50 μM) were allowed to equilibrate at room temperature in 100 mM potassium phosphate, pH 7.0, with 1 mM EDTA. The protein mixtures were quenched with N-ethylmaleimide and phosphoric acid and immediately separated by HPLC as described under "Experimental Procedures." Shown are the chromatograms from mixing reduced BCP with oxidized DsbA (red), and, displaced by 7 min and 0.01 absorbance units for ease of viewing, reduced DsbA mixed with oxidized BCP (blue).

***The pK_a of the Peroxidatic Cysteine of* E. coli *BCP Is <6, Similar to* X. fastidiosa *PrxQ,* S. typhimurium *AhpC and Other Prxs*.** To react efficiently with peroxides, the C_p in Prxs needs to be deprotonated; therefore Prx activity is supported by the lowered the pK_a of the C_p. Before embarking on pK_a analyses of BCP, we assessed the stability of this protein across a range of pH values to avoid conducting uninformative experiments. Both fluorescence measurements to monitor unfolding and experiments to evaluate activity retention after low or high pH treatment indicated that BCP is resistant to irreversible denaturation across the full pH range from 3 to 9. This result differs from that with AhpC, which showed instability in buffers below pH ~4.2 (Nelson *et al.*, 2008).

Attempts to measure the pH dependence of BCP activity were made through assessment of the competition between BCP and horseradish peroxidase (HRP) for hydrogen peroxide (Horta *et al.*, 2010; Nelson *et al.*, 2008; Ogusucu *et al.*, 2007), but the apparently slow reaction of BCP under these conditions did not allow us to use this approach as it competed very poorly with HRP. We therefore turned to an approach whereby absorbance at 240 nm is used to monitor the protonation state of cysteine residues in proteins (Benesch *et al.*, 1955; Kortemme *et al.*, 1996; Nelson *et al.*, 2008; Roberts *et al.*, 2005). Given the stability results described above, the ε_{240} was determined for both oxidized and reduced wild-type BCP over the pH range between 3 and 9. While the oxidized protein did not exhibit a significant pH-dependent change in ε_{240}, the reduced protein exhibited a single apparent pK_a value of 5.76 ± 0.08 (Figure 3-6a). Although reduced, wild type BCP possesses three cysteinyl residues, data

obtained are consistent with titration of only one thiol group, or multiple thiol groups with indistinguishable pK_a values around 5.8. As our interest is very specifically in the pK_a value of the peroxidatic Cys that lies within the active site, mutants were prepared removing one (the C_r, Cys50) or both (Cys50 and Cys99) of the other Cys residues in the protein by replacing them with Ser. In each of these mutants, the pH dependence of ε_{240} was shifted slightly to the right, yielding values of 6.05 ± 0.07 and 6.16 ± 0.05 for C50S and C50,99S, respectively. In contrast, the mutant lacking C_p (C45S) is much more reminiscent of the oxidized protein and seems to lack any clear increase in absorbance as the pH increases (Figure 3-6a). Curiously, the magnitude of the absorbance change was very similar for both C_r mutants (C50S and C50,100S) and the wild type protein, suggesting that each of these curves reflects primarily, or solely, the C_p thiol/thiolate status. The upward shift of about 0.3 to 0.4 pH units for both mutants which lack the C_r likely reflects the moderate influence this residue has on the C_p pK_a, presumably through structural and electrostatic perturbations near the active site imparted by this mutation.

To provide an independent measure of the pK_a of the C_p thiol group, we evaluated the rate of reaction of BCP with H_2O_2 using rapid manual mixing of enzyme (20 uM) and substrate (40 uM), quenching of the reaction with the FOX reagent, and subsequent spectrophotometric analysis to detect peroxide disappearance at time points from 1 to 15 s. Under these conditions, a first order rate of around 0.17 s^{-1} was obtained at pH 7 which, when divided by the concentration of BCP used, yields a second order rate constant of 9×10^3 M^{-1} s^{-1},

matching well with the V_{max}/K_m value for peroxide established in the steady state assays with Trx1. As shown in Figure 3-6b, titration of the BCP peroxide reactivity gave a remarkably similar pK_a value of 5.87 ± 0.16, strongly supporting the interpretation that the pK_a value of ~5.8 observed for the wild type, reduced enzyme by monitoring absorbance changes at 240 nm predominantly reflects titration of the C_p thiol group. This pK_a value for BCP is quite similar to those of other Prxs studied previously (Ferrer-Sueta *et al.*, 2011), including *X. fastidiosa* PrxQ (at 6.2), and *S. typhimurium* AhpC (at 5.9) (Horta *et al.*, 2010; Nelson *et al.*, 2008).

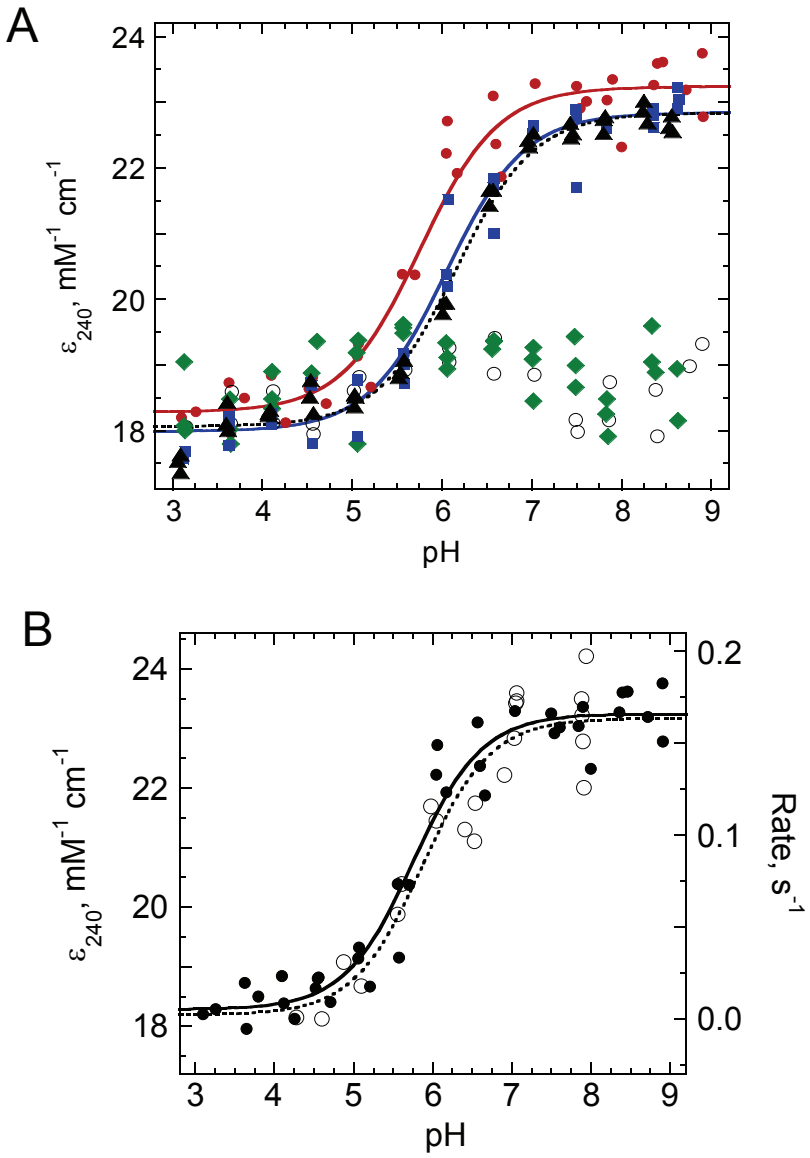
A
24
22
20
18
ε_{240}, mM^{-1} cm^{-1}
3
4
5
6
7
8
9
pH
B
24
22
20
18
ε_{240}, mM^{-1} cm^{-1}
0.2
0.1
0.0
Rate, s^{-1}
3
4
5
6
7
8
9
pH

Figure 3-6. Effects of pH on absorbance at 240 nm (panels A and B), and activity measured by the FOX assay (panel B) for BCP proteins. To generate data shown in both panels, the A_{240} and A_{280} values for reduced BCP (25 μM) were measured over a range of pH values and converted to ε_{240} as described in Experimental Procedures. Assuming the change in absorbance reflects a simple thiolate:thiol equilibrium, the pK_a values were calculated from the plot of ε_{240} versus pH by direct fit to Equation 3. Values shown are for wild type (red circles), C50S (blue squares) and C50,99S (black triangles) BCP, along with the respective pK_a fit curves (solid red, solid blue and dotted black, respectively). Data for C45S (green triangles) and oxidized wild type BCP (open circles) are also shown. In panel B, peroxide reduction rates (right axis) were assessed using the Fox assay to measure peroxide levels after rapid mixing with BCP (over a time course of 1 to 15 s), monitoring the decrease in absorbance at 595 nm after addition of the reagent (open circles and dotted line for the fit to Equation 3). These data are overlaid with the data from panel A with wild type, reduced BCP (closed circles and solid line) to illustrate the agreement between these independently-derived apparent pK_a values.

CONCLUSIONS

With these studies, wild-type BCP from *E. coli* joins the ranks of the relatively few Prxs across the diverse family which can use glutaredoxins as the source of reducing equivalents for peroxide reduction (Clarke *et al.*, 2010; Reynolds *et al.*, 2002; Rouhier *et al.*, 2002; Rouhier and Jacquot, 2003). The fact that BCP can take advantage of the availability of multiple forms of both Trx and Grx, in part due to its very high redox potential, and exhibits activity with both small and large hydroperoxide substrates makes it a potentially very important back-up system in cells under stress with compromised redox pathways. This functional flexibility may therefore offset the notably slow turnover (with k_{cat}/K_m for peroxide ~10^4 M^{-1} s^{-1}) catalyzed by BCP in the face of two other *E. coli* Prxs (AhpC and Tpx) with higher peroxide specificities and greater activities with the preferred substrates. Interestingly, the present data indicate that BCP reactivity by steady state analysis does reflect a slow rate of reaction of the reduced enzyme with H_2O_2 (Fig. 5b). This is in contrast to the findings with *Xylella fastidiosa* PrxQ, for which the first step of peroxide reaction is actually much faster (~10^7 M^{-1} s^{-1}) than its overall k_{cat}/K_m for H_2O_2 (~10^4 M^{-1} s^{-1}) (Horta *et al.*, 2010). Both *E. coli* BCP and *X. fastidiosa* PrxQ do, however, stabilize the thiolate form of the peroxidatic Cys in the active site to about the same degree (pK_a values of about 5.8 and 6.2, respectively) (Horta *et al.*, 2010).

Although the BCP/PrxQ subfamily members can confidently be grouped together based on sequence analyses which emphasize features near the active site (Copley *et al.*, 2004; Nelson *et al.*, 2011; Soito *et al.*, 2011), they are a very

diverse set of proteins spread across much of the phylogenetic tree. With the present data, we note that *E. coli* BCP has the highest redox potential (-146 mV at pH 7), and poplar PrxQ the lowest redox potential (-325 mV at pH 7), among all Prxs studied so far, indicating quite different structural attributes for the disulfide bonds in these proteins. It is now clear that some BCP/PrxQ proteins are monomeric, while others are dimeric. Even the second order reaction rate with H_2O_2 is now known to vary by as much as 3 orders of magnitude across the subfamily (Horta *et al.*, 2010). It is perhaps this very "adaptability" that has led to the persistence of this subfamily through much of evolution, adapting to fill a need in the various organisms that express it (Atack *et al.*, 2008; Hicks *et al.*, 2010; Jeong *et al.*, 2000; Wang *et al.*, 2005).

REFERENCES

Åslund, F., Berndt, K. D., and Holmgren, A. (1997). Redox potentials of glutaredoxins and other thiol-disulfide oxidoreductases of the thioredoxin superfamily determined by direct protein-protein redox equilibria. *J Biol Chem*. **272,** 30780-6.

Åslund, F., Ehn, B., Miranda-Vizuete, A., Pueyo, C., and Holmgren, A. (1994). Two additional glutaredoxins exist in *Escherichia coli*: glutaredoxin 3 is a hydrogen donor for ribonucleotide reductase in a thioredoxin/glutaredoxin 1 double mutant. *Proc Natl Acad Sci U S A*. **91,** 9813-7.

Atack, J. M., Harvey, P., Jones, M. A., and Kelly, D. J. (2008). The *Campylobacter jejuni* thiol peroxidases Tpx and Bcp both contribute to aerotolerance and peroxide-mediated stress resistance but have distinct substrate specificities. *J Bacteriol*. **190,** 5279-90.

Baba, T., Ara, T., Hasegawa, M., Takai, Y., Okumura, Y., Baba, M., Datsenko, K. A., Tomita, M., Wanner, B. L., and Mori, H. (2006). Construction of *Escherichia coli* K-12 in-frame, single-gene knockout mutants: the Keio collection. *Mol Syst Biol*. **2,** 2006 0008.

Baker, L. M., and Poole, L. B. (2003). Catalytic mechanism of thiol peroxidase from *Escherichia coli*. Sulfenic acid formation and overoxidation of essential CYS61. *J Biol Chem*. **278,** 9203-11.

Bardwell, J. C., McGovern, K., and Beckwith, J. (1991). Identification of a protein required for disulfide bond formation in vivo. *Cell*. **67,** 581-9.

Benesch, R. E., Lardy, H. A., and Benesch, R. (1955). The sulfhydryl groups of crystalline proteins. I. Some albumins, enzymes, and hemoglobins. *J Biol Chem*. **216,** 663-76.

Clarke, D. J., Mackay, C. L., Campopiano, D. J., Langridge-Smith, P., and Brown, A. R. (2009). Interrogating the molecular details of the peroxiredoxin activity of the *Escherichia coli* bacterioferritin comigratory protein using high-resolution mass spectrometry. *Biochemistry*. **48,** 3904-14.

Clarke, D. J., Ortega, X. P., Mackay, C. L., Valvano, M. A., Govan, J. R., Campopiano, D. J., Langridge-Smith, P., and Brown, A. R. (2010). Subdivision of the bacterioferritin comigratory protein family of bacterial peroxiredoxins based on catalytic activity. *Biochemistry*. **49,** 1319-30.

Copley, S. D., Novak, W. R., and Babbitt, P. C. (2004). Divergence of function in the thioredoxin fold suprafamily: evidence for evolution of peroxiredoxins from a thioredoxin-like ancestor. *Biochemistry*. **43,** 13981-95.

D'Ambrosio, K., Limauro, D., Pedone, E., Galdi, I., Pedone, C., Bartolucci, S., and De Simone, G. (2009). Insights into the catalytic mechanism of the Bcp family: functional and structural analysis of Bcp1 from *Sulfolobus solfataricus*. *Proteins*. **76,** 995-1006.

Dietz, K. J. (2011). Peroxiredoxins in Plants and Cyanobacteria. *Antioxid Redox Signal*. in press.

Dietz, K. J., Jacob, S., Oelze, M. L., Laxa, M., Tognetti, V., de Miranda, S. M., Baier, M., and Finkemeier, I. (2006). The function of peroxiredoxins in plant organelle redox metabolism. *J Exp Bot*. **57,** 1697-709.

El Hajjaji, H., Dumoulin, M., Matagne, A., Colau, D., Roos, G., Messens, J., and Collet, J. F. (2009). The zinc center influences the redox and thermodynamic properties of *Escherichia coli* thioredoxin 2. *J Mol Biol*. **386,** 60-71.

Eschenbach, D. A., Davick, P. R., Williams, B. L., Klebanoff, S. J., Young-Smith, K., Critchlow, C. M., and Holmes, K. K. (1989). Prevalence of hydrogen peroxide-producing *Lactobacillus* species in normal women and women with bacterial vaginosis. *J Clin Microbiol*. **27,** 251-256.

Fernandes, A. P., Fladvad, M., Berndt, C., Andresen, C., Lillig, C. H., Neubauer, P., Sunnerhagen, M., Holmgren, A., and Vlamis-Gardikas, A. (2005). A novel monothiol glutaredoxin (Grx4) from *Escherichia coli* can serve as a substrate for thioredoxin reductase. *J Biol Chem*. **280,** 24544-52.

Ferrer-Sueta, G., Manta, B., Botti, H., Radi, R., Trujillo, M., and Denicola, A. (2011). Factors affecting protein thiol reactivity and specificity in peroxide reduction. *Chem Res Toxicol*. **24,** 434-50.

Hall, A., Karplus, P. A., and Poole, L. B. (2009). Typical 2-Cys peroxiredoxins - structures, mechanisms and functions. *Febs J*. **276,** 2469-77.

Hall, A., Nelson, K., Poole, L., and Karplus, P. A. (2011). Structure-based insights into the catalytic power and conformational dexterity of peroxiredoxins. *Antioxid Redox Signal*. in press.

Hawkins, H. C., and Freedman, R. B. (1991). The reactivities and ionization properties of the active-site dithiol groups of mammalian protein disulphide-isomerase. *Biochem J*. **275 (Pt 2),** 335-9.

Hicks, L. D., Raghavan, R., Battisti, J. M., and Minnick, M. F. (2010). A DNA-binding peroxiredoxin of *Coxiella burnetii* is involved in countering oxidative stress during exponential-phase growth. *J Bacteriol*. **192,** 2077-84.

Holmgren, A. (1981). Thioredoxin: structure and functions. *Trends Biochem Sci*. **6,** 26-29.

Holmgren, A., Ohlsson, I., and Grankvist, M. L. (1978). Thiroedoxin from *Escherichia coli*. Radioimmunological and enzymatic determinations in wild type cells and mutants defective in phage T7 DNA replication. *J Biol Chem*. **253,** 430-6.

Horta, B. B., de Oliveira, M. A., Discola, K. F., Cussiol, J. R., and Netto, L. E. (2010). Structural and biochemical characterization of peroxiredoxin Qbeta from *Xylella fastidiosa*: catalytic mechanism and high reactivity. *J Biol Chem*. **285,** 16051-65.

Imlay, J. A. (2008). Cellular defenses against superoxide and hydrogen peroxide. *Annu Rev Biochem*. **77,** 755-76.

Jaeger, J., Sorensen, K., and Wolff, S. P. (1994). Peroxide accumulation in detergents. *J Biochem Biophys Methods*. **29,** 77-81.

Jeong, W., Cha, M. K., and Kim, I. H. (2000). Thioredoxin-dependent hydroperoxide peroxidase activity of bacterioferritin comigratory protein (BCP) as a new member of the thiol-specific antioxidant protein (TSA)/Alkyl hydroperoxide peroxidase C (AhpC) family. *J Biol Chem*. **275,** 2924-30.

Jönsson, T. J., Ellis, H. R., and Poole, L. B. (2007). Cysteine reactivity and thiol-disulfide interchange pathways in AhpF and AhpC of the bacterial alkyl hydroperoxide reductase system. *Biochemistry*. **46,** 5709-21.

Kim, S. J., Woo, J. R., Hwang, Y. S., Jeong, D. G., Shin, D. H., Kim, K., and Ryu, S. E. (2003). The tetrameric structure of *Haemophilus influenza* hybrid Prx5 reveals interactions between electron donor and acceptor proteins. *J Biol Chem*. **278,** 10790-8.

König, J., Baier, M., Horling, F., Kahmann, U., Harris, G., Schurmann, P., and Dietz, K. J. (2002). The plant-specific function of 2-Cys peroxiredoxin-mediated detoxification of peroxides in the redox-hierarchy of photosynthetic electron flux. *Proc Natl Acad Sci U S A*. **99,** 5738-43.

Kortemme, T., Darby, N. J., and Creighton, T. E. (1996). Electrostatic interactions in the active site of the N-terminal thioredoxin-like domain of protein disulfide isomerase. *Biochemistry*. **35,** 14503-11.

Ladner, J. E., Parsons, J. F., Rife, C. L., Gilliland, G. L., and Armstrong, R. N. (2004). Parallel evolutionary pathways for glutathione transferases: structure and mechanism of the mitochondrial class kappa enzyme rGSTK1-1. *Biochemistry*. **43,** 352-61.

Laue, T. M., Shah, B. D., Ridgeway, T. M., and Pelletier, S. L., Computer-aided interpretation of analytical sedimentation data for proteins. In: S. E. Harding, et al., Eds.), Analytical ultracentrifugation in biochemistry and polymer science. The Royal Society of Chemistry, Cambridge, 1992, pp. 90-125.

Lennon, B. W., and Williams, C. H., Jr. (1995). Effect of pyridine nucleotide on the oxidative half-reaction of *Escherichia coli* thioredoxin reductase. *Biochemistry*. **34,** 3670-7.

Liao, S. J., Yang, C. Y., Chin, K. H., Wang, A. H., and Chou, S. H. (2009). Insights into the alkyl peroxide reduction pathway of *Xanthomonas campestris* bacterioferritin comigratory protein from the trapped intermediate-ligand complex structures. *J Mol Biol*. **390,** 951-66.

Lundstrom, J., and Holmgren, A. (1993). Determination of the reduction-oxidation potential of the thioredoxin-like domains of protein disulfide-isomerase from the equilibrium with glutathione and thioredoxin. *Biochemistry*. **32,** 6649-55.

Miller, R. A., and Britigan, B. E. (1997). Role of oxidants in microbial pathophysiology. *Clin Microbiol Rev*. **10,** 1-18.

Nelson, K. J., Knutson, S. T., Soito, L., Klomsiri, C., Poole, L. B., and Fetrow, J. S. (2011). Analysis of the peroxiredoxin family: Using active-site structure and sequence information for global classification and residue analysis. *Proteins*. **79,** 947-64.

Nelson, K. J., Parsonage, D., Hall, A., Karplus, P. A., and Poole, L. B. (2008). Cysteine pK_a values for the bacterial peroxiredoxin AhpC. *Biochemistry*. **47,** 12860–12868.

Neumann, C. A., Krause, D. S., Carman, C. V., Das, S., Dubey, D. P., Abraham, J. L., Bronson, R. T., Fujiwara, Y., Orkin, S. H., and Van Etten, R. A. (2003). Essential role for the peroxiredoxin Prdx1 in erythrocyte antioxidant defence and tumour suppression. *Nature*. **424,** 561-5.

Nordstrand, K., Aslund, F., Meunier, S., Holmgren, A., Otting, G., and Berndt, K. D. (1999). Direct NMR observation of the Cys-14 thiol proton of reduced *Escherichia coli* glutaredoxin-3 supports the presence of an active site thiol-thiolate hydrogen bond. *FEBS Lett*. **449,** 196-200.

Ogusucu, R., Rettori, D., Munhoz, D. C., Soares Netto, L. E., and Augusto, O. (2007). Reactions of yeast thioredoxin peroxidases I and II with hydrogen peroxide and peroxynitrite: Rate constants by competitive kinetics. *Free Radic Biol Med*. **42,** 326-34.

Ortenberg, R., Gon, S., Porat, A., and Beckwith, J. (2004). Interactions of glutaredoxins, ribonucleotide reductase, and components of the DNA replication system of *Escherichia coli*. *Proc Natl Acad Sci U S A*. **101,** 7439-44.

Parsonage, D., Desrosiers, D. C., Hazlett, K. R., Sun, Y., Nelson, K. J., Cox, D. L., Radolf, J. D., and Poole, L. B. (2010a). Broad specificity AhpC-like peroxiredoxin and its thioredoxin reductant in the sparse antioxidant defense system of *Treponema pallidum*. *Proc Natl Acad Sci U S A*. **107,** 6240-5.

Parsonage, D., Karplus, P. A., and Poole, L. B. (2008). Substrate specificity and redox potential of AhpC, a bacterial peroxiredoxin. *Proc Natl Acad Sci U S A*. **105,** 8209-14.

Parsonage, D., Reeves, S. A., Karplus, P. A., and Poole, L. B. (2010b). Engineering of fluorescent reporters into redox domains to monitor electron transfers. *Methods Enzymol*. **474,** 1-21.

Parsonage, D., Youngblood, D. S., Sarma, G. N., Wood, Z. A., Karplus, P. A., and Poole, L. B. (2005). Analysis of the link between enzymatic activity and oligomeric state in AhpC, a bacterial peroxiredoxin. *Biochemistry*. **44,** 10583-92.

Philo, J. S. (1997). An improved function for fitting sedimentation velocity data for low-molecular-weight solutes. *Biophys J*. **72,** 435-44.

Philo, J. S. (2000). A method for directly fitting the time derivative of sedimentation velocity data and an alternative algorithm for calculating sedimentation coefficient distribution functions. *Anal Biochem*. **279,** 151-63.

Poole, L. B. (2005). Bacterial defenses against oxidants: mechanistic features of cysteine-based peroxidases and their flavoprotein reductases. *Arch Biochem Biophys*. **433,** 240-54.

Poole, L. B., Godzik, A., Nayeem, A., and Schmitt, J. D. (2000a). AhpF can be dissected into two functional units: tandem repeats of two thioredoxin-like folds in the N-terminus mediate electron transfer from the thioredoxin reductase-like C-terminus to AhpC. *Biochemistry*. **39,** 6602-15.

Poole, L. B., Reynolds, C. M., Wood, Z. A., Karplus, P. A., Ellis, H. R., and Li Calzi, M. (2000b). AhpF and other NADH:peroxiredoxin oxidoreductases, homologues of low Mr thioredoxin reductase. *Eur J Biochem*. **267,** 6126-33.

Potamitou, A., Holmgren, A., and Vlamis-Gardikas, A. (2002). Protein levels of *Escherichia coli* thioredoxins and glutaredoxins and their relation to null mutants, growth phase, and function. *J Biol Chem*. **277,** 18561-7.

Reynolds, C. M., Meyer, J., and Poole, L. B. (2002). An NADH-dependent bacterial thioredoxin reductase-like protein in conjunction with a glutaredoxin homologue

form a unique peroxiredoxin (AhpC) reducing system in *Clostridium pasteurianum*. *Biochemistry*. **41,** 1990-2001.

Ritz, D., Patel, H., Doan, B., Zheng, M., Aslund, F., Storz, G., and Beckwith, J. (2000). Thioredoxin 2 is involved in the oxidative stress response in *Escherichia coli*. *J Biol Chem*. **275,** 2505-12.

Roberts, B. R., Wood, Z. A., Jönsson, T. J., Poole, L. B., and Karplus, P. A. (2005). Oxidized and synchrotron cleaved structures of the disulfide redox center in the N-terminal domain of *Salmonella typhimurium* AhpF. *Protein Sci*. **14,** 2414-20.

Rouhier, N., Gelhaye, E., Gualberto, J. M., Jordy, M. N., De Fay, E., Hirasawa, M., Duplessis, S., Lemaire, S. D., Frey, P., Martin, F., Manieri, W., Knaff, D. B., and Jacquot, J. P. (2004). Poplar peroxiredoxin Q. A thioredoxin-linked chloroplast antioxidant functional in pathogen defense. *Plant Physiol*. **134,** 1027-38.

Rouhier, N., Gelhaye, E., and Jacquot, J. P. (2002). Glutaredoxin-dependent peroxiredoxin from poplar: protein-protein interaction and catalytic mechanism. *J Biol Chem*. **277,** 13609-14.

Rouhier, N., Gelhaye, E., Sautiere, P. E., Brun, A., Laurent, P., Tagu, D., Gerard, J., de Fay, E., Meyer, Y., and Jacquot, J. P. (2001). Isolation and characterization of a new peroxiredoxin from poplar sieve tubes that uses either glutaredoxin or thioredoxin as a proton donor. *Plant Physiol*. **127,** 1299-309.

Rouhier, N., and Jacquot, J. P. (2003). Molecular and catalytic properties of a peroxiredoxin-glutaredoxin hybrid from *Neisseria meningitidis*. *FEBS Lett*. **554,** 149-53.

Rouhier, N., and Jacquot, J. P. (2005). The plant multigenic family of thiol peroxidases. *Free Radic Biol Med*. **38,** 1413-21.

Ryan, C. S., and Kleinberg, I. (1995). Bacteria in human mouths involved in the production and utilization of hydrogen peroxide. *Arch Oral Biol*. **40,** 753-763.

Soito, L., Williamson, C., Knutson, S. T., Fetrow, J. S., Poole, L. B., and Nelson, K. J. (2011). PREX: PeroxiRedoxin classification indEX, a database of subfamily assignments across the diverse peroxiredoxin family. *Nucleic Acids Res*. **39,** D332-7.

Storz, G., Jacobson, F. S., Tartaglia, L. A., Morgan, R. W., Silveira, L. A., and Ames, B. N. (1989). An alkyl hydroperoxide reductase induced by oxidative stress in *Salmonella typhimurium* and *Escherichia coli*: genetic characterization and cloning of *ahp*. *J Bacteriol*. **171,** 2049-55.

Van Holde, K. E., Physical Biochemistry. Prentice-Hall, Inc., Englewood Cliffs, NJ, 1971, pp. 110-136.

Veine, D. M., Mulrooney, S. B., Wang, P. F., and Williams, C. H., Jr. (1998). Formation and properties of mixed disulfides between thioredoxin reductase from *Escherichia coli* and thioredoxin: evidence that cysteine-138 functions to initiate

dithiol-disulfide interchange and to accept the reducing equivalent from reduced flavin. *Protein Sci*. **7,** 1441-50.

Wang, G., Olczak, A. A., Walton, J. P., and Maier, R. J. (2005). Contribution of the *Helicobacter pylori* thiol peroxidase bacterioferritin comigratory protein to oxidative stress resistance and host colonization. *Infect Immun*. **73,** 378-84.

Winterbourn, C. C. (2008). Reconciling the chemistry and biology of reactive oxygen species. *Nat Chem Biol*. **4,** 278-86.

Wood, Z. A., Poole, L. B., Hantgan, R. R., and Karplus, P. A. (2002). Dimers to doughnuts: redox-sensitive oligomerization of 2-cysteine peroxiredoxins. *Biochemistry*. **41,** 5493-504.

Wood, Z. A., Poole, L. B., and Karplus, P. A. (2003). Peroxiredoxin evolution and the regulation of hydrogen peroxide signaling. *Science*. **300,** 650-3.

Woolston, C. M., Storr, S. J., Ellis, I. O., Morgan, D. A., and Martin, S. G. (2011). Expression of thioredoxin system and related peroxiredoxin proteins is associated with clinical outcome in radiotherapy treated early stage breast cancer. *Radiother Oncol*.

Wunderlich, M., and Glockshuber, R. (1993). Redox properties of protein disulfide isomerase (DsbA) from *Escherichia coli*. *Protein Sci*. **2,** 717-26.

Xia, B., Vlamis-Gardikas, A., Holmgren, A., Wright, P. E., and Dyson, H. J. (2001). Solution structure of *Escherichia coli* glutaredoxin-2 shows similarity to mammalian glutathione-S-transferases. *J Mol Biol*. **310,** 907-18.

Yamamoto, Y., Ritz, D., Planson, A. G., Jonsson, T. J., Faulkner, M. J., Boyd, D., Beckwith, J., and Poole, L. B. (2008). Mutant AhpC peroxiredoxins suppress thiol-disulfide redox deficiencies and acquire deglutathionylating activity. *Mol Cell*. **29,** 36-45.

Zhang, B., Wang, Y., and Su, Y. (2009). Peroxiredoxins, a novel target in cancer radiotherapy. *Cancer Lett*. **286,** 154-60.

Chapter 4

THE CATALYTIC RELEVANCE OF DISULFIDE BOND FORMATION IN *E. COLI* BCP

Stacy A. Reeves, Derek Parsonage, Leslie B. Poole

The following manuscript is in preparation for submission. Experiments involving the intermediate formation rates of *Escherichia coli* BCP are ongoing. Upon completion of future experiments, this manuscript will be submitted for publication. Reeves performed the kinetic experiments, gel shift studies, and prepared the manuscript. Dr. Parsonage assisted Reeves with sulfenic acid formation experiments. Dr. Poole is serving in an advisory and editorial capacity.

Peroxiredoxins possess an active site motif centered around a cysteine that reacts with peroxides called the “peroxidatic” cysteine or C_P. During the first phase of Prx catalysis the C_P attacks its peroxide (ROOH) substrate creating both sulfenic acid (Cys-SOH) on the enzyme and the reduced ROH product. After sulfenic acid formation, peroxiredoxins return the $C_P$to its active fully reduced form by 3 distinct mechanisms; 1-Cys, typical 2-Cys, and atypical 2-Cys (Figure 4-1) (Wood *et al* 2003). In typical and atypical 2-Cys Prxs, sulfenic acid is resolved with the formation of a disulfide bond between C_P and the resolving cysteine (C_R) (Ellis and Poole 1997; Jeong *et al* 2000, Rouhier *et al* 2002; Rouhier *et al* 2004; Trujillo *et al* 2006, Clarke *et al* 2010). The major difference between both 2-Cys mechanisms is the location of the C_R. The typical 2-Cys Prxs are dimeric and form intersubunit disulfide bonds with the C_R on a second subunit to resolve sulfenic acid. Conversely, in atypical 2-Cys Prxs, an intrasubunit disulfide bond is formed between C_P and a C_R farther down the same polypeptide chain.

BCP/PrxQ subfamily was originally classified based on the presence of a C_PXXXXC_R motif and a highly conserved TPVCTKE motif spanning the C_P (Copley *et al* 2004). The second cysteine; however, is not universally conserved in the BCP subfamily (Copley *et al* 2004, Hall *et al* 2010, Nelson 2011). In atypical 2-Cys BCPs, the resolving cysteine can be found in 1 of 2 locations: 5 residues downstream from the C_P (C_PXXXXC_R) or 35 residues downstream from the C_P in the α3 helix, akin to the Tpx subfamily (Copley *et al* 2004, Wakita *et al* 2007). The remainder of the BCP/PrxQ proteins employ a 1-Cys mechanism.

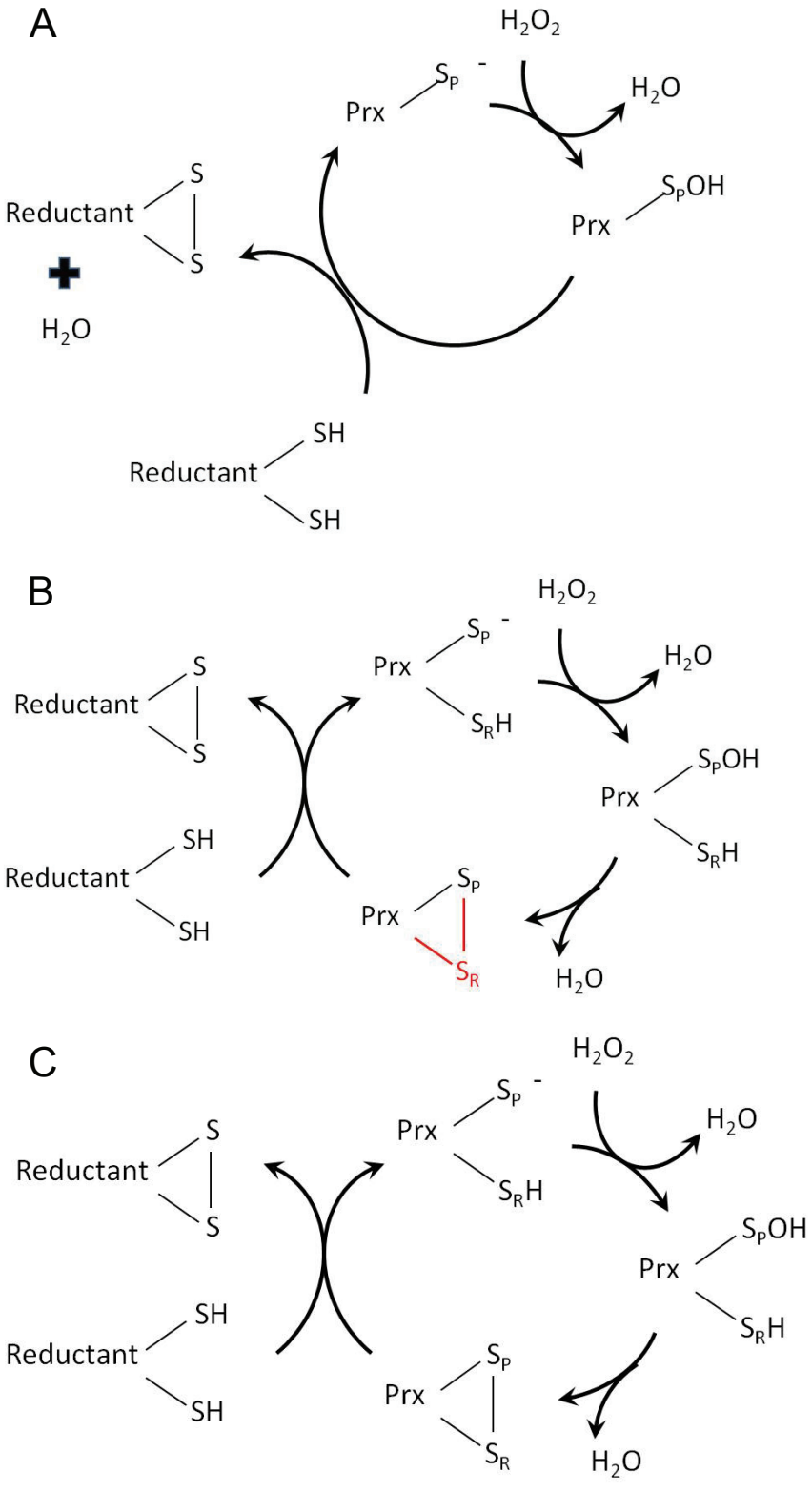
A
H_2O_2
S_P -
Prx
H_2O
S_POH
Prx
S
Reductant
S
H_2O
SH
Reductant
SH
B
H_2O_2
S_P -
Prx
H_2O
S_RH
S
Reductant
S
S_POH
Prx
S_RH
SH
Reductant
SH
S_P
Prx
S_R
H_2O
C
H_2O_2
S_P -
Prx
H_2O
S_RH
S
Reductant
S
S_POH
Prx
S_RH
SH
Reductant
SH
S_P
Prx
S_R
H_2O

Figure 4-1. Examples of peroxiredoxin mechanisms. Depicted are the 3 types of mechanisms utilized by peroxiredoxins. The formation of sulfenic acid on the C_P is a universal feature among Prxs. The differences between the mechanisms reflect the variations in sulfenic acid reduction. (A) The 1-Cys Prxs are resolved by exogenous reducing substrates for reactivation. (B) In typical 2-Cys, the resolving Cys sulfur (S_R, red) comes from a resolving cysteine on another subunit, thus forming an inter-subunit disulfide bond. (C) The C_R of atypical 2-Cys Prxs is found on the same subunit. In all pathways, the Prxs are typically recycled by dithiol-containing reductants.

The BCP/PrxQ subfamily is suggested to be most representative of the ancestral precursor of modern Prxs (Copley *et al* 2004, Hall *et al* 2011). These proteins may initially have begun as 1-Cys Prxs and evolved resolving cysteines over time, and in different locations. Other subfamilies exhibit C_R conservation as high as 99% as is seen for the AhpC subfamily, while the position of the C_R varies greatly in the BCP/PrxQ subfamily, with 54% in helix α2 and 7% in helix α3, leaving 39% as expected 1-Cys (Nelson 2011). Virtually half the members of this group do not possess a resolving cysteine which calls into question not only the mechanism of *Ec*BCP, but also the catalytic competence of active site disulfide bonds.

*Ec*BCP possesses the C_PXXXXC_R motif. While it has a total of 3 cysteine residues (Cys45, Cys50, Cys99), only the mutation of the absolutely conserved cysteine (Cys45) resulted in complete loss of thiol peroxidase activity (Jeong *et al* 2000). Additionally, mutating the resolving cysteine still allows for the reduction of sulfenic acid in members of other Prxs subfamilies in which the C_R location is highly conserved; however the reduction reaction does experience decreased activity (Ellis and Poole 1997; Rouhier *et al* 2002; Baker and Poole 2003; Rouhier *et al* 2004; Trujillo *et al* 2006). It is entirely possible that *Ec*BCP may function as both a 2-Cys and a 1-Cys peroxiredoxin, even in the presence of the second active site cysteine (C_R). Analytical ultracentrifugation studies described in the previous chapter using reduced and oxidized *Ec*BCP confirmed the monomeric nature of *Ec*BCP in solution. Along with data from other investigators (Jeong *et al* 2000, Clarke *et al* 2009), these studies eliminated the possibility of

BCP forming an intersubunit disulfide bond similar to the typical 2-Cys Prxs (see previous chapter).

In mutational studies conducted on a plant BCP homologue (PrxQ), researchers discovered that a second mechanism was operable in the presence of certain reducing substrates. In these studies, a resolving cysteine mutant of Poplar PrxQ demonstrated increased activity for a reducing substrate (a Grx) that the wild-type enzyme could not use (Rouhier *et al* 2004). If this extends to *Ec*BCP, this enzyme may utilize either a 1-Cys or an atypical 2-Cys mechanism depending on the availability of reducing substrates.

GSH reportedly inhibited Trx-linked turnover of *Burkholderia cenocepacia* BCP (*Bc*BCP), a naturally occurring 1-Cys BCP, due to the formation of an irresolvable GSH-BCP complex (Clarke *et al* 2010). Clarke *et al* contend that the GSH/Grx system is not efficient for reducing 2-Cys Prxs, yet it is the preferred reductant of 1-Cys BCP subfamily members and is capable of inhibiting the TrxR/Trx system (Clarke *et al* 2010). However, as described in Chapters 2 and 3, our studies show that Grx1, not GSH, serves as a direct reductant for *Ec*BCP (Parsonage *et al* 2010). If the GSH/Grx system is the preferred pathway for 1-Cys BCPs, then *Ec*BCP resolving cysteine mutants (C50S) should only demonstrate increased efficiency in Grx-linked peroxidase experiments. In mutational studies of a resolving cysteine mutant of PrxQ, activity increased for all reductants, including thioredoxin (Rouhier *et al* 2004). These data suggest that the presence of a resolving cysteine may sacrifice overall activity in order to

protect the C_P against over-oxidation by additional equivalents of peroxide substrate.

The first studies regarding peroxidase activity of *Ec*BCP C_R mutants were conducted in 2000. Jeong *et al* conducted mutational experiments on *Ec*BCP to determine the functionality of each cysteine residue in the active site. The experiments were strictly aimed at identifying the catalytic cysteine by measuring the antioxidant activity of each cysteine mutants. Their results verified C45 as the catalytic cysteine. Surprisingly, in those studies, the C50S mutant retained ~80% of its ability to protect against oxidative stress (Jeong *et al* 2000). At the time, no true V_{max} or K_m values were given for this activity as neither substrate (reductant or H_2O_2) was varied, but the data suggested a possible 1-Cys mechanism for *Ec*BCP (Jeong *et al* 2000). Other studies have examined the activity of resolving cysteine mutants of *Ec*BCP (Clarke *et al* 2009), but only with the present work, reported herein, have kinetic parameters for *Ec*BCP C_R mutants been determined.

Previous studies confirmed disulfide bond formation in oxidized *Ec*BCP, but they have yet to definitely prove its formation during turnover or its catalytic competence (Jeong *et al* 2000, Clark *et al* 2009). The experiments were not conducted in the presence of a reductant and were primarily designed to trap and map disulfide bonds. The data presented in this chapter calls into question the necessity for disulfide bond formation between C45 and C50 during *Ec*BCP turnover. In fact, possible mechanisms may differ based on the type of reductant, i.e. Trx and Grx, and its availability *in vivo*. The studies described in

this chapter tested the hypothesis that *Ec*BCP exhibits a 1-Cys peroxidase mechanism, but is not limited to this particular mechanism. Our strategy has been to determine the ability of each reductant to reduce disulfide bonds (k_4) and to measure the formation rates of each intermediate during turnover of *Ec*BCP (Figure 4-2). The relative rate of intramolecular disulfide (k_3) formation compared to direct intermolecular disulfide formation with each reductant (k_2) will determine which mechanism is preferred during turnover.

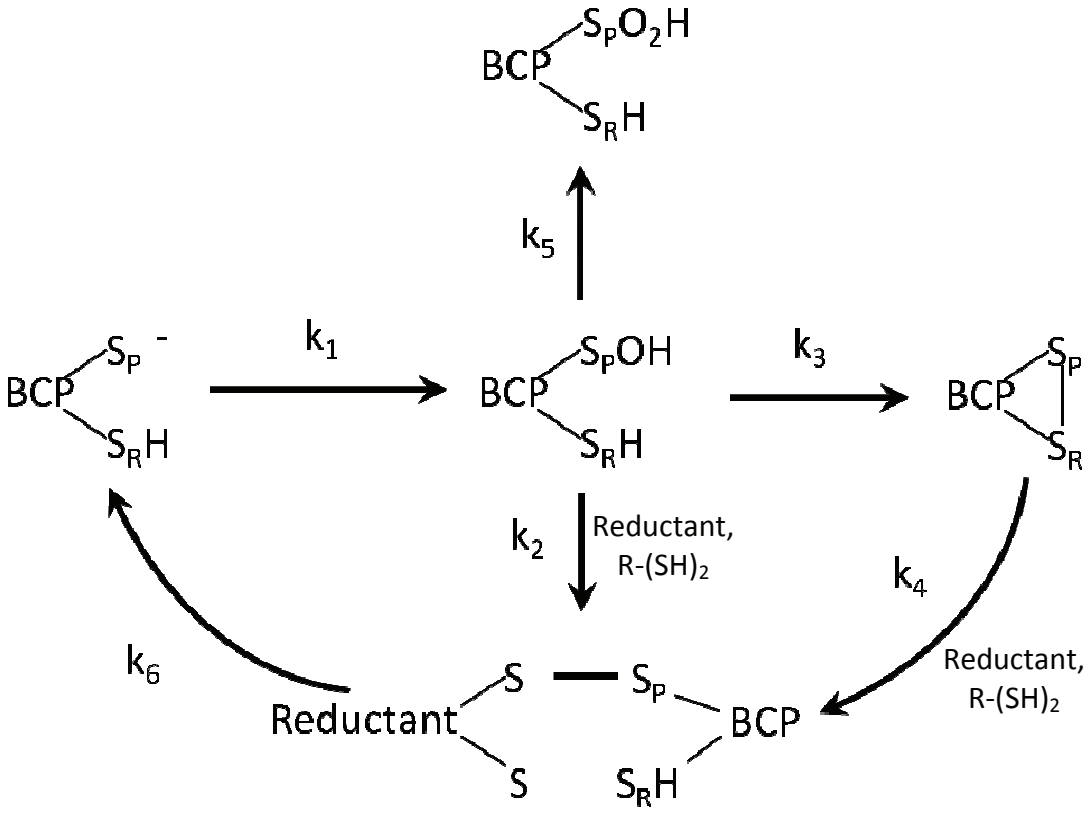

Figure 4-2. *E. coli* BCP Kinetic Intermediates. An illustration of the various *Ec*BCP intermediates and the corresponding rate of formation. Currently, the proposed *Ec*BCP pathway involves k_1, k_3, k_4, and k_6. The k_2 pathway represents turnover through a 1-Cys Prx mechanism.

METHODS

Mutagenesis, Expression and Purification of Proteins. All mutations were introduced as described previously in Chapters 2 and 3. The BCP, Trx1 and $Grx1_{F6W}$ proteins were expressed and purified as described in Chapter 3. In addition, another mutant of Grx1, the C14S mutant ($Grx1_{C14S}$, which removes the resolving Cys of the CXXC active site), was expressed and purified for these studies as previously described (Yamamoto *et al* 2008).

Stopped Flow Spectral Analysis to Measure Wild-Type and Mutant BCP Turnover With Trx and $Grx1_{F6W}$. As previously described in Chapter 2, a sensitive assay was developed that monitors Trx and mutant $Grx1_{F6W}$ oxidation. Pre-reduced Trx1 or $Grx1_{F6W}$ (10 μM final concentrations after mixing), were mixed with 0.5 μM *Ec*BCP and the reaction buffer (50 mM phosphate buffer with 1 mM EDTA at pH 7) in one syringe while varying concentrations (25 μM – 500 μM) H_2O_2 were added to the same buffer in the second syringe of an Applied Photophysics SX.18MV stopped-flow spectrophotometer. *E. coli* BCP peroxidase activity was measured by monitoring the change in fluorescence of oxidized reductant, with excitation at 280 nm and emission >320 nm (using an emission filter). Fluorescence changes were calibrated by measuring the total change in fluorescence upon oxidation of 10 μM Trx or $Grx1_{F6W}$ by excess peroxide, described in more detail in Chapter 2, and converted to μM/min using Equation 1 in Chapter 3. The initial rate of fluorescence decrease was determined by linear regression of the data during the first 2 seconds of the

reaction at 25ºC. Values for V_{max} and K_m for peroxide were obtained by fitting the experimental data to the Michaelis-Menten equation using Kaleidagraph.

Analysis of the Rate of Peroxide Reduction (k_1) of Wild-type and Mutant BCP. Peroxide reduction rates were assessed using the FOX assay to measure peroxide levels at various time points after the addition of wild-type or mutant BCP. Equal volumes (25 µL) of 50 µM H_2O_2 were added to 25 µM *E. coli* BCP (final concentrations after mixing) in 10 mM Borate-Phosphate-Citrate buffer (pH 7 before quenching with 1 mL of FOX reagent after various time points between 1 and 15 s. A standard curve was created by adding FOX reagent to known H_2O_2 concentrations between 10 and 50 µM. Samples from each reaction along with standard curve samples were transferred to 96 well plates and the absorbance at 595 nm was measured on a Tecan Sapphire2 plate reader. Data were fit to an exponential decay curve and rates were calculated based on observed rates and peroxide concentrations.

Measurement of Glutaredoxin Complex Formation with EcBCP Sulfenic Acid By Gel Shift Assay. All proteins were first prereduced by DTT for 1 hr and excess DTT was removed by PD10 column filtration in 50 mM phosphate buffer at pH 7. Equal volumes (50 µl) of equimolar concentrations (60 µM) of *Ec*$BCP_{C50,99S}$ and $Grx1_{C14S}$ were combined. Next, 100 µl of 60 µM H_2O_2 was added, yielding final concentrations of 15 µM reductant and 30 µM H_2O_2. Aliquots were removed at various time points and quenched with 0.2 M N-ethylmaleimide (NEM). Grx-BCP complex was visualized by resolving the samples on a SDS-PAGE gel and staining with GelCode Blue.

Measurement of Glutaredoxin Complex Formation with EcBCP Disulfide By A Gel Shift Assay. Proteins were prereduced by DTT for 1 hr and excess DTT was removed by PD10 column filtration in 50 mM phosphate buffer at pH 7. Reduced *Ec*BCP was oxidized by incubation with 10 mM H_2O_2 for 2 min in order to generate disulfide bonds. Excess H_2O_2 was removed similarly to DTT. Equal volumes (50 μl) of equimolar concentrations (20 μM) of oxidized *Ec*BCP and $Grx1_{C14S}$ were combined. Aliquots were removed at various time points and quenched with 0.2 M NEM. Grx-BCP complex was visualized after resolution by SDS-PAGE as described above.

RESULTS

EcBCP Behaves as a Robust 1-Cys Prx in the Absence of the Resolving Cysteine. To test the ability of BCP to utilize a 1-Cys mechanism and to compare the effectiveness of this mechanism with multiple reducing substrates, stopped-flow spectral analyses of wild-type and mutant *Ec*BCP proteins were conducted using Trx (Figure 4-3a) and $Grx1_{F6W}$ (Figure 4-3b). The rate of reaction was monitored by observing decreasing fluorescence associated with oxidation of the reductant. The V_{max} rates for C50S and C50,99S mutants were up to 2.5-fold and 19-fold faster than for wild-type *Ec*BCP with Trx and $Grx1_{F6W}$, respectively (Table 4-I). In the previous chapter, V_{max}/K_m for ROOH remained constant across a range of Trx concentrations for *Ec*BCP, which established the validity of using this number to compare reductants, even when comparing them at a single reductant concentration. Values for V_{max}/K_m (ROOH) determined for both mutants were <2-fold different than those for wild-type *Ec*BCP with both reductants, Trx1 and $Grx1_{F6W}$ (Table 4-1). Interestingly, the V_{max}/K_m values were very similar when comparing $EcBCP_{C50,99S}$ and $Grx1_{F6W}$ with wild-type *Ec*BCP and Trx1, the reportedly preferred reductant of *Ec*BCP. A significant loss of activity was typically observed in mutational studies of other 2 Cys-containing Prx subfamilies and if the BCP/PrxQ subfamily is reminiscent of the precursor of modern day Prxs, then it is possible that even 2-Cys members of the BCP/PrxQ subfamily may function more efficiently as 1-Cys Prxs (Ellis and Poole 1997;

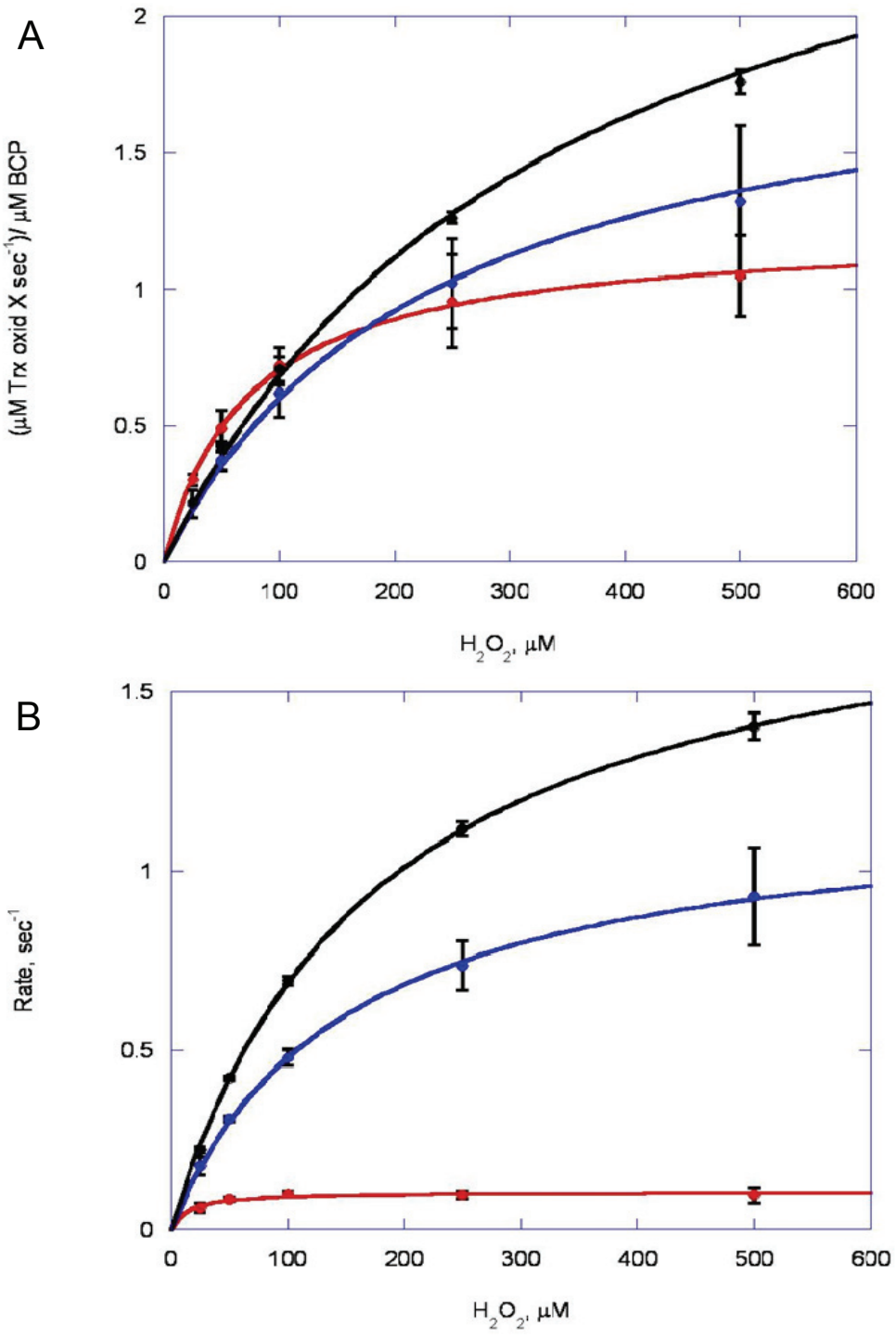
A
(μM Trx oxid X sec-1)/ μM BCP
2
1.5
1
0.5
0
0
100
200
300
400
500
600
H2O2, μM
B
Rate, sec-1
1.5
1
0.5
0
0
100
200
300
400
500
600
H2O2, μM

Figure 4-3. *E. coli* BCP utilizes a robust 1-Cys mechanism in the absence of the resolving cysteine. In panel A, the rate of reaction was measured by monitoring the change in fluorescence of 10 μM oxidized Trx1 in the presence of 0.5 μM *Ec*BCP (wild-type or mutants), and 25-500 μM H_2O_2 in 50 mM phosphate and 1 mM EDTA, at pH 7. In panel B, 10 μM $Grx1_{F6W}$ was used in place of Trx1. In both panels, red represents the data with wild-type *Ec*BCP, blue with *Ec*BCP_{C50S}, and black with *Ec*$BCP_{C50,99S}$.

Table 4-I: Steady-state Kinetics Parameters of Wild-Type and Mutant BCP With Varying Concentrations Of H_2O_2

Protein Reductant, at 10 *μM*	BCP	$V_{max, app}$ *(μM/s)/ μM* BCP	$K_{m, app}$ for ROOH *μM*	V_{max}/K_m M^{-1} s^{-1}
Trx1	Wild-type	1.21 ± 0.02	76.1 ± 3.77	1.6×10^4
	C50S	1.85 ± 0.05	204 ± 17.31	9.1×10^3
	C50,99S	3.03 ± 0.08	343 ± 21.10	8.9×10^3
$Grx1_{F6W}$	Wild-type	0.10 ± 0.006	14.6 ± 4.9	7.2×10^3
	C50S	1.14 ± 0.002	135 ± 1.3	8.4×10^3
	C50,99S	1.90 ± 0.039	176 ± 294	1.1×10^4

Jeong *et al* 2000, Rouhier *et al* 2002; Baker and Poole 2003; Rouhier *et al* 2004; Trujillo *et al* 2006).

The Rate of SOH Formation (k_1) Is Unaffected By the C_R. We predicted that the resolving cysteine does not play a significant role in C_P activation or peroxide activation for attack; therefore, a rapid mix/acid quench assay was used to determine the influence of C_R on SOH formation by measuring H_2O_2 disappearance in the presence of wild-type and C50,99S *Ec*BCP (Figure 4-4). Under these pseudo-first order conditions (with H_2O_2 in excess), first order rate constant divided by the H_2O_2 concentration yielded a second order rate constant (k_1) of wild-type BCP with peroxide (or formation rate of SOH) of 6.76 x 10^3 M^{-1} s^{-1}, while *Ec*$BCP_{C50,99S}$ exhibited a slightly slower rate, at 5.76 x 10^3 M^{-1} s^{-1}. The comparable rates demonstrated between wild-type and mutant *Ec*BCP indicate that Cys50 does not affect active site chemistry. Therefore, differences in activity between wild-type and mutant can be attributed to changes in the rate of disulfide bond formation or reductant interactions. This experiment provided the rate of sulfenic acid formation (k_1 in Figure 4-2).

Measurement of the Formation of the Grx1 Complex With 1-Cys Ec*BCP *(k_2) by Gel Shift Analysis. In recently reported studies, Brown and coworkers demonstrated that *Bc*BCP (a naturally occurring 1-Cys BCP) was able to use GSH as a reductant in combination with Grx1 to reduce the mixed disulfide bond between glutathione and BCP (Clarke *et al* 2010). Our data, described in the preceding chapter, also demonstrated that the Grx system is capable of reducing

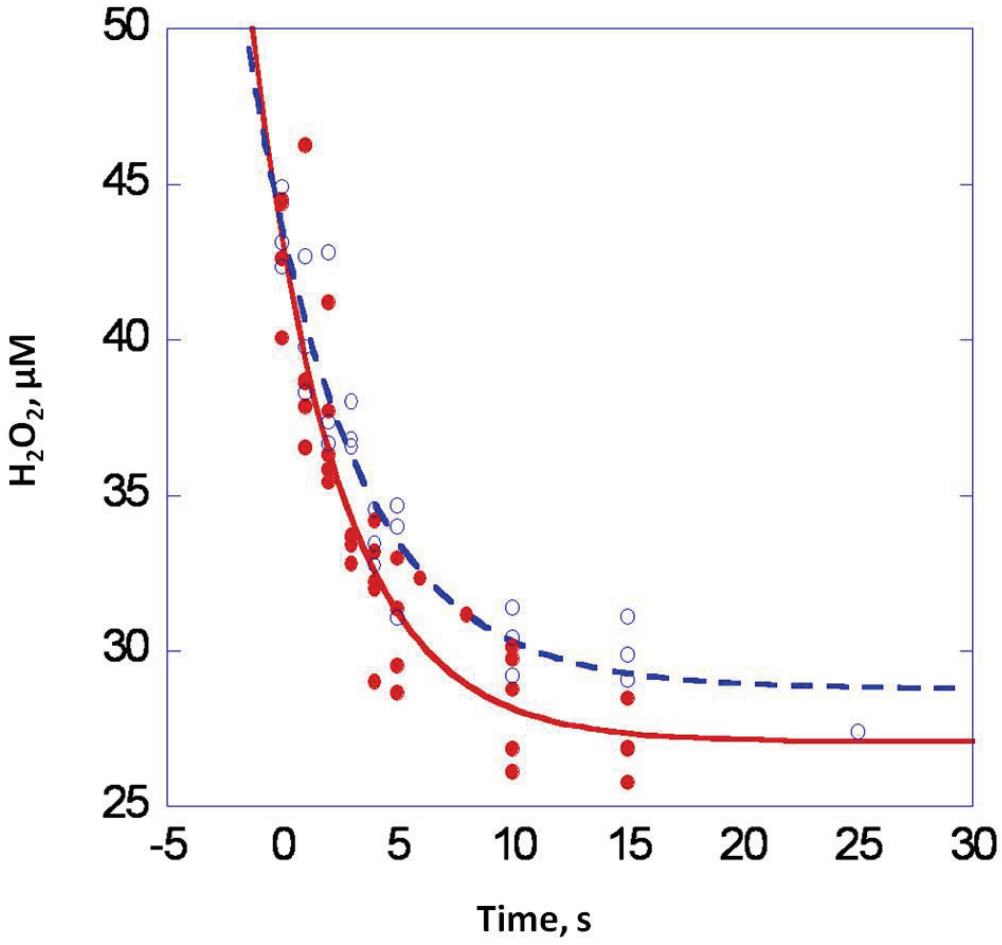

Figure 4-4. Determination of the rate of SOH formation (k_1) for the reaction of 25 µM *Ec*BCP with 50 µM H_2O_2, in the absence or presence of the C_R. Peroxide disappearance was measured after the addition of wild-type or mutant C50,99S *Ec*BCP using the FOX acid quench method as described in Chapter 3. Data were fit to a single exponential decay curve for both wild-type *Ec*BCP (red) and *Ec*BCP$_{C50,99S}$ (blue).

oxidized *Ec*BCP; however, this reduction occurs in the absence of GSH, with Grx1 serving as the direct substrate (Parsonage *et al* 2010). To determine the rate of Grx1 disulfide formation with the BCP sulfenic acid (k_2), we monitored complex formation using gel shift analysis (Figure 4-5). The reaction mixture containing equimolar concentrations of reduced *Ec*$BCP_{C50,99S}$ and $Grx1_{C14S}$ was incubated with H_2O_2 and rapid complex formation was observed. The rate of complex formation under these conditions occured at approximately the same rate as sulfenic acid formation (Fig. 4-4). The rate of reaction measured using this method depends on both k_1 and k_2; therefore, higher concentrations of H_2O_2 are needed in order to prevent the reaction from being rate limited by k_1. However, we have an initial indication from these studies that k_2 is greater than ~ 0.3 s^{-1}.

By comparing k_2 with the rate of k_3 and k_4 once we have them, we will be able to determine if sulfenic acid formation alone is sufficient for turnover of *Ec*BCP with Grx1, bypassing disulfide bond formation. In additional experiments, wild-type *Ec*BCP will replace the mutant in order to measure complex formation in the presence of the resolving cysteine, although initial efforts to determine k2 values with wild-type EcBCP, described in the next section, suggest that stopped flow kinetic approaches will be required. The experiment conducted with $Grx1_{C14S}$ will also be repeated with mutated Trx (C35S) replacing $Grx1_{C14S}$.

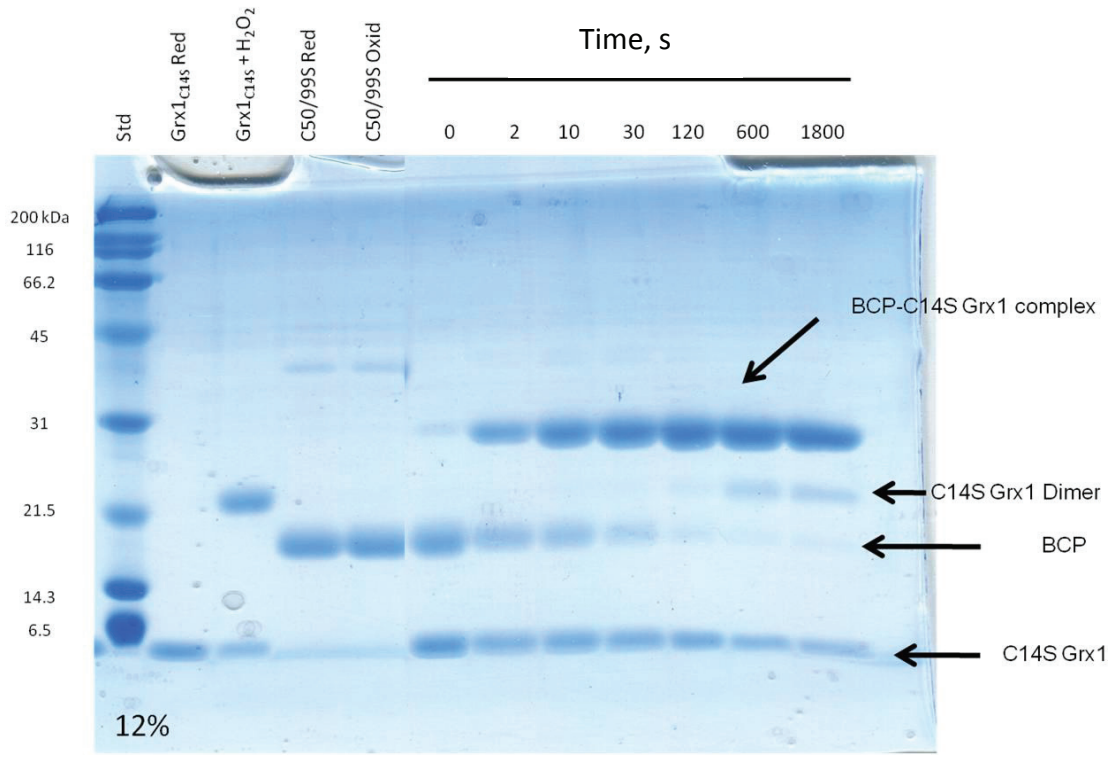

Figure 4-5. Determination of the rate of formation of Grx1 in complex with the BCP sulfenic acid (k_2). H_2O_2 (30 μM) was added to 15 μM of pre-reduced *Ec*BCP (C50,99S) and 15 μM $Grx1_{C14S}$. Aliquots were removed at various time points and quenched with 0.2 M NEM. Proteins were resolved by SDS-PAGE and Grx-BCP complex formation was visualized after staining with GelCode Blue.

Measurement of the Resolution of Disulfide Bonds in Oxidized EcBCP (k_4) By Trx or Grx1. The next set of gel shift assays was designed to measure the reduction rate (k_4) of $Grx1_{C14S}$ for disulfide-bonded *Ec*BCP. Similar to the previous experiment, equimolar concentrations of prereduced $Grx1_{C14S}$ were incubated with *Ec*BCP, which in this case was pre-oxidized to form the C45-C99 disulfide bond (Figure 4-6). At various time points, aliquots were removed and quenched using 0.2 M NEM. As shown in Fig. 4-6, no complex was observed on the gel, suggesting that either Grx1 is unable to reduce disulfide-bonded *Ec*BCP, or the back reaction to yield oxidized BCP and the thiol form of Grx_{C14S} is more thermodynamically favorable. These and other data suggest that disulfide bonds may serve as poor substrates for Grx1 (Clarke *et al* 2010).

The next set of experiments will be conducted with mutant Trx_{C35S} instead of mutant $Grx1_{C14S}$ and may yield vastly different results (i.e., Trx- *Ec*BCP complex formation) given the known propensity for Trx1 to reduce disulfide bonds in proteins. The implications of such results would be that Trx1 is the preferred reductant *Ec*BCP when it contains an intramolecular disulfide, but not necessarily during turnover.

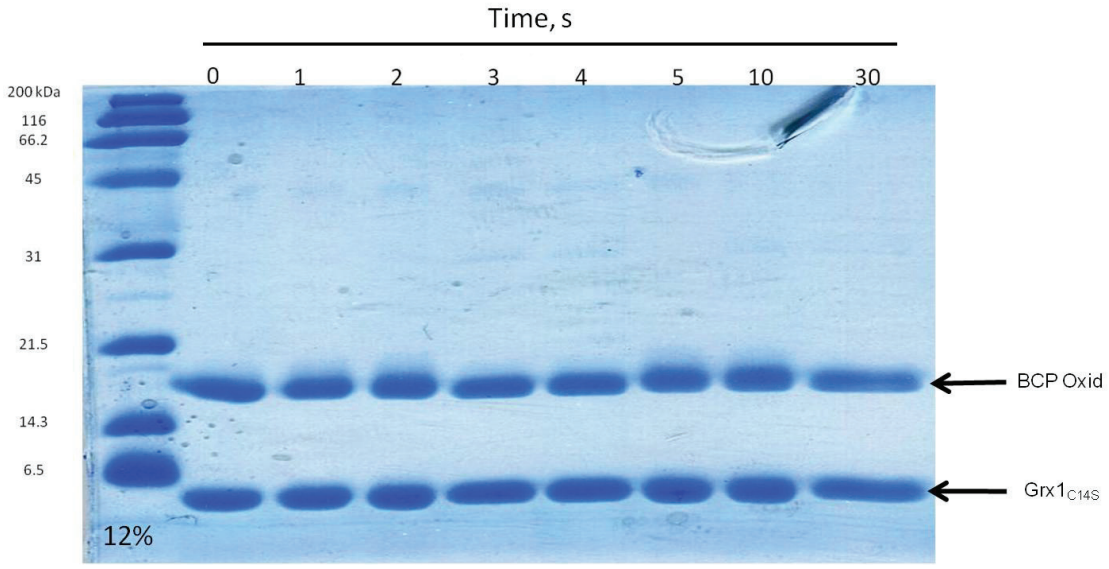

Figure 4-6. Determination of the rate of formation of Grx1 in complex with BCP disulfide (k_4). Pre-reduced $Grx1_{C14S}$ (20 μM) was added to 20 μM of pre-oxidized (disulfide bonded) *Ec*BCP. Aliquots were removed at various time points and quenched with 0.2 M NEM. Proteins were resolved by SDS-PAGE and Grx-BCP complex formation was visualized after staining with GelCode Blue.

DISCUSSION

In this study we established that *Ec*BCP is capable of performing as a 1-Cys Prx through stopped-flow spectral analysis of *Ec*BCP resolving cysteine mutants, highlighting the versatility of the *Ec*BCP mechanism. Pursuing this further, another group showed that when a putative resolving cysteine was inserted into the active site of a 1-Cys BCP member (*Bc*BCP) to create the L49C mutant which resembles *Ec*BCP (Clarke *et al* 2010), L49C could indeed utilize a 2-Cys mechanism in the presence of Trx.

With Trx1 as reductant, the V_{max}/K_m for hydrogen peroxide decreased less than 2-fold from wild-type to C50,99S *Ec*BCP, while the V_{max}/K_m increased slightly from wild-type to the C50,99S mutant with Grx1. This is consistent with previous studies of the poplar PrxQ resolving cysteine mutant (Rouhier *et al* 2004), where the corresponding C_R mutant demonstrated greatly increased activity compared to wild-type PrxQ in the presence of Grx. Together, these data suggest that Grx is a relatively poor disulfide bond reductase and is better suited for sulfenic acid resolution than for disulfide bond reduction (Rouhier *et al* 2004, Clarke *et al* 2010). In another study, the 1-Cys BCP from *Burkholderia cenocepacia* (BcBCP, mentioned above) demonstrated higher activity with the GSH/Grx system than with the Trx system. Moreover, GSH was able to inhibit activity in the presence of the Trx system (Clarke *et al* 2010). In addition, another group demonstrated that a mitochondrial 1-Cys Prx (Prx1p) in yeast is capable of antioxidant defense, but only when coupled with GSH/Grx (Pedrajas *et al* 2010). Following this further, a 1-Cys Prx (BiPrx1) found in *Bombus ignitus*

is incapable of utilizing Trx as a reductant (Hu *et al* 2010). In some cases, 2-Cys Prxs prefer the GSH/Grx reducing system, as is the case with SLL1621, a 2-Cys Prx found in the cyanobacteria, *Synechocystis sp. PCC 6803*, which showed 10-20% more activity with Grx than with Trx (Hosoya-Matsuda *et al* 2005). Conclusions drawn from the aforementioned studies are bolstered by the data obtained from C_R mutational studies presented in this chapter and other sources that also showed increased Grx-dependent activity in the absence of C_R (Rouhier *et al* 2004).

It is entirely possible that intramolecular disulfide bond formation during turnover in 2-Cys BCPs will be dependent on reductant concentration and the role of the resolving cysteine in the BCP/PrxQ subfamily may be to protect the catalytic cysteine from overoxidation in the absence of satisfactory reductant levels, even though this may sacrifice some degree of efficiency in turnover, and may impose a greater limitation on the reductants that can be used for regeneration. In the Prx catalytic cycle, sulfenic acid forms at the C_P as an intermediate and is not generally as stable as sulfinic acid (SO_2H) or disulfide bonds (Yang 2002, Wagner *et al* 2002, Prouzet-Mauleon *et al* 2002). As presented in Chapter 3, the catalytic efficiency of many Prxs (~10^7 M^{-1} s^{-1}) is significantly greater than that of *Ec*BCP. Although removing the resolving cysteine increased activity during turnover, it did not increase it enough to put *Ec*BCP on par with other peroxiredoxins. Sluggish peroxidase turnover with reductants results in generation of a SOH group that is susceptible to overoxidation in 1-Cys Prxs, and this susceptibility may have been the driving

force behind the evolution of the resolving cysteine in the BCP/PrxQ subfamily. Attempts by Clark *et al.*to trap SOH for mass spectrometric analysis proved difficult due to disulfide bond or sulfinic acid (SO_2H) formation in *Ec*BCP_{C50S} (Clarke *et al* 2009). Our lab has observed that SOH is readily converted to SO_2H during mass spectrometry analysis, so it is unclear from the experiments by Clarke *et al* whether sulfinic acid is ever formed during normal turnover.

Further studies with *Ec*BCP proteins are planned to answer questions surrounding the formation and reduction of disulfide bonds. In order to test for proposed preference of Grx1 for SOH reduction, parallel investigations involving wild-type and mutant Trx and Grx proteins will be conducted with *Ec*BCP in various forms, e.g. reduced, sulfenic acid and disulfide bonded forms. The data generated from the proposed experiments will elucidate the mechanism of *Ec*BCP and contribute to our emerging understanding of catalysis among members of the BCP/PrxQ subfamily.

REFERENCES

Baker, L. M., and Poole, L. B. (2003). Catalytic mechanism of thiol peroxidase from *Escherichia coli*. Sulfenic acid formation and overoxidation of essential CYS61. *J Biol Chem*. **278,** 9203-11.

Clarke, D. J., Mackay, C. L., Campopiano, D. J., Langridge-Smith, P., and Brown, A. R. (2009). Interrogating the molecular details of the peroxiredoxin activity of the *Escherichia coli* bacterioferritin comigratory protein using high-resolution mass spectrometry. *Biochemistry*. **48,** 3904-14.

Clarke, D. J., Ortega, X. P., Mackay, C. L., Valvano, M. A., Govan, J. R., Campopiano, D. J., Langridge-Smith, P., and Brown, A. R. (2010). Subdivision of the bacterioferritin comigratory protein family of bacterial peroxiredoxins based on catalytic activity. *Biochemistry*. **49,** 1319-30.

Copley, S. D., Novak, W. R., and Babbitt, P. C. (2004). Divergence of function in the thioredoxin fold suprafamily: evidence for evolution of peroxiredoxins from a thioredoxin-like ancestor. *Biochemistry*. **43,** 13981-95.

Ellis, H. R., and Poole, L. B. (1997). Roles for the two cysteine residues of AhpC in catalysis of peroxide reduction by alkyl hydroperoxide reductase from *Salmonella typhimurium*. *Biochemistry*. **36,** 13349-56.

Hall, A., Nelson, K., Poole, L., and Karplus, P. A. (2011). Structure-based insights into the catalytic power and conformational dexterity of peroxiredoxins. *Antioxid Redox Signal* 15, 795-815.

Hosoya-Matsuda, N., Motohashi, K., Yoshimura, H., Nozaki, A., Inoue, K., Ohmori, M., and Hisabori, T. (2005). Anti-oxidative stress system in cyanobacteria. Significance of type II peroxiredoxin and the role of 1-Cys peroxiredoxin in Synechocystis sp. strain PCC 6803. *J Biol Chem*. **280,** 840-6.

Jeong, W., Cha, M. K., and Kim, I. H. (2000). Thioredoxin-dependent hydroperoxide peroxidase activity of bacterioferritin comigratory protein (BCP) as a new member of the thiol-specific antioxidant protein (TSA)/Alkyl hydroperoxide peroxidase C (AhpC) family. *J Biol Chem*. **275,** 2924-30.

Nelson, K. J., Knutson, S. T., Soito, L., Klomsiri, C., Poole, L. B., and Fetrow, J. S. (2011). Analysis of the peroxiredoxin family: Using active-site structure and sequence information for global classification and residue analysis. *Proteins*. **79,** 947-64.

Parsonage, D., Reeves, S. A., Karplus, P. A., and Poole, L. B. (2010). Engineering of fluorescent reporters into redox domains to monitor electron transfers. *Methods Enzymol*. **474,** 1-21.

Pedrajas, J. R., Padilla, C. A., McDonagh, B., and Barcena, J. A. (2010). Glutaredoxin participates in the reduction of peroxides by the mitochondrial 1-CYS peroxiredoxin in *Saccharomyces cerevisiae*. *Antioxid Redox Signal*. **13,** 249-58.

Prouzet-Mauleon, V., Monribot-Espagne, C., Boucherie, H., Lagniel, G., Lopez, S., Labarre, J., Garin, J., and Lauquin, G. J. (2002). Identification in *Saccharomyces cerevisiae* of a new stable variant of alkyl hydroperoxide reductase 1 (Ahp1) induced by oxidative stress. *J Biol Chem*. **277,** 4823-30.

Rouhier, N., Gelhaye, E., Gualberto, J. M., Jordy, M. N., De Fay, E., Hirasawa, M., Duplessis, S., Lemaire, S. D., Frey, P., Martin, F., Manieri, W., Knaff, D. B., and Jacquot, J. P. (2004). Poplar peroxiredoxin Q. A thioredoxin-linked chloroplast antioxidant functional in pathogen defense. *Plant Physiol*. **134,** 1027-38.

Rouhier, N., Gelhaye, E., and Jacquot, J. P. (2002). Glutaredoxin-dependent peroxiredoxin from poplar: protein-protein interaction and catalytic mechanism. *J Biol Chem*. **277,** 13609-14.

Trujillo, M., Mauri, P., Benazzi, L., Comini, M., De Palma, A., Flohe, L., Radi, R., Stehr, M., Singh, M., Ursini, F., and Jaeger, T. (2006). The mycobacterial thioredoxin peroxidase can act as a one-cysteine peroxiredoxin. *J Biol Chem*. **281,** 20555-66.

Wagner, E., Luche, S., Penna, L., Chevallet, M., Van Dorsselaer, A., Leize-Wagner, E., and Rabilloud, T. (2002). A method for detection of overoxidation of cysteines: peroxiredoxins are oxidized in vivo at the active-site cysteine during oxidative stress. *Biochem J*. **366,** 777-85.

Wakita, M., Masuda, S., Motohashi, K., Hisabori, T., Ohta, H., and Takamiya, K. (2007). The significance of type II and PrxQ peroxiredoxins for antioxidative stress response in the purple bacterium *Rhodobacter sphaeroide*s. *J Biol Chem*. **282,** 27792-801.

Wood, Z. A., Schröder, E., Harris, J. R., and Poole, L. B. (2003). Structure, mechanism and regulation of peroxiredoxins. *Trends Biochem Sci*. **28,** 32-40.

Yang, K. S., Kang, S. W., Woo, H. A., Hwang, S. C., Chae, H. Z., Kim, K., and Rhee, S. G. (2002). Inactivation of human peroxiredoxin I during catalysis as the result of the oxidation of the catalytic site cysteine to cysteine-sulfinic acid. *J Biol Chem*. **277,** 38029-36.

Chapter 5

CONCLUSIONS

Escherichia coli bacterioferritin comigratory protein (*Ec*BCP) is a peroxiredoxin which catalyzes the reduction of hydrogen peroxide and alkyl hydroperoxides. *Ec*BCP possesses a conserved Prx active site structure centered around the peroxidatic cysteine which forms a cysteine sulfenic acid upon reaction with peroxides. This cysteine subsequently forms a disulfide bond with an active site resolving cysteine (intramolecular) or a reductant (intermolecular) during reductive recycling. Additionally, *Ec*BCP exhibited a broad specificity for reductants and peroxide substrates, potentially allowing BCP to remain fully active and functional under varying cellular conditions. The work in this dissertation provides both kinetic and biochemical details surrounding the role and function of *E. coli* BCP.

Chapter 2 of this dissertation was published in Methods of Enzymology in 2010. It reports the discovery of a Grx reducing pathway for *Ec*BCP and describes the construction and application of a mutant Grx fluorescent redox reporter. Chapter 3 of this dissertation describes the kinetic and biochemical and redox properties of *Ec*BCP; this chapter has been submitted for review and publication to *Biochemistry*. Chapter 4 examines the formation and catalytic competence of disulfide bonded BCP. The combined works presented in this dissertation better characterize residue functions and rates of reaction of *Escherichia coli* bacterioferritin comigratory protein.

The Engineering of a Glutaredoxin Fluorescent Redox Reporter. In previous studies of a plant BCP homologue, PrxQ, Grx was able to support as low level of peroxidase activity, although substitution of the C_R with Ser led to

increased peroxidase activity using this same reductant (Rouhier, 2004). Based on a shared sequence identity with poplar PrxQ of ~40%, it was predicted that *Ec*BCP would exhibit activity in the presence of Grx. In NADPH linked peroxidase assays, our studies showed that Grx was capable of serving as a reductant for *Ec*BCP. Stopped-flow spectral analysis utilizing wild type Grx1 proved to be problematic because of low fluorescence mission intensity. Therefore, a mutant of Grx1 was created with a redox state-sensitive fluorescent reporter (F6W) near the active site, based on the position of the fluorescent Trp28 in thioredoxin. The added Trp residue produced a measurable 2-fold difference in fluorescence between reduced and oxidized redox states. $Grx1_{F6W}$ served as a useful tool in subsequent Grx-dependent stopped-flow investigations of *Ec*BCP described in Chapter 3.

Ec*BCP *is a Monomer. Previous studies utilized SDS PAGE analysis to determine oligomeric state, although this method tests only for covalent linkage of subunits (Jeong *et al.*, 2000). Other investigations using high resolution mass spectrometry suggested that BCP behaves as a monomer, but these studies also did not address the oligomeric state of *Ec*BCP in solution (Clarke *et al.*, 2009). Investigations into oligomeric states of other peroxiredoxins have revealed that protein concentration can affect the oligomeric state (Wood *et al.*, 2002, Parsonage *et al.*, 2005). Consequently, analytical ultracentrifugation was used to accurately determine sedimentation coefficient and the molecular weight of reduced and oxidized *Ec*BCP in solution. During analytical ultracentrifugation

studies, BCP behaved as a monomer in solution eliminating the possibility of a mechanism including intersubunit disulfide bond formation.

Broad Substrate Specificity of E. coli BCP. BCP exists in two states, a reduced dithiol state and a chemically modified oxidized state as a direct result of peroxide reduction. A detailed bisubstrate kinetic analysis of *Ec*BCP was conducted by stopped-flow investigation using varying amounts of Trx and H_2O_2 as substrates. A Hanes-Woolf analysis of the *Ec*BCP kinetic data presented in Chapter 3 is consistent with a ping-pong mechanism as expected for this protein. From these investigations, a turnover rate was observed that was 67-fold faster than those previously recorded and the catalytic efficiency (V_{max}/K_m) of *Ec*BCP was determined to be ~10^4 M^{-1} s^{-1} (Chapter 3). Furthermore, *Ec*BCP demonstrated an increase in rate proportional to Trx1 concentrations suggesting the reaction was not saturated even at concentrations as high as 80 μM Trx. To put this in perspective, the K_m of AhpC, another *E. coli* peroxiredoxin, toward its designated reductant, AhpF, is 5.9 μM (Parsonage *et al.*, 2008).

As *Ec*BCP exhibited higher activity with H_2O_2 than had been previously appreciated, we also analyzed the ability of *Ec*BCP to reduce other organic substrates, and specifically the bulky tertiary hydroperoxides t-butyl hydroperoxide (tBHP) and cumene hydroperoxide (CHP). *Ec*BCP demonstrated comparable peroxidase activity when acting upon H_2O_2 and cumene hydroperoxide (CHP). These results show that BCP is equally active with at least some organic hydroperoxide substrates.

An exploration of other potential reductants of BCP was conducted using NADPH-linked assays and stopped-flow spectral analysis, revealing that Grx1, Grx3, and Trx2 also act as reductants of *Ec*BCP. The V_{max} of BCP and H_2O_2 when utilizing Trx1 as an electron donor was noted to be 2.5-fold faster than with Trx2 or Grx1, and ~5.6-fold faster than Grx3. Trx1 and $Grx1_{F6W}$ demonstrated similar V_{max}/K_m values despite the large differences in V_{max} and K_m.

The versatility of *Ec*BCP activity led us to further investigate underlying biochemical features of this enzyme. One important aspect of redox centers within enzymes is their midpoint reduction (redox) potential. The redox potentials of the four Trx and Grx redoxins shown to recycle *Ec*BCP range from -198 mV (for Grx3) to -284 mV (for Trx1) (Moore *et al.*, 1964, Krause & Holmgren, 1991, Krause *et al.*, 1991, Aslund *et al.*, 1997). Our kinetic studies using Trx and Grx proteins provided a starting point for estimating the redox potential of BCP because reduction pathways (electron donation) proceed in the direction of increasing redox potential (Moore *et al.*, 1964, Aslund *et al.*, 1997). Investigations described in Chapter 3 yielded a value for the redox potential of -146 mV at pH 7 for *Ec*BCP that is higher than any previously reported peroxiredoxin. For example, AhpC proteins from *Treponema pallidum* and *Salmonella typhimurium* exhibit redox potentials of -192 ± 2 and -178 ± 0.4 mV, respectively (Steiner *et al.*, 1981, Parsonage *et al.*, 2008). This higher value for *Ec*BCP partially explains the reducing substrate versatility exhibited by *Ec*BCP.

***Increases In Peroxidase Activity Of Ec*BCP *Via Direct Reduction Of Sulfenic Acid By Grx*.** Disulfide bonds are about 40% weaker than C-C and C-

H bonds, making them ideal for serving as redox switches and signaling (Sevier & Kaiser, 2002). In recent studies, *Ec*BCP was described as an atypical 2-Cys Prx after the intramolecular disulfide bond in this protein was mapped to C45-C50 by high resolution mass spectometry (Clarke *et al.*, 2009). However, the findings did not prove formation or catalytic competency of disulfide bonds under normal cellular conditions and any assumptions regarding the *in vivo* formation of disulfide bonds should be based on experiments conducted in the presence of cellular reducing systems (Jeong *et al.*, 2000, Clarke *et al.*, 2009). The data presented in Chapter 4 shows that BCP is capable of exhibiting a robust 1-Cys mechanism in the absence of the resolving cysteine. Surprisingly, the catalytic efficiency of the mutant nearly doubled for *Ec*BCP$_{C50S}$ (compared with wild type) with Grx1 serving as the electron donor. Based on C_R mutant studies of *Ec*BCP and other subfamily members, it is entirely possible that 2-Cys containing members of the BCP/PrxQ subfamily are capable of 1-Cys activity in the presence of Grx (Rouhier, 2004, Clarke *et al.*, 2010). Gel shift assays proved that *Ec*BCP can efficiently form intermolecular disulfide bonds with mutant Grx1. However, mutant Grx1 was incapable of forming a stable complex with oxidized (disulfide bonded) wild type *Ec*BCP. These findings suggest that Grx prefers SOH reduction as opposed to disulfide bond reduction.

E. coli BCP Potentially Serves as a Peroxidase of Last Resort. *E. coli* possess various H_2O_2 scavengers, such as catalase, glutathione, superoxide dismutase, BtuE, and two other Prxs, Tpx and AhpC. The role of *Ec*BCP has not been cleared defined. The studies conducted and presented in this dissertation

shed new light on the possible *in vivo* role of *Ec*BCP. While the catalytic efficiency of *Ec*BCP is small (10^4 M^{-1} s^{-1}) when compared to other Prxs (~10^6-10^8 M^{-1} s^{-1}), catalase (~10^6 M^{-1} s^{-1}), and glutathione peroxidases (~10^8 $M^{-1}s^{-1}$), the low turnover rates associated with *Ec*BCP do not automatically imply unimportance (Hillar *et al.*, 2000, Pineyro *et al.*, 2011, Ross *et al.*, 2011). Deletions of *bcp* in *E. coli* resulted in hypersensitivity to H_2O_2, t-BHP, and linoleic acid hydroperoxide as measured by decreased colony size and survival rates (Jeong *et al.*, 2000, Wang *et al.*, 2005). Ultimately, BCP demonstrated a broad specificity for peroxides, with comparable rates for H_2O_2, a small molecule, and the larger CHP. This suggests the active site of BCP is capable of accommodating both large and small substrates resulting in broader specificity and potentially higher K_m values for peroxide substrates and various reductants. In one study, the ability of *Ec*BCP to reduce linoleic acid hydroperoxide was 5-fold greater than for other substrates; as a result, researchers claimed the role of *Ec*BCP was in fatty acid or lipid hydroperoxide reduction (Jeong *et al.*, 2000). However, *E. coli* does not contain the polyunsaturated fatty acids that are most prone to lipid peroxidation, making it unclear whether this is a physiologically relevant activity.

The presumed infinite K_m and marginal V_{max} of *E. coli* BCP results in a somewhat low V_{max}/K_m around 10^4 M^{-1} s^{-1} (presented in Chapter 3). *Ec*BCP demonstrated increasing V_{max} with increasing reductant concentrations, while maintaining catalytic efficiency. Under normal conditions, the intracellular concentrations of H_2O_2 are well below the K_m of *Ec*BCP forcing it to continually

operate under limiting conditions. Since *Ec*BCP is capable of using multiple reductants *in vivo*, then it stands to reason that *in vitro* assays with a single reductant do not accurately depict all of the cytoplasmic interactions of *Ec*BCP during turnover. These assays are necessary for accurately determining V_{max} and K_m for various BCP substrates, but they may be missing something about the *in vivo* function of BCP. The data presented in this dissertation suggests that greater amounts of reductant are available than apparent when measuring each individual reductant, resulting in increased H_2O_2 scavenging (Figure 5-1).

In studies assessing the importance of Trx and Grx protein *in vivo*, only the monocysteinic Grx4 proved indispensible to *E. coli* survival (Fernandes & Holmgren, 2004). The remaining genes in the Trx and Grx pathways can be knocked out individually without significantly decreasing cell survival (although simultaneous Trx and Grx impairment stops cell division). The lack of necessity of each of these may be the reason why *Ec*BCP possesses such broad specificity for reductants. It is able to scour the cytoplasm for all possible reductants based on availability (Figure 5-2). Because of the reported decrease in levels of Grx1 from exponential to stationary phase, it is unlikely that Grx1 serves as a major reductant of BCP during stationary phase. However, Grx1 expression is upregulated (along with Trx1 and Trx2) in the absence of catalase, and in the absence of Trx1 Grx1 cellular levels increase 20~30 fold (Potamitou, 2002).

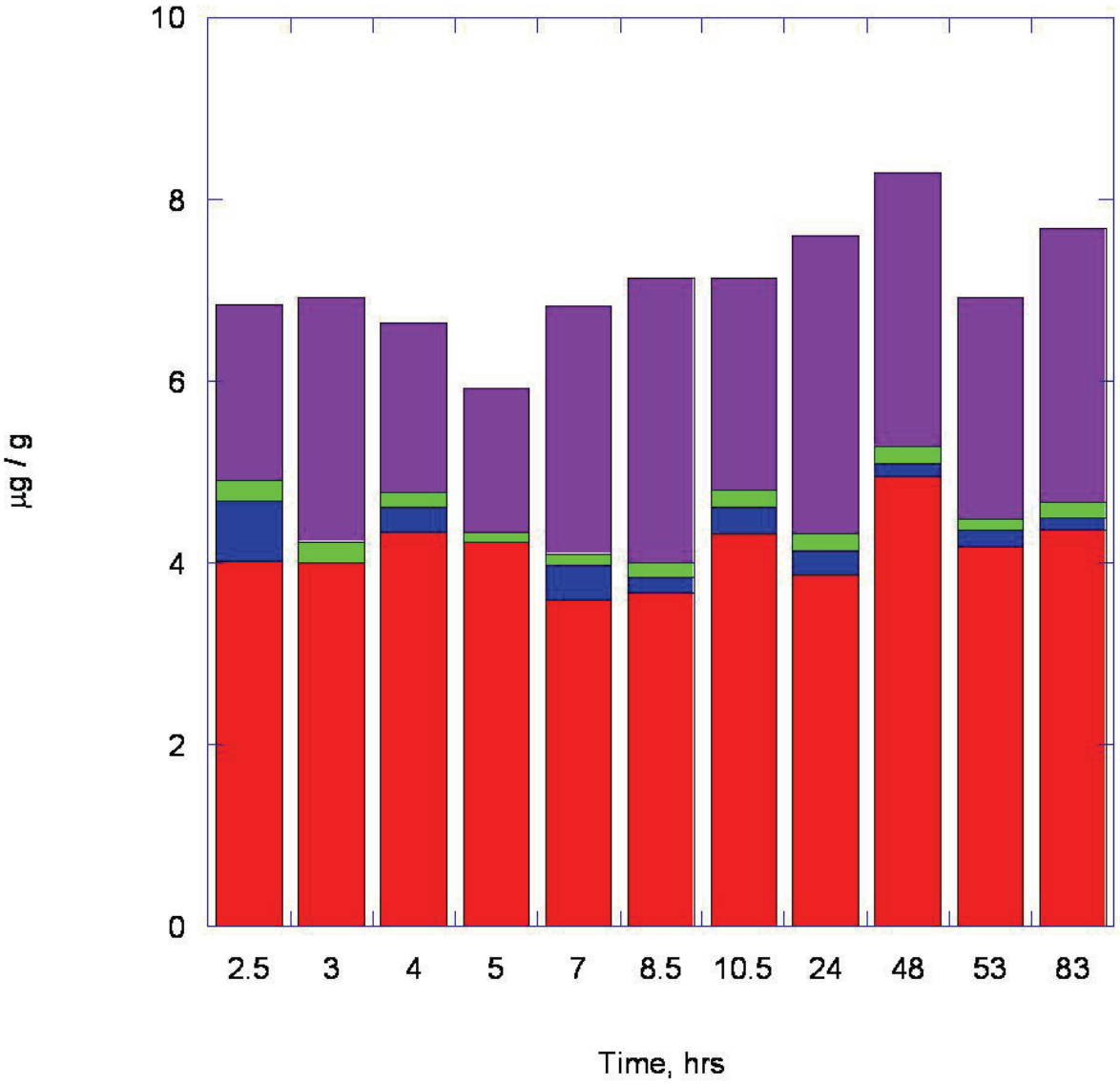

Figure 5-1. Greater amounts of reductant are available to *Ec*BCP than apparent when measuring levels with each individual reductant. Reductant levels of Trx1 (purple), Trx2, (green), Grx1 (blue), and Grx3 (red) were measured over time in *Escherichia coli* (Meyer *et al.*, 2009) and plotted to indicate the total reductants available to BCP over time.

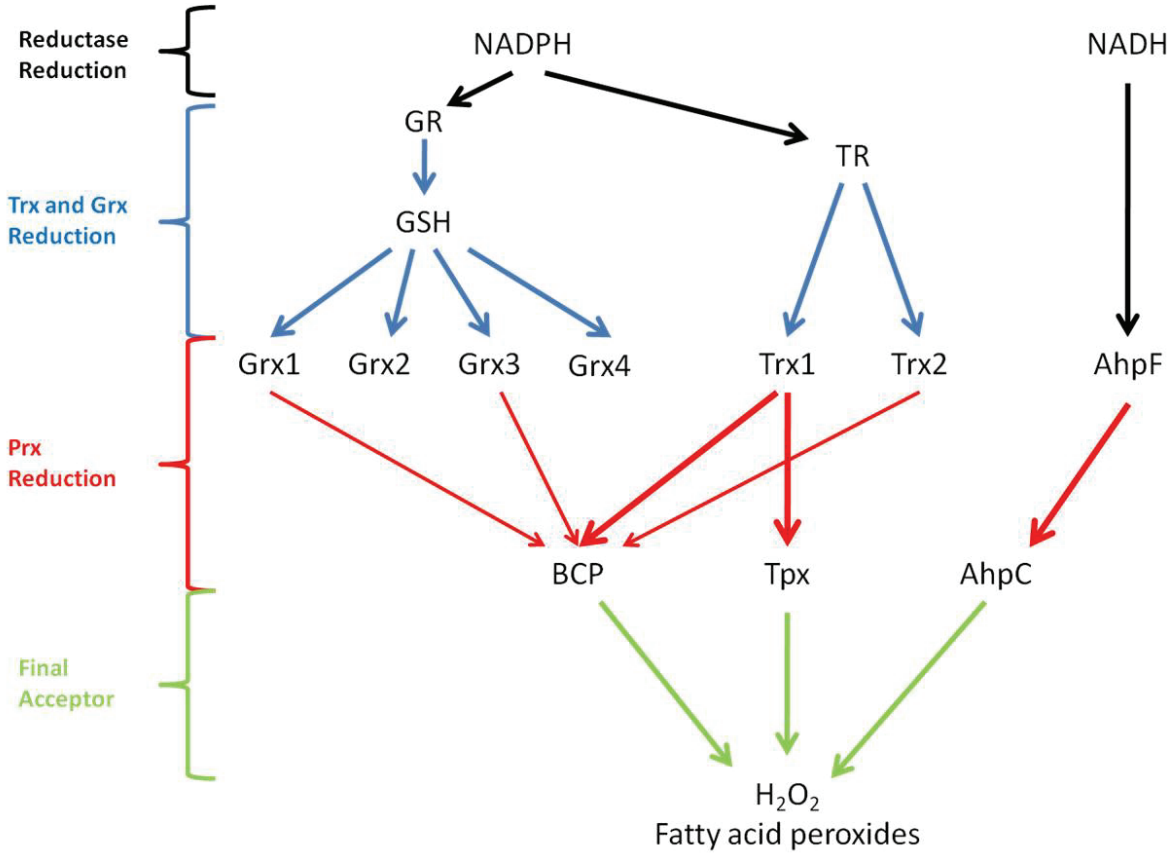

Figure 5-2. The reductive recycling pathways for *E. coli* Prxs. This figure highlights the unique NADH-dependent pathway of AhpC and the redundancy of Trx and Grx reductants for BCP. The thicker arrows indicate preferred reduction pathways.

Studies show *Ec*BCP is upregulated during peroxide distress (Fournier *et al.*, 2006). The absence of BCP in the oxyR regulon raises questions about the effectiveness of gene products from the OxyR regulon as reductants for BCP. The transcription factor OxyR is activated by H_2O_2 during oxidative stress and induces the expression of antioxidant machinery (KatG, AhpCF, Tpx) and reducing proteins like Grx1, Trx2 and glutathione reductase (Carmel-Harel & Storz, 2000, Ritz *et al.*, 2000, Pomposiello & Demple, 2001).

The BCP/PrxQ Subfamily is the Most Similar to the Progenitor of Modern Day Prxs. The biochemical features associated with *Ec*BCP are possible remnants of earlier Prxs. The first Prxs would have been simple. They would have utilized a 1-Cys mechanism allowing them to behave as a monomer, both functionally and structurally, as is the case with *Ec*BCP. A broad specificity for peroxide substrates and reductants imparted versatility, but is associated with lower catalytic efficiency linked to high substrate K_m values. The high K_m of *Ec*BCP for peroxides may have evolved as a necessity to prevent substrate saturation and because bacteria possessing only one type of Prx needed to have that particular Prx function under many oxidative conditions. The widespread nature of the BCP/PrxQ subfamily is probably a byproduct of its origin.

The complexity of evolution can be seen in comparisons between BCP/PrxQ and other Prx subfamilies and this complexity applies not only to oxidative stress defense mechanisms, but also to the defenders themselves, i.e. peroxiredoxins. Evolutionary changes occurred over the passage of time resulting in several key changes among Prxs. Firstly, a highly conserved

resolving cysteine arose in many Prx subfamilies, while the resolving cysteine is only present in ~54% of BCP/PrxQ members. Secondly, many Prxs developed increased specificity and lower K_m values for certain substrates at the cost of peroxidase versatility. Finally, peroxiredoxins transitioned from monomeric to dimeric quaternary structures (and larger) in a possible attempt to protect active site pockets.

Future studies for E. coli BCP. Based on the discovery of efficient turnover for resolving cysteine mutants with both Trx1 and $Grx1_{F6W}$, additional kinetic studies to elucidate the mechanism of *E. coli* BCP are warranted. As described in Chapters 3 and 4, rapid mix acid quench titrations were used to determine the rate of formation (k_1) of sulfenic acid, the first intermediate formed during catalysis. Additionally, gel shift assays have been used and will be further employed to determine formation rates of some of the remaining *Ec*BCP kinetic intermediates (Fig. 4-2). Disulfide bond reduction rates (k_4) will be measured in assays combining oxidized *Ec*BCP and resolving cysteine mutants of Trx or Grx1. By measuring the formation of *Ec*BCP -reductant complex formation, k_4 can be determined. Further experimentation may require stopped flow and/or quenched flow kinetic analysis to determine these rate constants with wild type proteins, as well. By determining the rates of intermediate formation (k_1 - k_4), we will be able to fully assess the formation and catalytic competence of the C45-C50 disulfide bond in *Ec*BCP.

In vitro studies in this dissertation tested for defined interactions under defined conditions, while *in vivo* studies will be of particular value in assessing

the physiological functions of *Ec*BCP. With that in mind, *in vivo* functional assays to investigate peroxide scavenging function of *Ec*BCP with and without the resolving cysteine would be of great interest. *In vivo* studies are complicated by the presence of catalase, a H_2O_2 scavenger that may mask the effectiveness of *Ec*BCP. Fortunately, catalase cannot degrade organic hydroperoxides; therefore, tBOOH and CHP can be used as substrates to more accurately measure the activity of *Ec*BCP. These studies may also be complicated by the two Prx proteins in *E. coli*, AhpC and Tpx (Jacobson *et al.*, 1989, Poole & Ellis, 1996, Poole *et al.*, 2000, Poole, 2005, Tao, 2008). A deletion strain of *E. coli* could be generated which lacks all three Prx family members, AhpC, Tpx and BCP. Although this strain may be hypersensitive to peroxide stress, we still anticipate that it can be generated and stable under rich media culture conditions based on many other studies of similar mutants. Expression vectors for wild type and mutant BCP could then be transformed into this strain, with C45S serving as a negative control, and these strains could then be tested for peroxide hypersensitivity and scavenging capacity using complementary assay approaches. One approach is disk diffusion assays which measure the level of protective peroxidase activity as assessed by small or large zones of bacterial killing on plates with H_2O_2, tBHP or CHP spotted onto paper disks placed at the center of each plate (as described by (Seaver & Imlay, 2001). Percentages of surviving bacteria expressing wild-type and mutant *Ec*BCP can also be statistically analyzed by plating serial dilutions after treatment with multiple concentrations of peroxide substrates (Poole & Ellis, 1996). Finally, the *in vivo*

capacity of the bacteria containing wild type and mutant expression plasmids to scavenge organic hydroperoxides could be tested using the Fox assay to look at disappearance of peroxide over time (Klomsiri 2005).

REFERENCES

Aslund, F., Berndt, K. D., and Holmgren, A. (1997) Redox potentials of glutaredoxins and other thiol-disulfide oxidoreductases of the thioredoxin superfamily determined by direct protein-protein redox equilibria, *J Biol Chem 272*, 30780-30786.

Carmel-Harel, O., and Storz, G. (2000) Roles of the glutathione- and thioredoxin-dependent reduction systems in the *Escherichia coli* and saccharomyces cerevisiae responses to oxidative stress, *Annu Rev Microbiol 54*, 439-461.

Clarke, D. J., Mackay, C. L., Campopiano, D. J., Langridge-Smith, P., and Brown, A. R. (2009) Interrogating the molecular details of the peroxiredoxin activity of the *Escherichia coli* bacterioferritin comigratory protein using high-resolution mass spectrometry, *Biochemistry 48*, 3904-3914.

Clarke, D. J., Ortega, X. P., Mackay, C. L., Valvano, M. A., Govan, J. R., Campopiano, D. J., Langridge-Smith, P., and Brown, A. R. (2010) Subdivision of the bacterioferritin comigratory protein family of bacterial peroxiredoxins based on catalytic activity, *Biochemistry 49*, 1319-1330.

Fernandes, A. P., and Holmgren, A. (2004) Glutaredoxins: glutathione-dependent redox enzymes with functions far beyond a simple thioredoxin backup system, *Antioxid Redox Signal 6*, 63-74.

Fournier, M., Aubert, C., Dermoun, Z., Durand, M., Moinier, D., and Dolla, A. (2006) Response of the anaerobe Hildenborough to oxidative conditions: proteome and transcript analysis, *Biochimie 88*, 85-94.

Hillar, A., Peters, B., Pauls, R., Loboda, A., Zhang, H., Mauk, A. G., and Loewen, P. C. (2000) Modulation of the activities of catalase-peroxidase HPI of *Escherichia coli* by site-directed mutagenesis, *Biochemistry 39*, 5868-5875.

Jacobson, F. S., Morgan, R. W., Christman, M. F., and Ames, B. N. (1989) An alkyl hydroperoxide reductase from Salmonella typhimurium involved in the defense of DNA against oxidative damage. Purification and properties, *J Biol Chem 264*, 1488-1496.

Jeong, W., Cha, M. K., and Kim, I. H. (2000) Thioredoxin-dependent hydroperoxide peroxidase activity of bacterioferritin comigratory protein (BCP) as a new member of the thiol-specific antioxidant protein (TSA)/Alkyl hydroperoxide peroxidase C (AhpC) family, *J Biol Chem 275*, 2924-2930.

Krause, G., and Holmgren, A. (1991) Substitution of the conserved tryptophan 31 in *Escherichia coli* thioredoxin by site-directed mutagenesis and structure-function analysis, *J Biol Chem 266*, 4056-4066.

Krause, G., Lundstrom, J., Barea, J. L., Pueyo de la Cuesta, C., and Holmgren, A. (1991) Mimicking the active site of protein disulfide-isomerase by substitution of proline 34 in *Escherichia coli* thioredoxin, *J Biol Chem 266*, 9494-9500.

Meyer, Y., Buchanan, B. B., Vignols, F., and Reichheld, J.-P. (2009) Thioredoxins and Glutaredoxins: Unifying elements in redox biology, *Ann Rev Genetics 43*, 335-367.

Moore, E. C., Reichard, P., and Thelander, L. (1964) Enzymatic Synthesis of Deoxyribonucleotides.V. Purification and Properties of Thioredoxin Reductase from *Escherichia coli* B, *J Biol Chem 239*, 3445-3452.

Parsonage, D., Karplus, P. A., and Poole, L. B. (2008) Substrate specificity and redox potential of AhpC, a bacterial peroxiredoxin, *Proc Natl Acad Sci U S A 105*, 8209-8214.

Parsonage, D., Youngblood, D. S., Sarma, G. N., Wood, Z. A., Karplus, P. A., and Poole, L. B. (2005) Analysis of the link between enzymatic activity and oligomeric state in AhpC, a bacterial peroxiredoxin, *Biochemistry 44*, 10583-10592.

Pineyro, M. D., Arcari, T., Robello, C., Radi, R., and Trujillo, M. (2011) Tryparedoxin peroxidases from *Trypanosoma cruzi*: high efficiency in the

catalytic elimination of hydrogen peroxide and peroxynitrite, *Arch Biochem Biophys 507*, 287-295.

Pomposiello, P. J., and Demple, B. (2001) Redox-operated genetic switches: the SoxR and OxyR transcription factors, *Trends Biotechnol 19*, 109-114.

Poole, L. B. (2005) Bacterial defenses against oxidants: mechanistic features of cysteine-based peroxidases and their flavoprotein reductases, *Arch Biochem and Biophys 433*, 240-254.

Poole, L. B., and Ellis, H. R. (1996) Flavin-dependent alkyl hydroperoxide reductase from *Salmonella typhimurium*. 1. Purification and enzymatic activities of overexpressed AhpF and AhpC proteins, *Biochemistry 35*, 56-64.

Poole, L. B., Reynolds, C. M., Wood, Z. A., Karplus, P. A., Ellis, H. R., and Li Calzi, M. (2000) AhpF and other NADH:peroxiredoxin oxidoreductases, homologues of low Mr thioredoxin reductase, *Eur J Biochem 267*, 6126-6133.

Potamitou, A. (2002) Protein levels of *Escherichia coli* Thioredoxins and Glutaredoxins and their relation to null mutants, growth phase, and function, *J Biol Chem 277*, 18561-18567.

Ritz, D., Patel, H., Doan, B., Zheng, M., Aslund, F., Storz, G., and Beckwith, J. (2000) Thioredoxin 2 is involved in the oxidative stress response in *Escherichia coli*, *J Biol Chem 275*, 2505-2512.

Ross, J. R., Porter, B. E., Buckley, P. T., Eberwine, J. H., and Robinson, M. B. (2011) mRNA for the EAAC1 subtype of glutamate transporter is present in neuronal dendrites in vitro and dramatically increases in vivo after a seizure, *Neurochem Int 58*, 366-375.

Rouhier, N. (2004) Poplar Peroxiredoxin Q. A Thioredoxin-linked chloroplast antioxidant functional in pathogen defense, *Plant Physiology 134*, 1027-1038.

Seaver, L. C., and Imlay, J. A. (2001) Alkyl hydroperoxide reductase Is the primary scavenger of endogenous hydrogen peroxide in *Escherichia coli*, *Journal of Bacteriology 183*, 7173-7181.

Sevier, C. S., and Kaiser, C. A. (2002) Formation and transfer of disulphide bonds in living cells, *Nat Rev Mol Cell Biol 3*, 836-847.

Steiner, B., McLean, I., and Graves, S. (1981) Redox potential and survival of virulent *Treponema pallidum* under microaerophilic conditions, *Br J Vener Dis 57*, 295-301.

Tao, K. (2008) Subcellular localization and in vivo oxidation-reduction kinetics of thiol peroxidase in *Escherichia coli*, *FEMS Microbiol Lett 289*, 41-45.

Wang, G., Olczak, A. A., Walton, J. P., and Maier, R. J. (2005) Contribution of the *Helicobacter pylori* thiol peroxidase bacterioferritin comigratory protein to oxidative stress resistance and host colonization, *Infect Immun 73*, 378-384.

Wood, Z. A., Poole, L. B., Hantgan, R. R., and Karplus, P. A. (2002) Dimers to doughnuts: redox-sensitive oligomerization of 2-cysteine peroxiredoxins, *Biochemistry 41*, 5493-5504.

Stacy Reeves, MPH, PhD

Wake Forest University School of Medicine
Department of Biochemistry
Molecular Genetics and Genomics Program
Medical Center Boulevard
Telephone: (336)716-6370, E-mail: streeves@wfubmc.edu

Education

Ph.D., Molecular Genetics and Genomics, Wake Forest University School of Medicine, Winston-Salem, NC. Degree anticipated August 2011
Advisor: Dr. Leslie Poole, Professor of Biochemistry

MPH, Environmental Health, Fort Valley State University, Fort Valley, GA. May 2009

Bachelor of Science, Biology, Fort Valley State University, Fort Valley, GA. June 1996

Doctoral Research: Wake Forest University School of Medicine, Winston Salem, NC. 08/2004-present. Advisor: Dr. Leslie Poole

The primary focus of my research has been to determine the catalytic mechanism of a peroxiredoxin known as bacterioferritin comigratory protein (BCP). As part of my research, I have classified the resolving mechanism of BCP, investigated the role of active site residues in modulating catalytic activity, and determined the redox potential and pKa values of wild type and mutant BCP. Highlights include:

1. We published a method for inserting a fluorescent redox reporter into glutaredoxin 1 (Parsonage D, Reeves SA, Karplus PA, Poole LB. (2010) Methods Enzymol 474, 1-21.) The inserted tryptophan increased fluorescence of the mutated protein allowing for stopped-flow fluorescence analysis of *E. coli* BCP peroxidase activity.

2. We submitted a paper detailing the kinetic and thermodynamic features of the *E. coli* peroxiredoxin known as bacterioferritin comigratory protein (BCP) (Reeves SA, Parsonage D., Nelson K., Poole LB. (*in submission*). BCP is versatile peroxiredoxin responsible for scavenging peroxides in the cytoplasm. BCP possesses the highest recorded redox potential for a peroxiredoxin to date.

3. BCP demonstrated a robust 1-Cys mechanism during mutational studies. The catalytic efficiency of BCP increases in resolving cysteines mutants using Grx1 as a reductant. Additionally, BCP capable of using multiple reductants for scavenging purposes.

Academic Awards

2010 Minority and Indigenous Fellow, The Biotechnology Institute

2010 Pincus Award, Federation of American Societies for Experimental Biology, Anaheim, CA

2010 MARC Travel Award, Federation of American Societies for Experimental Biology, Anaheim, CA

2008 MARC Travel Award, Federation of American Societies for Experimental Biology, San Diego, CA

Publications

Parsonage D, Reeves S, Karplus PA**,** Poole LB. 2010. Engineering of fluorescent reporters into redox domains to monitor electron transfer. In Methods in Enzymology (474):1-21.

Reeves SA, Parsonage D., Nelson K., Poole LB. Kinetic and Thermodynamic Features Reveal That *E. coli* BCP Is an Unusually Versatile Peroxiredoxin. *Biochemistry* (*in revision by Biochemistry*).

Poster Presentations

Biochemical Features Supporting the Flexible Role of *E. coli* BCP in Antioxidant Defense. 25th Anniversary Symposium of the Protein Society, Boston, MA 2011

Kinetic characterization of a BCP-class peroxiredoxin from Escherichia coli Experimental Biology Meeting, Anaheim, CA April 2010

Oligomeric state and utilization of various substrates by a BCP-class peroxiredoxin from *Escherichia coli*. Wake Forest Graduate Student Research Day, Winston-Salem, NC 2009

Oligomeric state and utilization of various substrates by a BCP-class peroxiredoxin from *Escherichia coli.* Experimental Biology Meeting, San Diego, CA April 2008

Oligomeric state and utilization of various substrates by a BCP-class peroxiredoxin from *Escherichia coli*. Society for Free Radical Biology and Medicine 14th Annual Meeting, Washington, DC 2007

References

Leslie Poole, Ph.D., Professor
Director, Center for Structural Biology
Wake Forest University School of Medicine
Medical Center Blvd.
Winston-Salem, North Carolina 27157
Office: 336-716-6711
Email: lbpoole@wfubmc.edu

Mark O. Lively, Ph.D., Professor
Translational Science Institute
Institute for Regenerative Medicine
Wake Forest University School of Medicine
Medical Center Blvd.
Winston-Salem, North Carolina 27157
Office: 336-716-2969
Email: mlively@wfubmc.edu

Kim Nelson, Ph.D., Professor
Department of Biochemistry
Wake Forest University School of Medicine
Medical Center Blvd.
Winston-Salem, North Carolina 27157
Office: 336-716-6370
Email: kinelson@wfubmc.edu